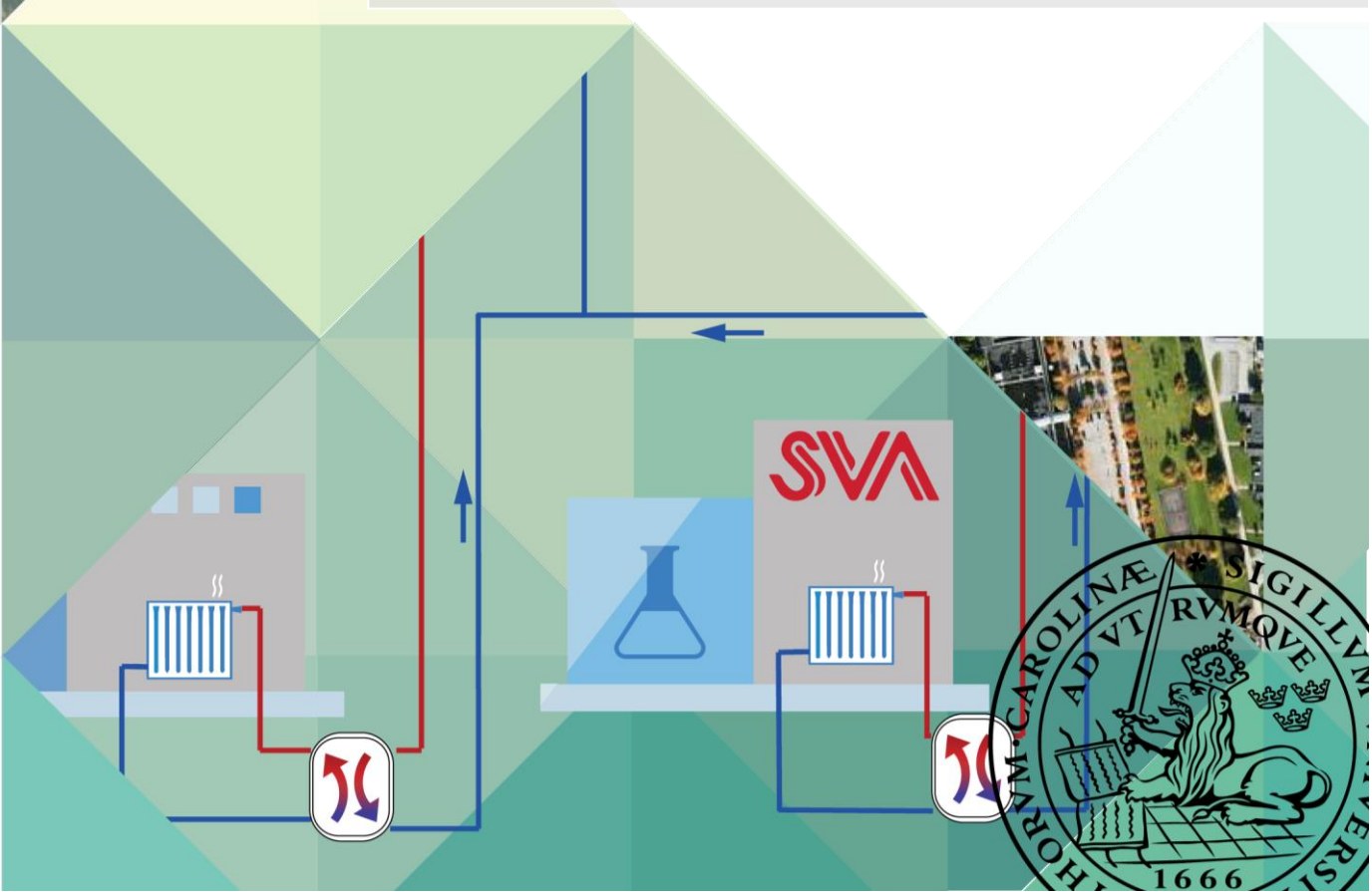# WASTE HEAT STORAGE AND UTILIZATION FOR THE CASE OF NATIONAL VETERINARY INSTITUTE (SVA), UPPSALA, SWEDEN

Stanislav Proshyn & Iryna Bulich

Master thesis in Energy-efficient and Environmental Buildings

Lund University

Lund University, with eight faculties and a number of research centres and specialized institutes, is the largest establishment for research and higher education in Scandinavia. The main part of the University is situated in the small city of Lund which has about 112,000 inhabitants. A number of departments for research and education are, however, located in Malmö. Lund University was founded in 1666 and has today a total staff of 6,000 employees and 47,000 students attending 280 degree programmes and 2,300 subject courses offered by 63 departments.

Master Programme in Energy-efficient and Environmental Building Design

This international programme provides knowledge, skills and competencies within the area of energy-efficient and environmental building design in cold climates. The goal is to train highly skilled professionals, who will significantly contribute to and influence the design, building or renovation of energy-efficient buildings, taking into consideration the architecture and environment, the inhabitants' behaviour and needs, their health and comfort as well as the overall economy.

The degree project is the final part of the master programme leading to a Master of Science (120 credits) in Energy-efficient and Environmental Buildings.

Examiner: Dennis Johansson (Lund University, Division of Building Services)
Supervisor: Saqib Javed (Lund University, Division of Building Services)
Co-supervisor: Anton Mickelsson (Helenius Ingenjörsbyrå AB)

Keywords: waste heat; direct distribution; thermal energy storage; hot water storage tank; borehole seasonal storage; heat pump; IDA ICE plant modelling; savings-to-investment ratio; life-cycle costs.

Thesis: EEBD - # / 17

Abstract

The incineration furnace at National Veterinary Institute (SVA) in Uppsala, Sweden, runs approximately 2,150 hours a year and generates a large amount of waste heat. Some of this heat is partially recovered, and is used for heating one of the main buildings during the furnace operation. However, around 2,000 MWh is wasted annually due to unavailability of any storage system. This wasted heat is approximately equivalent to the heating demand of 160 average Swedish single-family houses.

This work aims to investigate different options allowing to use the waste heat as an energy source in neighbouring buildings and reduce the amount of purchased heating energy. The study initiates with the quantitative analysis of available waste heat and heating demand of nearby buildings. Based on this analysis, four options for the management and use of excess waste heat have been selected for detailed evaluation.

The first option considered in this work is to use a storage tank to provide the main building with heating during the furnace non-operating time. For this option, special attention has been paid to the tank sizing technique. The second option studied in detail in this work is to maximize the instantaneous use of waste heat by providing direct heating to nearby buildings. This implies the supply of waste heat directly to the buildings during the furnace operating time. In this context, a strategy has been developed to determine the optimal order for connecting different buildings depending on their demand profiles and distance from the furnace. In the third option, the instantaneous use of waste heat and hot water storage tanks has been studied simultaneously in various combinations. Finally, in the fourth option an underground thermal energy storage (UTES) system assisted by a ground-source heat pump (GSHP) has been considered for seasonal heat storage. The performance of the UTES and the GSHP system has been optimized by evaluating different strategies to maximise the source-side entering temperature to the heat pump.

All the above-mentioned options have been implemented in the building energy simulation program IDA ICE (Advanced level). For each option, the overall energy performance and corresponding energy savings have been evaluated. The economic feasibility of each option has been assessed and compared to other options based on life-cycle cost (LCCs) analysis. Overall, this study contributes to the understanding of heat management between different buildings and underlines the importance of demands and availability analysis to determine the optimal solution.

Acknowledgments

Contribution

The first part of the work, including analysis and processing of the measured data of heating demand and waste heat profiles, was performed by both authors. Following the discussion on this, the design options were proposed as a result of collaborative brainstorming. Literature review section was also done in cooperation. After that, however, the work was split between the two authors. Stanislav undertook the water storage tank manual calculations and simulations, and Iryna performed simulations on instantaneous connection and parametric analysis. Stanislav contributed to the LCC calculation and investigation of all related costs. The section with the different combinations of water storage tanks and instantaneous connection is a result of joint work of both authors. The borehole system was designed by Iryna, while Stanislav was assessing the heat pump performance. Both authors equally contributed to the report writing. Illustrations were created by Iryna.

Abbreviations

ATES	Aquifer Thermal Energy Storage
BHE	Borehole Heat Exchanger
BTES	Borehole Thermal Energy Storage
COP	Coefficient of Performance
CXA	Coaxial pipe with annular inlet
CXC	Coaxial pipe with centred inlet
DH	District Heating
DHW	Domestic Hot Water
EED	Earth Energy Designer
GSHP	Ground-Source Heat Pump
HP	Heat Pump
HT-BTES	High-Temperature Borehole Thermal Energy Storage
HTF	Heat Transfer Fluid
KLIMP	Swedish climate investigating program
LCC	Life Cycle Cost
NPV	Net Present Value
PCM	Phase Change Materials
PTES	Pit Thermal Energy Storage
PV	Present Value
SIR	Savings-to-Investment Ratio
SMHI	Swedish Meteorological and Hydrological Institute
SPF	Seasonal Performance Factor
SVA	National Veterinary Institute of Sweden
TES	Thermal Energy Storage
TTES	Tank Thermal Energy Storage
UTES	Underground Thermal Energy Storage

Table of content

"Sustainability, ensuring the future of life on Earth,
is an infinite game, the endless expression of generosity
on behalf of all."

Paul Hawken

1 Introduction

This work has been carried out in cooperation with Helenius Ingenjörsbyrå, Uppsala, on the request of Akademiska Hus who owns a premises where a considerable amount of excess waste heat is generated. A large part of the generated thermal energy cannot be utilized due to a time lag between availability and demand of energy. The mismatch occurs over a wide timescale ranging from a few hours to several weeks.

The aim of this work has therefore been to find the solutions for the maximum excess heat utilization. In this case, a part of the energy purchased from the district heating (DH) network can be replaced with the excess energy, which is dissipated at present. This will result in reduction of building operation costs and environmental impact.

Thermal energy storage (TES) is the solution that has the potential to abolish the mismatch between heat availability and heating demands. By implementing a TES system, not only savings in energy can be achieved, but also a peak power shaving, allowing the size and pumping power of the equipment to be reduced, can be accomplished. The questions addressed in this work are also related to a common problem in renewable energy of balancing the fluctuating power generation with the constantly changing demand.

Another way to solve the current task is to connect more buildings directly to a heat source and thus utilize waste energy without using any TES system. Then, the generated excess heat will be used instantaneously. The key idea in this regards is to find the buildings with the most suitable heating demands.

1.1 Background

Akademiska Hus is one of Sweden's largest real estate companies, which owns and manages university and college buildings as well as student housings in various parts of the country. It owns a complex of buildings in Uppsala, which is subleased to National Veterinary Institute (SVA). The SVA is the Swedish national administrative authority that specializes in veterinary expertise and animals' disease research and uses the site for veterinary clinic, laboratory premises and offices (SVA, 2017).

The SVA is situated in four buildings in Uppsala (see Figure 1.1). In Building 14, a destruction furnace is used for incineration purposes. The process releases a large amount of waste heat, which is available for approximately nine hours per working day all year around. About 3,600 MWh of thermal energy is produced yearly, from which 1,600 MWh is used for heating Building 14 during the operating hours of the furnace. The remaining 2,000 MWh is not utilized and is dumped to the DH network free of charge. During non-operating time of the furnace – mainly nights and weekends – the heating demand of the building is met through the energy purchased from the DH company, Vattenfall.
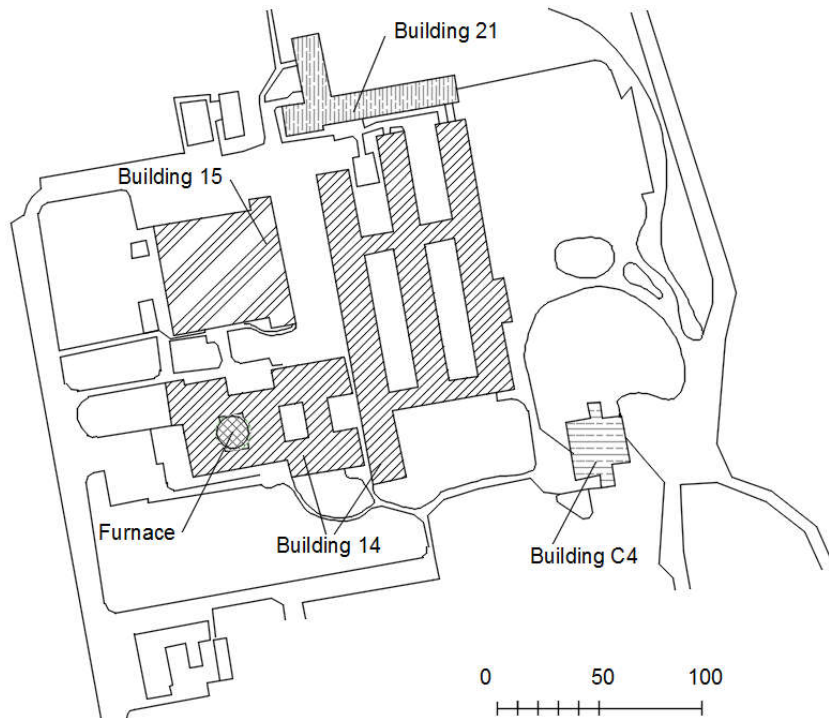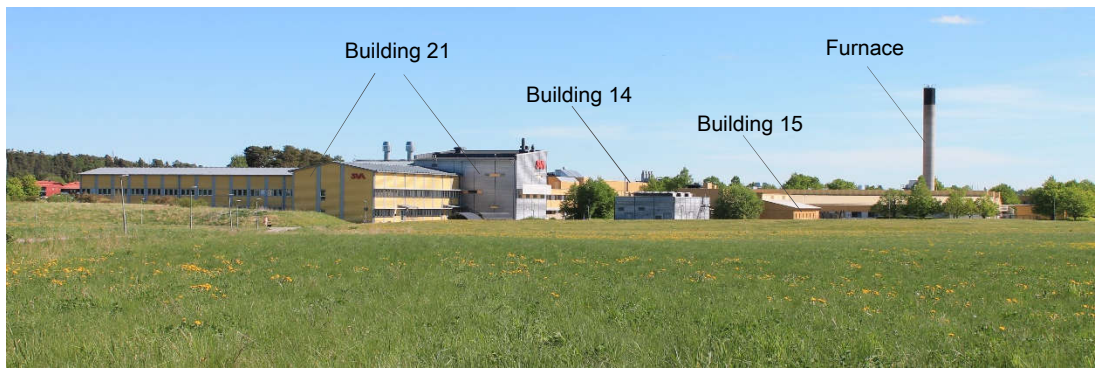
Figure 1.1: Site and layout of SVA buildings in Uppsala.

Akademiska Hus has an intention to become more energy independent by utilizing as much waste heat as possible from the 2,000 MWh/year currently dumped to the DH network. The main challenges to reach this target include:

- Largest heating demand is at night when furnace is not in operation,

- Significant part of waste heat is available during summer, because during winter it is already utilized for covering the heating demands of Building 14,

- Waste heat is not available on weekends making it challenging to reduce the peak load with a short-term storage tank.

1.2   Previous study

In 2016, Helenius Ingenjörsbyrå performed a project for SVA where two options (named *A* and *B*) of storing waste heat in water tank were studied. The aim was to find a solution to heat Buildings 14 and 15 during evenings and nights when the furnace is not in operation. *Option A* was to store the heat required for heating Building 14 during the non-operating furnace hours. For this purpose, the volume of the storage tank was estimated to be 145 m^3. *Option B* was to provide Building 15 with waste heat as well. For this, an appropriate volume of the tank was determined to be 25 m^3 larger than   for *Option A*. The capacity of the heat storage was determined by taking an average hourly demand (kW) during the March to May period multiplied by an assumed discharging time (15 hours). Although this approach of sizing a tank is a common practice, it failed to consider the demand in relation to the available excess heat. In addition, the tank was estimated to operate at 60 ˚C / 90 ˚C. The actual temperatures in the system were not considered.

The annual energy savings from *Option A* and *Option B* were estimated to be 1,000 and 1,300 MWh, respectively. With the first option, it was possible to use about 59 % of the available waste heat. The corresponding figure for the second option was estimated to be approximately 76 % of the available excess heat. More than 700 MWh/year would still be available after implementing any of these two options. Economic viability was estimated to be 4.0 MSEK for *Option A* and 4.4 MSEK for *Option B*. Payback period was estimated to be approximately five years. The installation costs were not considered in depth, and costs of system components including pumps, piping, control and peripherals were overlooked.

1.3   Aim and objectives

The most common TES technology is to use a water storage tank and the previous work done by Helenius Ingenjörsbyrå only focused on this solution. Also, storage tanks offer short-time storage excluding the possibility to utilize the large part of waste heat generated during summer. Therefore, in this study a ground storage to store excess heat at the time when heating demand is low has also been considered as a design option.

Thus, this work aims to determine the optimal way of waste heat management in the neighbouring buildings in terms of maximum usage, highest energy savings and economic viability. To attain this aim following set of objectives has been formulated:

- To analyse waste heat availability and the demands of adjacent buildings,

- To assess the possibility of direct (instantaneous) use of waste heat,

- To evaluate water tank as an option for short-time storage with a detailed sizing strategy,

- To analyse the possibility of seasonal ground storage.

1.4   Limitations

This study is subjected to a number of limitations, the most significant of which are listed here. Data for heat dumped to the DH network and heating demand profiles has been analysed based on the measurements of the year 2016 only. However, the heating demands have been normalized to the reference year.

Simplifications have been made when modelling systems in IDA ICE (EQUA, 2017) to avoid complex control mechanisms. This is explained in more details in sections *Methodology*, and *Discussion and Conclusions*. All the results and conclusions, based on the performance of system components including tank and heat pump, are simulation-based and no experiments or measurements have been performed.

Life-cycle cost (LCC) calculations have been performed with fixed values of discount rate and energy price growth rate. The numbers and parameters used in this work have been provided by Akademiska Hus. As per the contract between Akademiska Hus and the DH company, the price for district heating remains fixed over the year. The economic and financial calculations have been performed assuming a 15-year life-cycle period. In reality, the lifecycle of technical systems is typically over 25 years. A number of assumptions have also been made when estimating the costs and prices for different stages of the project. Where relevant, assumptions are mentioned in the corresponding sections.

The ground properties are mainly assumed values based on experience and knowledge of the ground structure in the area. The ground-source heat pump system has been simulated using two different software, IDA ICE and Earth Energy Designer (EED) (buildingphysics.com, 2017), which may have some effect on the system performance and results.

1.5 Outline

This thesis presents a case-study focused on the methods of waste heat utilization and storage. The main aspects considered in the work are short-term storage (water tank), direct use, and long-term storage using borehole thermal energy storage (BTES). The work is organized into five chapters. *Chapter 1* introduces the background and the problem, and explains objectives and limitations of the study. *Chapter 2* presents an overall explanation of TES concept, types and design methods, and provides examples of waste heat utilization projects. *Chapter 3* covers the analysis of the existing system and measured profiles of the demand and available heat based on the measurements taken in 2016. The section also assesses the overall potential to utilize and distribute the available waste heat between different SVA buildings. The approach taken for the design of each option is also described. *Chapter 4* presents results of all proposed options together with economic consideration. *Chapter 5* discusses the final results, sensitivity of the results, and evaluation of the chosen approach. It also elaborates in detail on the limitations of the conducted study and analyses how they affected the results.

2 Literature review

This chapter introduces TES and provides an overview of different storage types, storing durations, medias and design recommendations. Water tank and borehole thermal energy storage (BTES) systems employed in the current project are considered in more detail. Storage tanks are studied in regard to their sizing technique, stratification, investment costs and different fluid types. Borehole thermal energy storage systems are studied in regard to rock properties and borehole operation. The chapter also provides examples of some interesting waste heat utilization projects.

2.1 Overview of the TES types and design rules

Heat storage technologies are used in a wide variety and generally divided into three types: sensible, latent and thermo-chemical (Figure 2.1). *Sensible heat* is when temperature of a material increases and consequently increases the amount of energy in it. Water and rock are two examples of materials used for sensible storage. *Latent heat* is the energy needed for the change of the state of a material, for instance from ice to water and from water to steam. Water/ice and salt hydrate systems are used for latent storage in phase change materials (PCM). *Chemical heat* storage technology principle lies in breaking and forming of chemical bonds, which allows for storing a considerable part of energy per unit mass of storage material (Dincer & Rocen, 2011). Thermal energy storage can be designed for different time durations. Short-term storage (usually up to 24 hours) is used to reduce peak-power loads and to decrease size of the system. Diurnal storage permits smaller units and lower investment costs. In case if significant amount of waste heat is available, then the medium-term storage is recommended (ranging from several weeks to months). Finally, long-term storage takes into consideration seasonal variations of demand and allow for storing energy from the summer to autumn-winter period. Annual storage is considerably more cost demanding and its careful sizing is much more critical (Dincer & Rocen, 2011).
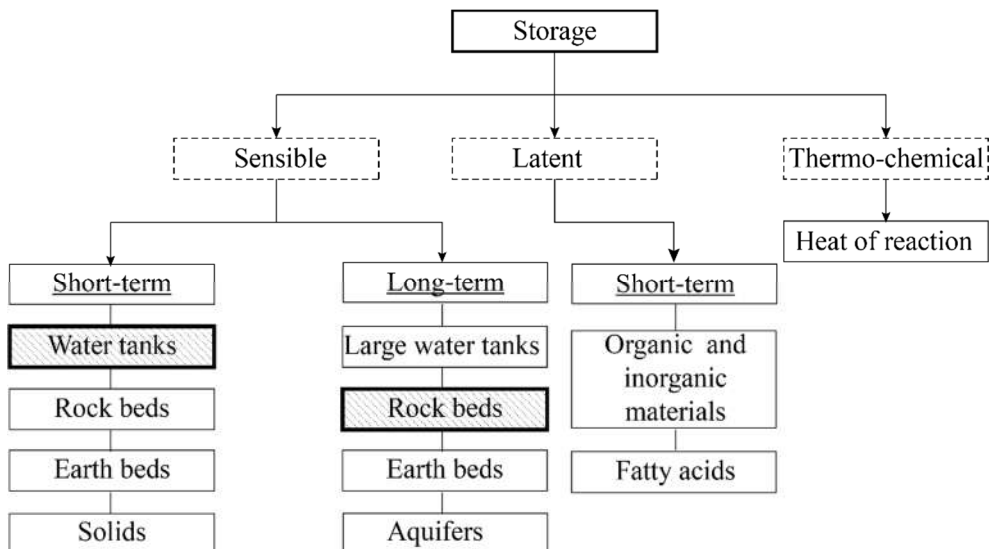

Figure 2.1: Classification of TES and storage mediums. High-lighted systems including water tank and bedrock systems are respectively used as short- and long-term storage options.

When designing a TES system, the first thing to be considered is the characteristic of the thermal storage itself. Generally, good thermal storage systems are considered to have high storage capacity, possibility of high heat transfer between heat transfer fluid (HTF) and the storage, possibility of reverse flow in the system, and low thermal losses. Volumetric thermal capacity is an important parameter that determines the ability to store sensible heat. Water has high thermal capacity of approximately 4.15 MJ/(m^3·K), which is almost three times higher than most ground formations such as clay, sand and gravel. Sedimentary and magmatic rock types have slightly higher volumetric thermal capacity, yet not as high as that of water (Cabeza, 2015).

The second, and an even more important issue to be addressed when designing a TES system is the use of an operation strategy tailored according to application, existing conditions, space restrictions and desired output. For example, the peak load, operative temperatures of the system, enthalpy drop and compatibility with existing system must be analysed (Cabeza, 2015). Apart from this, technical criteria such as life span, costs, efficiency, installation and environmental standards should also be considered. Control methods can also be complex, but very important to allow for.

2.2   Water tank storage

It is rather easy to design and model the performance of a sensible heat storage. However, one of its main disadvantages is that it requires large volumes. This is governed by Equation 1, where the capacity Q of the storage depends on the density ρ of the substance (in kg/m^3), its specific heat capacity C_p (in kJ/(kg·K)), storage volume V (in m^3) and temperature rise ΔT of storage (in K). This implies that a higher $\rho \cdot C_p$ is desired to decrease the volume. Hence, selection of appropriate storage material is an important aspect when designing a sensible heat storage (Ataer, 2006).

$$Q = V \cdot \rho \cdot C_p \cdot \Delta T \qquad [Q] = \text{kJ} \qquad (1)$$

Choice of the storage material depends largely on the desired temperature levels. For example, it is possible to reach temperatures of up to 220 ºC by using hot oil storage. Among others, vegetable oils are applicable for these purposes (Prinsloo & Dobson, 2015). The disadvantages of using oils are their degradation, safety problems, and costs. For these reasons, application of this material is usually considered in small storage systems (Ataer, 2006). Molten salt can be used for high-temperature applications (up to 560 ºC) (Way, 2008). However, they are highly corrosive.

Water is being widely used for storage temperatures below 100 ºC at atmospheric pressure. By using a pressurized equipment (tank, piping, etc.) it is also possible to store water above this temperature. However, it is seldom done mainly because of the high costs of such equipment. The advantages of water include its lower costs and easy availability, whereas freezing problems, corrosion, and temperature limits are the main drawbacks. Another advantage of using water is that energy can be easily pumped and transported to different places due to the liquid state of water.

The efficiency of a water storage tank largely depends on its thermal stratification – i.e. the ability of water to form layers of different temperatures. Cold water has a higher density and

therefore it sinks down, whereas hot water rises to the top, creating a temperature gradient throughout the height of the tank. Due to this, high temperature water can be supplied to the consumer from the top of the tank, while water at lower temperature can be drawn off from the bottom of the tank. This is particularly useful in solar heating installations, increasing the efficiency of the collector.

Ideal stratification is not possible to achieve due to a number of reasons. It is affected by the water flow entering the tank, its temperature, as well as by heat losses from the tank walls (Ataer, 2006). Pavlov and Olesen (2011) pointed out that in a cylindrical tank thermal stratification can be achieved even with high water flow rates. In addition to that, Lavan and Thompsom (1976) suggested that location of the water inlet to the tank has a great influence on the tank performance.

2.3 Borehole thermal energy storage

Development of the ground storage gained momentum during the oil crises of 1970s when long-term storage systems for solar energy were sought (Bourne-Webb et al., 2016). Several pilot studies were made in Scandinavia, and especially in Sweden in 1980s (Cabeza, 2015). Underground thermal energy storage (UTES) systems use the available heating or cooling during summer and winter periods, or from a waste heat process and store it in aquifers or boreholes (Javed, 2012). In the first case, groundwater carries the thermal energy to and from the aquifers and, thus, the heat is captured in groundwater or the soil around. This technology is widely used in Sweden and the Netherlands, for low-temperature systems (Cabeza, 2015). On the other hand, borehole thermal energy storage is based on the conduction mechanism in the solid material such as rock or soil. Hence, heat exchangers are needed for injection and extraction of heat. Borehole heat exchanger (BHE), a vertical or slightly inclined pipe, is placed in the borehole, filled with water or an antifreeze that is transferring energy from and to the ground and is backfilled with a grouting material (Javed & Spitler, 2016). This type of BHE is shown in Figure 2.2.

As seen in Figure 2.2, different configurations of pipe are possible: single U-pipe, double U-pipe, coaxial pipe with annular inlet (CXA) and coaxial pipe with centred inlet (CXC). BHE is usually used for depths up to 400 m. In rocky underground structure, e.g. in Sweden, it is also common to use water-filled boreholes instead of grouted ones (Spitler et al., 2016).
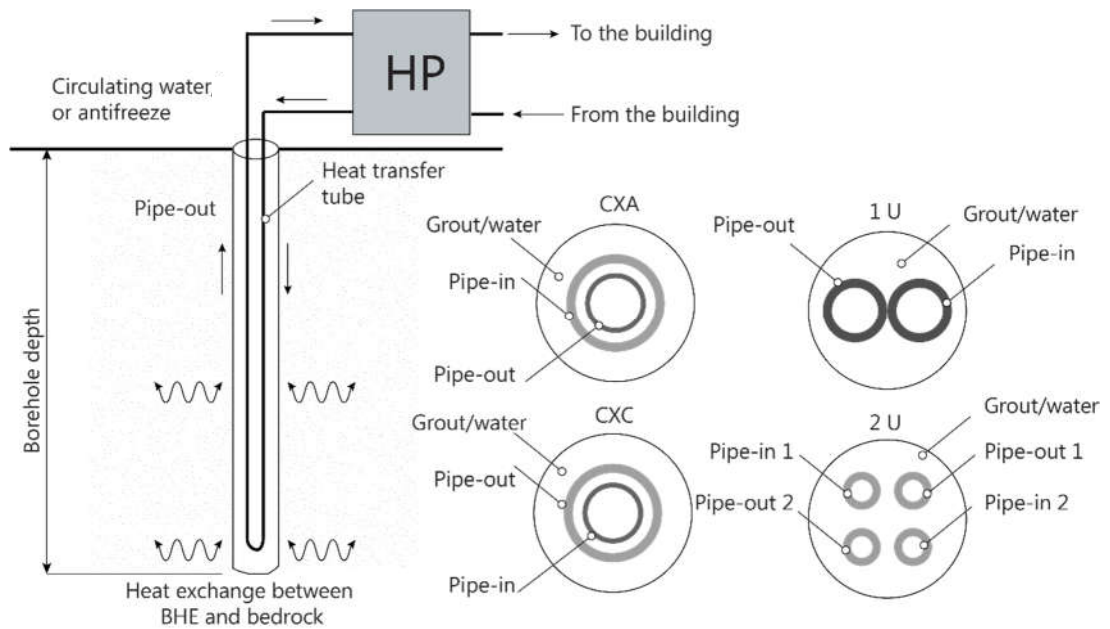
Figure 2.2: GSHP system with possible borehole configurations.[1]

The thermal conductivity in the ground ranges from 1–5 W/(m·K). The temperature in the top surface of the ground varies with ambient air temperature. At a depth of around 15 m the temperature remains constant throughout the year. Below that depth, temperature rises by approximately 3 K every 100 m. Because of the mutual thermal interaction between boreholes, the borehole field should be arranged with minimum surface and maximum volume (Javed, 2010). Thus, it is preferable to place the maximum number of boreholes in a close proximity to each other. Regular values for spacing between BHE ranges from 2 to 5 m (Cabeza, 2015).

Boreholes can be connected in series or in parallel. A parallel connection is often preferred because of shorter critical path for the pump (Manonelles, 2014). Since charging and discharging are dependent on the thermal conductivity of the ground, it is important to consider the flux at which heat is supplied to the ground. Sometimes, ground is not able to take all heat and additional buffer storage is needed. Because of the heat losses the temperatures from the heat source for charging the ground storage should be significantly higher than the return temperatures. When using a heat pump the temperature difference and storage capacity is higher and thus the smaller size of BHE is possible. If DH is used as a supplementary heat source then the minimum temperature from the ground should be equal to the district heating return temperature (Cabeza, 2015).

---

[1] Figure is adapted from Cabeza (2015).

2.4   Waste heat utilization related projects

Today, a large amount of waste heat is produced as a by-product of industrial processes, human activities and other processes, and is often disposed to the ambient environment. It is estimated that 20 % to 64 % of energy used by industrial processes is ultimately rejected to ambient as waste heat (Romagnoli, 2015). According to the Dutch statistical data mentioned in the work of Boer et al. (2006) around 80 % of processes in industry sector imply heat generation. Subsequently, this heat is dissipated through cooling towers, cooling water and flue gasses.

In large scale thermal systems, waste heat is rarely being recycled due to the mismatch in energy demand and waste heat availability, large distances between heat source and place of its utilization, and high installation and distribution costs. Instead of being wasted, excess heat can be collected, recovered and utilized by another process substituting electricity or fossil fuels with emission-free energy (Figure 2.3).
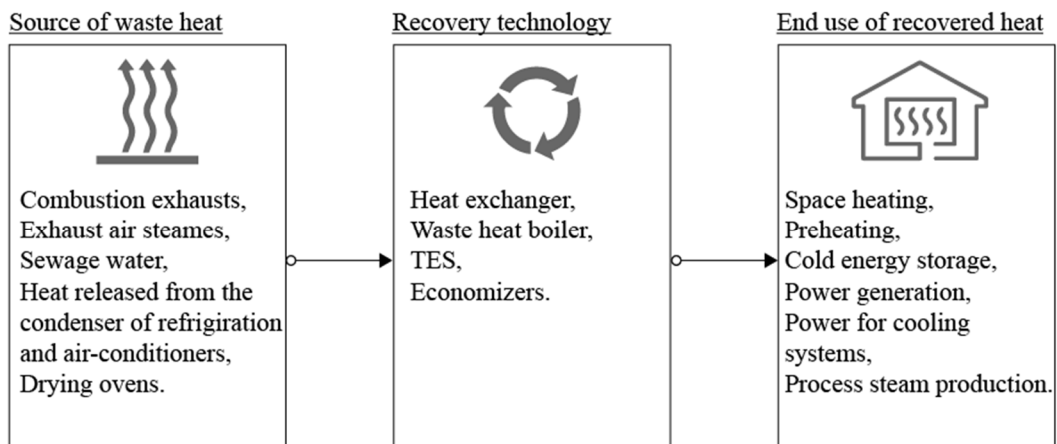

Figure 2.3: Waste heat sources and their utilization.

One of the large projects of waste heat management was successfully implemented and launched in 2010 in Lindås, Sweden (Andersson et al., 2009). There, the company ITT Water and Waste Water owns a plant, which manufactures submersible pumps and mixtures. There are melting ovens that release around 10 GWh of waste heat annually. High temperature borehole storage (HT-BTES) combined with two heat pumps of 400 kW and 600 kW were introduced to replace the DH connection. Waste heat was used as a heat source together with extract energy from ventilation system and the water basin was utilized for cooling. There were 140 boreholes, 150 m deep occupying 40 x 50 m of surface area. The operating temperatures of the system were reported to be 60 ˚C and 40 ˚C. The project was supported by KLIMP, one of the climate investment program aiming to reduce the climate change (The Swedish Environmental Protection Agency, 2009).

Another example of storing waste heat generated by high capacity diesel engines has been described in the work of Kiran and Reddy (2015). In this process, two-thirds of the energy was wasted as exhaust gases and other losses. The authors investigated the possibility of storing waste heat in a TES tank filled with PCM based on stearic acid and PCM paraffin. The storage was charged up to 60–70 ˚C and in this range the phase change from solid to

liquid occurred. After that, the temperature was increased up to 93 ˚C. Discharging occurred for 24 hours and during this time the temperature dropped to the ambient temperature.

Some new possibilities of mobile TES have also been reported in the literature. Owing to high storage capacity, PCM materials are made compact and portable which has led to new possibilities of transferring heat from one location to another. Examples of such mobile thermal energy storage have been demonstrated by Gurtner (2015) in a review of possibilities for industrial waste heat recovery. It has been shown that the mobile TES can be transferred from the charging station at a power plant to the discharging station at a demand side 8 km away. Such a mobile TES can be an alternative to long pipelines. Another work (Wang, 2010) related to mobile TES examined a solution of delivering transportable charged PCM from industrial plants, where the surplus of heat is present, to detached buildings in rural areas.

Waste heat can also be recovered to power[2]. For instance, in high temperature processes such as gas turbine or cyclic power plant operation (which produce steam at a temperature of 400 ˚C), temporarily available waste heat can be stored in thermal oil at a temperature as high as 550 ˚C. The storage time varies between three hours to several days. Then, hot steam is directed to steam turbine which transforms thermal energy to power with a thermal efficiency of 99 % (EnergyNest, 2017).

Also, these days, the heat exchange between multiple buildings with different thermal demands is becoming increasingly popular. Recent developments toward this, have been demonstrated in the Hikari project in Lyon, France. In this project a building complex with offices, residential and commercial units was designed as a plus energy block with a joint heat recovery system (SADEV, 2017). Loads were distributed in a way that simultaneous heating and cooling demands were avoided.

All case-studies mentioned above illustrate that TES enables flexible use of waste heat and can offer different opportunities for reducing primary energy use. The example with heat exchange between buildings shows the importance of studying demand profiles and matching them in the best possible way.

---

[2] In parallel with current work, Felix Ek from Uppsala University investigates the possibility to convert the excess heat produced in SVA to electricity using closed-loop gas turbines.

3   Methodology

This chapter is divided into three main sections. The first section deals with analysis of the available heat and demand profiles for the considered buildings. The second section briefly describes the current system arrangement and connection to the furnace and the DH plant. The third and the most extensive one, introduces the options proposed for waste heat utilization and simulations. Figure 3.1 sums up the two main approaches applied in this process. The first approach refers to the direct use of waste heat whereas the second approach concerns the possibility of storing the heat to be utilized later. Special attention has been paid to the modelling of system configurations in the software IDA ICE.

1) Instantaneous use

| Source of waste heat | o──────▶ | Distribution | o──────▶ | Buildings |
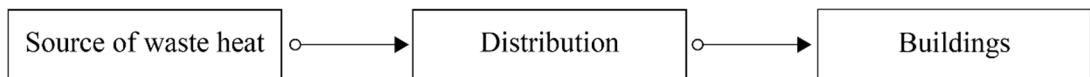
2) Instantaneous use and/or storage

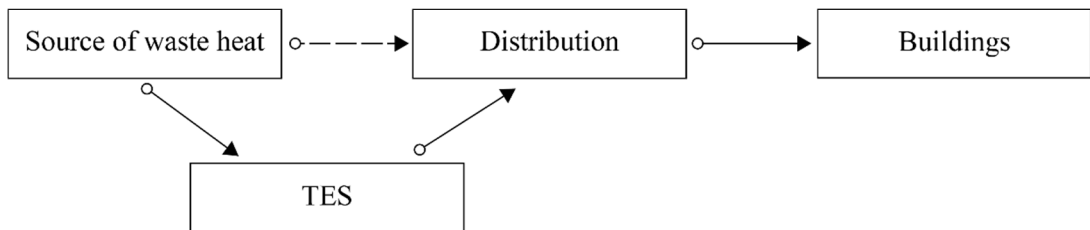| Source of waste heat | o──────▶ | Distribution | o──────▶ | Buildings |

TES

Figure 3.1: Heat utilization principles applied in the project.[3]

3.1   Analysis of heating demands and available heat profiles

Measured hourly values of the energy dumped to the district heating network as well as the heating demands of the buildings were available for the year 2016. Since the available data is year-specific, it was first adjusted to a reference year to get results for the most typical weather conditions. Swedish Meteorological and Hydrological Institute (SMHI) has developed an energy indexing method, which correlates the energy use to variation in weather conditions taking ambient air temperature, solar and wind exposure into account. The method also considers building standards, such as BBR (Boverket, 2015), and the location of the building (SMHI, 2016).

According to the method, the energy index values should be applied to the weather-dependent part of energy use, i.e. excluding domestic hot water (DHW) and household electricity. The measured data includes both space heating and DHW together without any clear distinction. Hence, energy use for space heating was calculated assuming 2 kWh/(m²·year) for DHW as suggested by (SVEBY, 2013) for office buildings. The average temperature for the year 2016

---

[3] Figure is adapted from Dincer & Rocen (2011).

was 1.6 °C warmer than the normal average temperature for the period 1981–2010. For this reason, energy indices listed in Table 3.1 were applied to the measured energy data.

Table 3.1: Monthly energy index values for Uppsala for the year of 2016.

Month	Energy index / %
January	112.3
February	91.8
March	87.6
April	100.5
May	82.2
June	72.0
July	41.2
August	100.0
September	62.0
October	99.8
November	104.1
December	87.6

After normalizing the data, the correlation between heating demands of different buildings and available waste heat was studied on monthly, daily and hourly basis. The monthly correlation was important to decide the preferred order of connecting the buildings to the available waste heat. The daily correlation was significant to analyse the demands on weekends, and to decide the storage tank size. The hourly correlation allowed to determine the amount of heat which could actually be used by the buildings.

Figure 3.2 shows the monthly profiles of available energy and energy required by different buildings. In total, 2,000 MWh of waste heat is available, which is enough to provide heating for approximately 160 average single-family houses in Sweden. As can be seen, a large amount of it is available during the summer months when heating demands of several buildings are minimal.
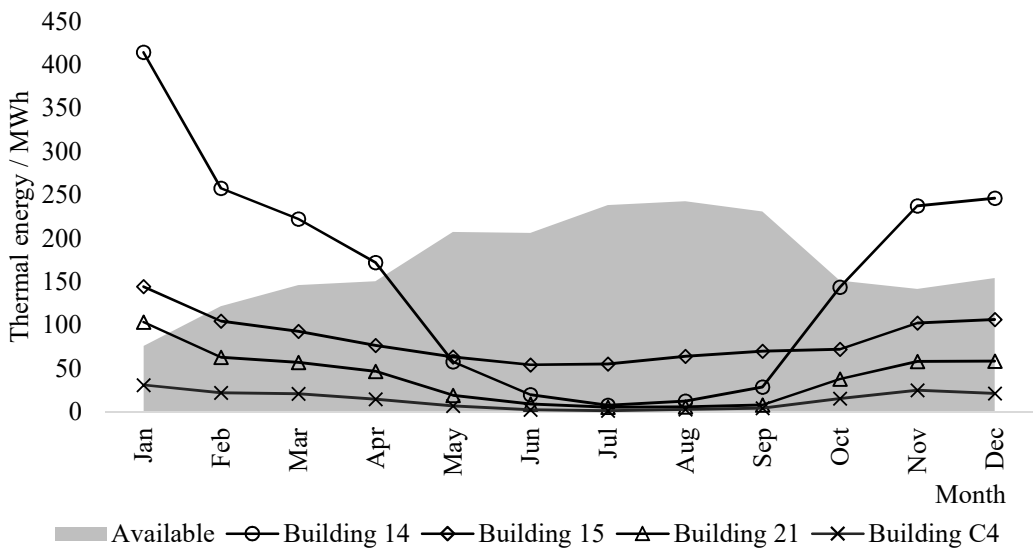
Figure 3.2: Available waste heat and monthly heating demands.

The heating demand shown in Figure 3.2 for Building 14 is only for non-operating hours of the furnace, since at other times it is already covered by the waste heat. The specific indoor air conditions of Building 15 require cooling to reach the desired relative humidity level and year-round heating to maintain the temperature. Hence, the building has a relatively high heating demand even in summer.

When looking at the monthly profile, it seems that there is plenty of heat available to cover the heating demands. However, the analysis of the daily profiles indicates the contrary. This is illustrated in Figure 3.3, which shows the profile of a typical winter day of Building 14. Waste heat covers 100 % of the demand during the day and a large amount of waste heat is still available afterwards. During the night, the heat is purchased from the DH company. The decrease in heating demand during the night is explained by the fact that ventilation flow rate is significantly lower at nights. The set point temperature remains the same for day and night.
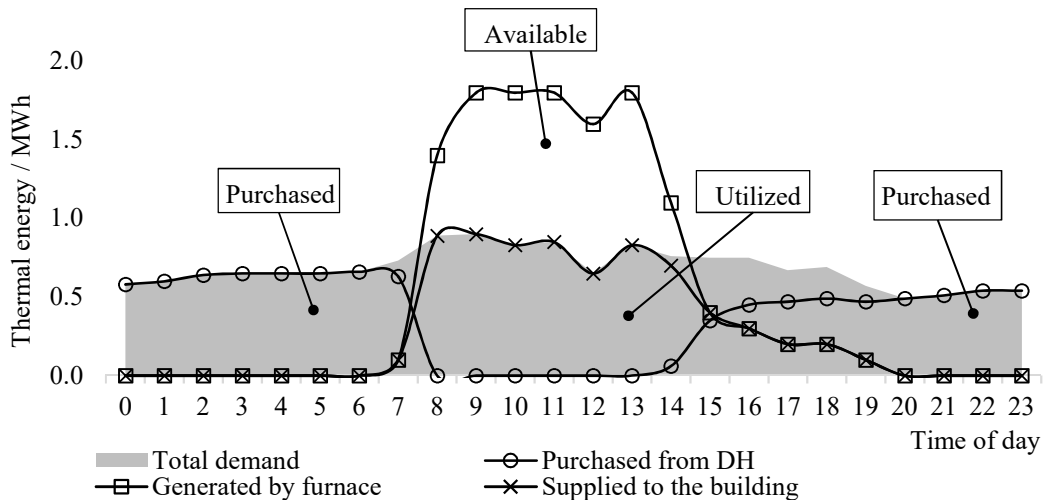
Figure 3.3: Purchased, available and used heat for Building 14 on December 15, 2016.

Table 3.2 shows the annual energy and peak power demands for Buildings 14, 15, 21 and C4. It can be noticed that despite the fact that heating demand of Building 14 is partially met by waste heat during the day, peak heating demands, which typically occur during the night when the furnace is not in operation, are still not reduced.

Table 3.2: Heating energies, specific heat used and peak demands for case study buildings.

	Area / m²	Annual heating purchased / MWh	Specific heat use / (kWh/m²)	Peak power / kW
Building 14 (DH only)	24,328	1,900	78	1,025
Building 15	6,561	1,090	166	303
Building 21	3,578	500	140	287
Building C4	793	179	225	125

At present, the district heating company charges no extra costs for covering the peak demands. However, for 2025 onwards a new contract will be negotiated, in which additional costs for covering peak demands may be imposed by the DH company.

3.2   Functional description of existing system

The schematic arrangement of the existing heating system with supply from the furnace and the DH network is shown in Figure 3.4. When the furnace is in operation, the heating demand of the Building 14 is totally covered by the waste heat generated from the furnace. The surplus heat is dumped to the DH network. On weekends and at nights, the heat is supplied to the Building 14 from the DH network by reversing the flow direction. Buildings 15, 21 and C4 are entirely heated by DH at present.
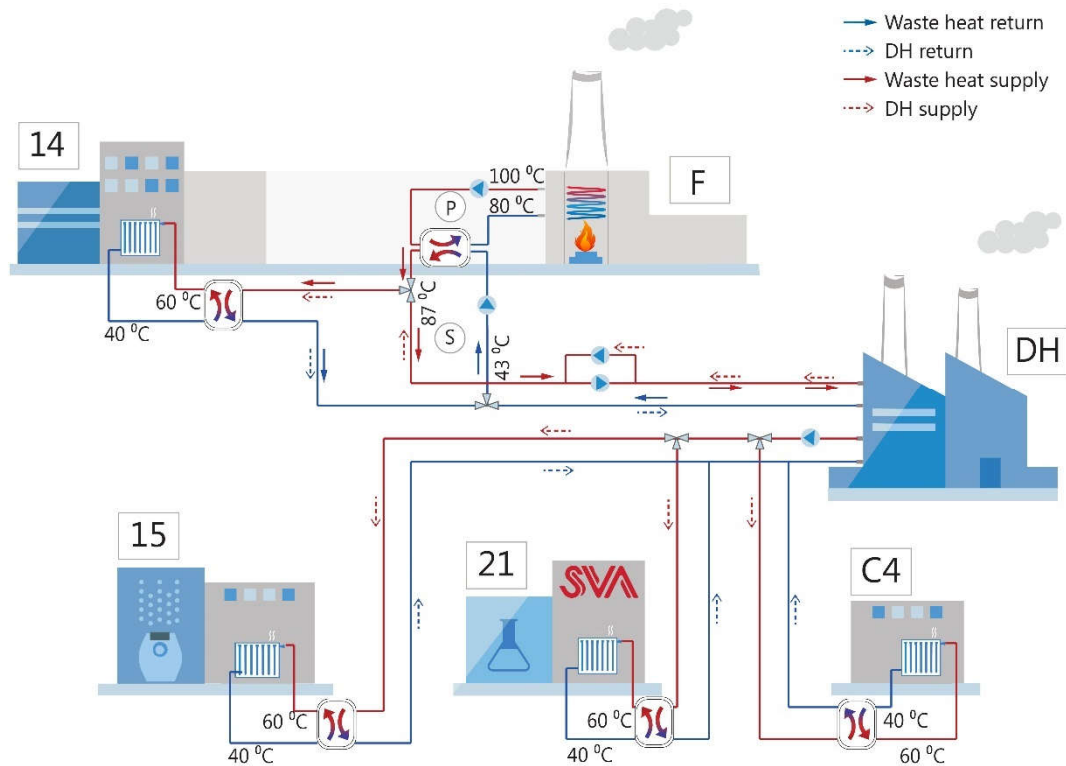
Figure 3.4: Schematic diagram of the existing heating system and connections between Furnace (F), Building 14, Building 15, Building 21, Building C4 and district heating (DH) network [4].

In Figure 3.4, the water on the primary side (*P*) is pressurized and is pumped at high temperatures to the HE. The temperature range varies, but on average, water is supplied at 100 ˚C and after passing the heat exchanger is cooled down to 80 ˚C. The secondary side (*S*) operates at mean temperatures of 43 ˚C and 87 ˚C as heat-exchanger entering and leaving temperatures, respectively. Because of high temperature and pressure on the primary side, special steel piping and auxiliary systems have been used (Figure 3.5 A). Building 14 is connected to the secondary side, which makes installation more feasible (Figure 3.5 B). The heat losses in the flat-plate heat exchanger used between primary and secondary side are on the scale of 2–3 %. Temperatures for supply and return systems for heat-exchanger entering and leaving temperatures to the buildings are considered to be 60 ˚C and 40 ˚C, respectively, as common for buildings of the same age group.

---

[4] The scheme has been simplified and should not be taken as the technical layout. This also applies to all other schematics presented in this thesis.
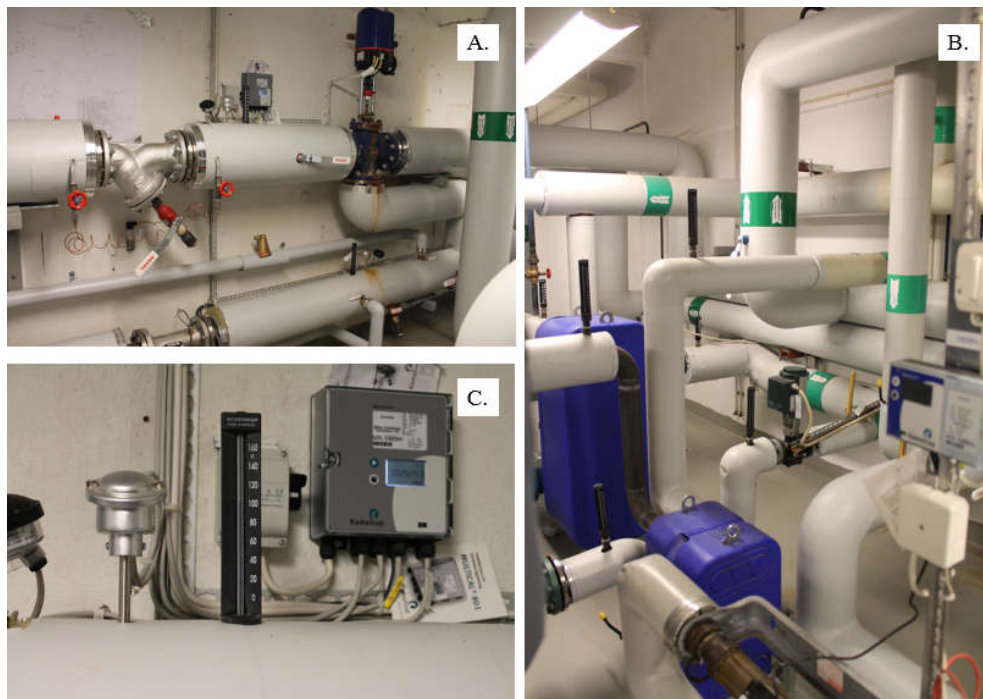
Figure 3.5: Technical room in Building 14 with A) primary side, B) secondary side, and C) auxiliary equipment for the heating system connection.

Technical connection of Building 14 and the furnace is shown as a flow-chart in Figure A1 (see Appendix A).

3.3 Design options

Four main design options considered and analysed in this thesis are summarized in Figure 3.6. The first design option was to consider a water tank for Building 14. As a second option, instantaneous use of waste heat (i.e. direct connection) with different order of connection for Buildings 15, 21 and C4 was investigated. The third option was to study various combinations of the direct connection and the water tank. Lastly, as the fourth option the combination of direct connection and a BTES system was studied.
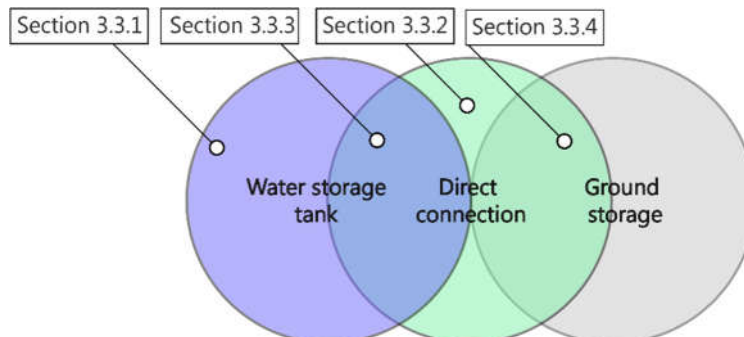

Figure 3.6: Approaches to waste heat utilization considered in this thesis.

3.3.1 Water tank

Since Building 14 already uses the waste heat during the day, the first study attempt was to minimize its dependence on the DH network. It is also the largest building considered in this project and has the highest heating demand too. This also means that the building offers a great potential for waste heat utilization. A hot water storage tank designed for the non-operating time of the furnace was considered for this purpose. This option is referred further in the thesis as *Option 1*.

Figure 3.7 shows the schematic diagram of this option. The tank has been designed to collect heat during the day and to provide the building with it after the furnace operating hours. This implies nearly nine hours of charging and 15 hours of discharging the tank. During the day, the excess heat from the furnace is supplied to Building 14. If the available heat is not enough, the rest is produced by district heating. On the other hand, if available heat is more than the heating demand of Building 14, then the excess heat is sent to the tank, where it is accumulated until the tank is fully charged to 87 ˚C. In case there is even more heat left, it is dumped to the district heating network. At night, the tank covers the heating demand of Building 14 and is discharged down to 43 ˚C. Sizing of the tank for weekend or other long duration periods was not considered because of significantly larger volume, space and investment requirements.
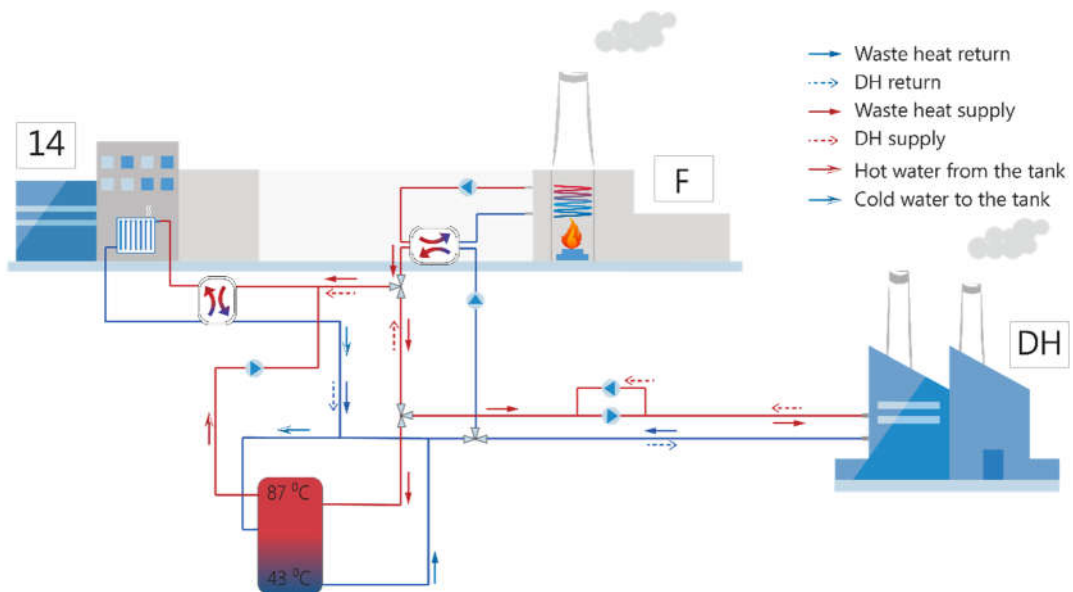
Figure 3.7: Schematic diagram of the heating system connection of Building 14, the furnace (F), district heating plant (DH) and the water tank for night storage.

3.3.1.1 Tank sizing

The volume of the tank was determined using Eq. 2, where ρ in kg/m³ is the water density, C_p in kJ/(kg·K) is the specific heat of water, ΔT in K is the temperature difference between hot and cold water and Q in kWh is the capacity of the storage.

$$V = \frac{Q \cdot 3600}{\rho \cdot C_p \cdot \Delta T} \qquad [V] = \text{m}^3 \qquad\qquad (2)$$

In the previous studies done by Helenius Ingenjörsbyrå (Mickelsson, 2016), the temperature difference (ΔT) was assumed to be 30 K. However, as was mentioned earlier in Section 3.2, a detailed analysis of the existing system showed that the average operating temperatures for supply and return on the secondary side are 87 ˚C and 43 ˚C, respectively. Thus, corresponding temperature difference of 44 K has been used for tank sizing calculations.

To assess the possibilities for storage and to determine the required tank capacity (Q), the profiles of available waste heat and heating demand of Building 14 have been analysed on a daily (24 hours) basis. Figure 3.8 shows corresponding profiles in the ascending order of the difference between the available waste heat and heating demand for each day of the furnace operation. The non-operating days of the furnace have been excluded from this analysis.
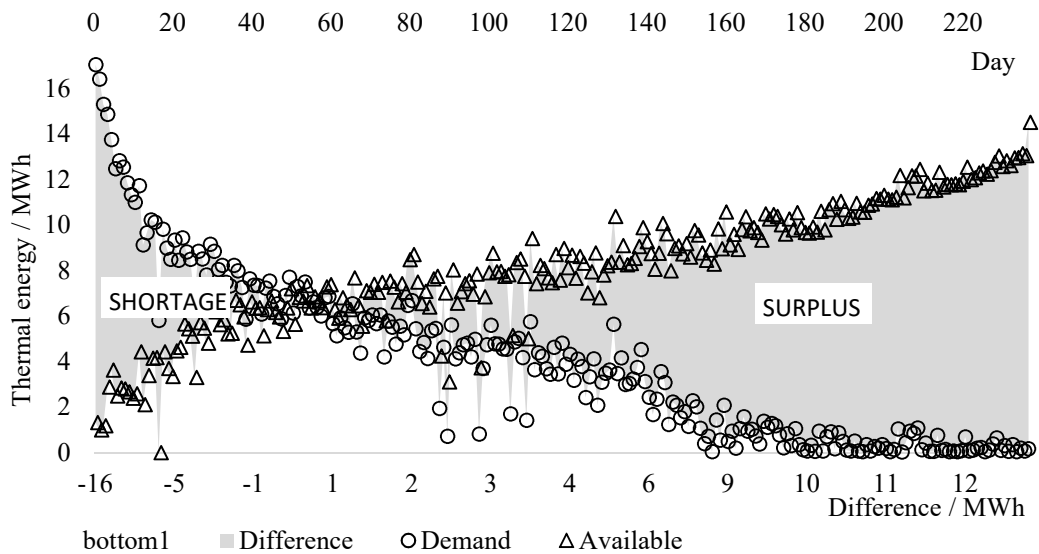

Figure 3.8: Difference in daily values of available waste heat and heating demands of Building 14 plotted in the ascending order (i.e. available minus demand). Only furnace operating days are considered.

As can be seen from Figure 3.8, there are nearly 50 days in a year when the amount of available waste heat during the day is less than the night demand. This shows the lack of capacity to cover the total demand even if all the available heat is stored (left side of the graph, i.e. shortage).

On the other hand, it is not reasonable to size the tank after the available capacity while there is no demand (right side of the graph, i.e. heat surplus). Consequently, the maximum storage capacity (Q) of the tank should correspond to the point when the difference between the available heat and the heating demand is close to zero. In this case zero difference lies at nearly 6.5 MWh.

Figure 3.9 illustrates the difference between available heat and the heating demand on the yearly time-frame. It can be observed that a constant energy deficit is present until the beginning of March. Closer look at this month reveals that starting from the second week onwards there is enough energy available to cover the entire demand (Figure 3.10).
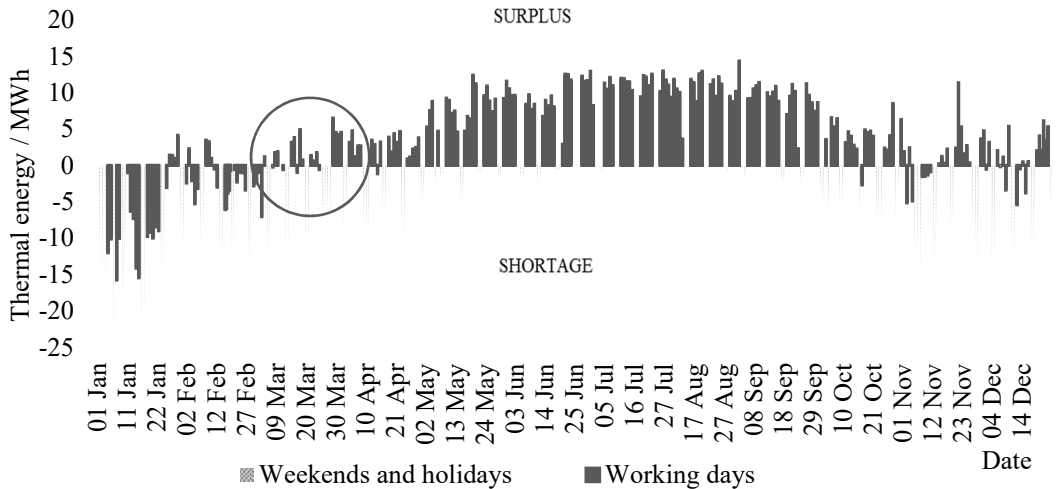

Figure 3.9: Difference between available heat and heating demand on a yearly time scale. The values for March, when the difference tends to become zero to positive, are circled.
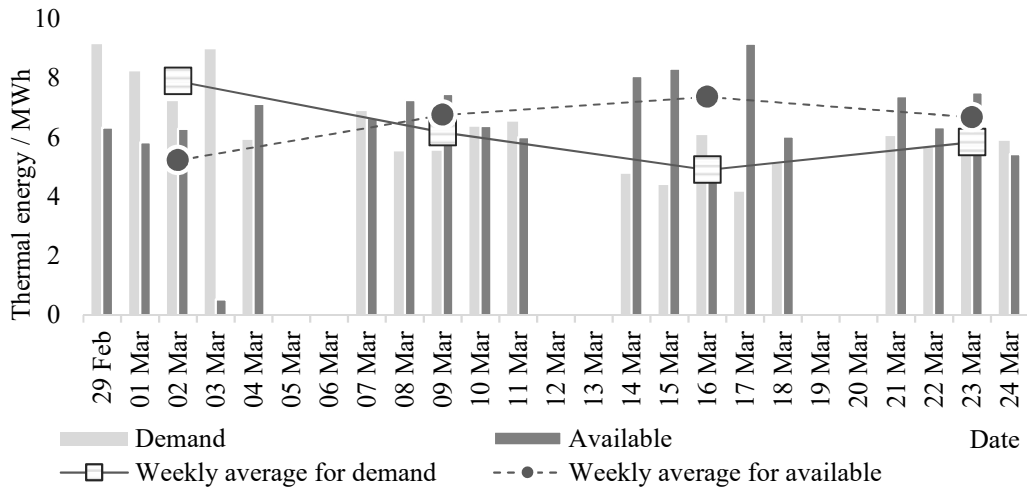
Figure 3.10: Daily values of the available waste heat and the heating demand for the month of March. Non-operating days of the furnace are excluded.

Thus, the maximum storage tank capacity is considered to be equal to the average load of the second week of March, i.e. around 6.5 MWh. This value also corresponds to the zero-difference calculation presented earlier in Figure 3.8. However, it should be noted that the optimal tank size determined based on LCC calculations may differ from the maximum size determined here.

3.3.1.2 Manual calculation

Having determined the maximum storage capacity of the tank (Q), the next step completed for Option 1 is to perform a manual calculation to estimate the tank storage output (i.e. thermal energy provided by the tank). The following approach has been used to determine the new demand (*ND*) of the building from the DH network. Daily sums of available energy (A_{daily}) and demand (D_{daily}) are retrieved from the hourly data. For any day:

if $A_{daily} \leq D_{daily} \leq Q$ then ND = 0;

if $D_{daily} \geq Q$ and $A_{daily} > D_{daily}$ then ND = A_{daily} - Q;

if $D_{daily} < Q$ and $A_{daily} \geq D_{daily}$ then ND = A_{daily} - D_{daily};

The approach describes an ideal situation when all the available heat is stored, and is used later to cover the demand. To account for dynamics in the system and heat losses from the tank, detailed simulations have been performed and are described in the next section. The results of the manual calculation are used as reference values to check the results of the simulation and performance of the mathematical modelling.

3.3.1.3 IDA ICE model

Simulations have been made using building energy simulation program IDA ICE (Advanced level), where user is able to create a specific plant configuration and custom algorithms in addition to the built-in configurations. In order to read the hourly heat generation profile in IDA ICE, the following procedure has been followed. The delivered power $q_{available}$, in both real life and IDA model, is represented by the water supplied at a certain mass flow rate $\dot{m}$ and at a certain temperature difference ΔT. Hence, the first step is to determine mass flow rate using Eq. 3, which has been implemented in the IDA model as shown in Figure 3.11.

$$\dot{m} = \frac{q_{available}}{\rho \cdot c_p \cdot \Delta T} \qquad [\,\dot{m}\,] = \text{kg/s} \qquad (3)$$
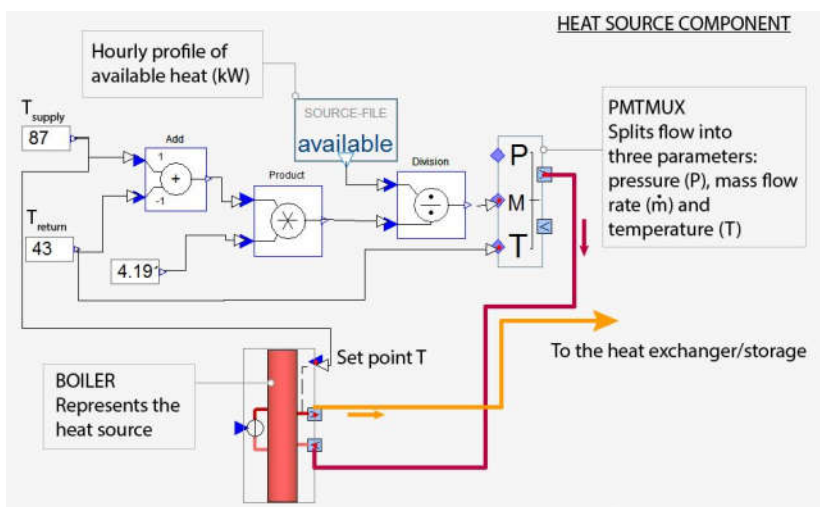

Figure 3.11: Modelling of heat source component in IDA ICE. The component converts the known available power (kW) to mass flow rate $\dot{m}$ (kg/s) at a fixed ΔT of 44K.

The calculated mass flow rate is first prescribed to M in the component PMTMUX with the lowest temperature fixed to 43 ˚C. The water is then sent to a boiler which heats it up to the set point of 87 ˚C. The temperatures are assumed to be constant over the year. From the boiler, mass flow rate is sent further to the storage or to the building connected through the heat exchanger. As a result, energy in kWh delivered by the boiler reflects corresponding profile of the available waste heat.

The same is repeated for the demand side using the heating demand profile (Figure 3.12). The only difference is that the chiller component works as a heat sink, and cools down the water from 60 ˚C to the prescribed leaving temperature of 40 ˚C.

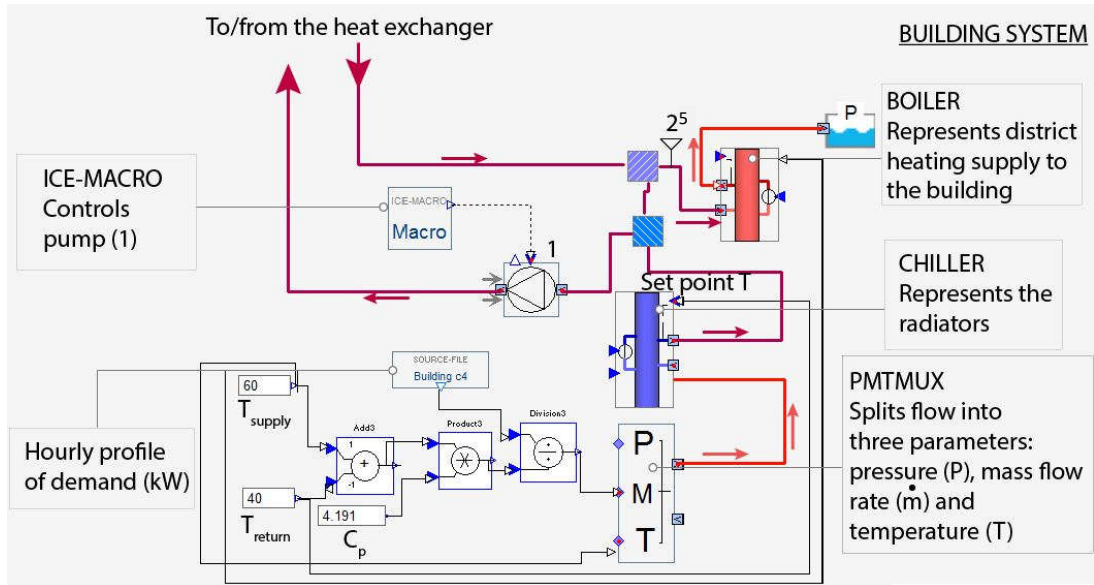*Figure 3.12: Building system component modelled in IDA[5]. Component converts known heating demand (kW) to mass flow rate ṁ for the given temperature difference ΔT.*

Nominal mass flow rate of *Pump 1* can be calculated using the same equation (i.e. Eq. 3), with $q_{available}$ being the peak power in the demand profile. Nominal mass flow rate is set to 12 kg/s. In order to avoid errors, the mass flow rate of the pump in each time step should be equal to the mass flow from the chiller. Another issue is that due to high temperature water on the furnace side of the HE, the building side of the HE may get overheated. Both these issues can be resolved by using a Proportional Integral (PI) control mechanism in the control Macro of *Pump 1* (Figure 3.13).

---

[5] The sensor (2) is not a component in IDA and is shown to illustrate the point in the scheme where the process variable is taken from PI controller iterations.
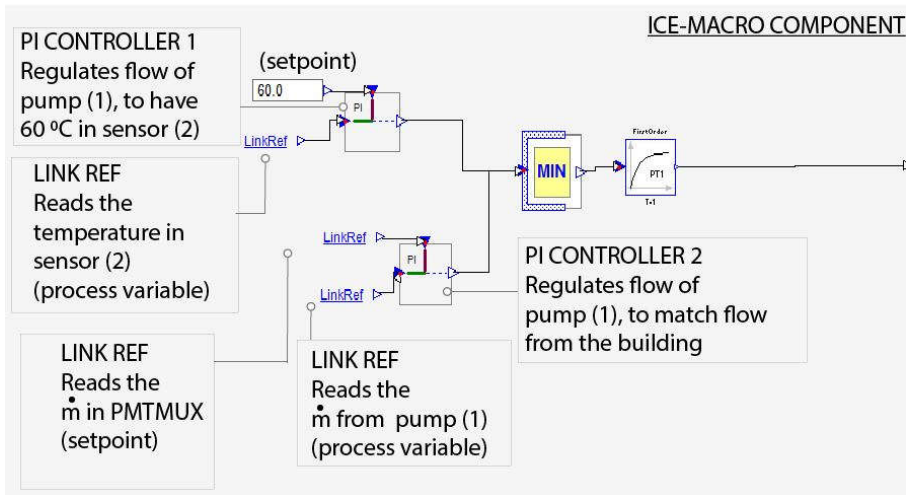
Figure 3.13: Details of Macro component. To be considered together with Figure 3.12.

The PI control is a variation of Proportional Integral Derivative (PID) control. The latter represents a feedback control system that is a real physical controller and is widely used in different applications, such as control for valves, dampers, heating elements. For each time step, it calculates the error between the desired set point and the actual measured process variable. If the error is zero and the set point is equal to process variable, then the output from the controller is zero. In case of a disparity, small adjustments are applied to bring the process variable closer to the set point. The process is repeated until there is no error (Peacock, 2016). The PID control process is also shown in Figure 3.14.
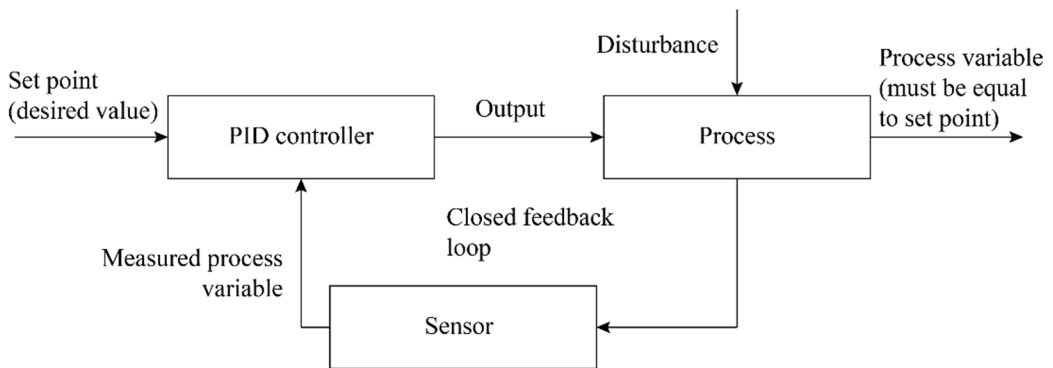
Figure 3.14: The PID control process explained through a block-diagram.[6]

The PID control mechanism includes three coefficients: proportional, integral and derivative, denoted as *P*, *I* and *D*, respectively. The name of the control type is also defined by them. The coefficient *P* is responsible for present error value. The coefficient *I* accounts also for errors in the past and is able to track the error over time by integrating it. the coefficient *D* predicts

---

[6] Figure adapted from Peacock (2016).

the future trend by analysing the change of the error over time if the present signal is too weak (Peacock, 2016).

In Figure 3.12 the PI controller inside the Macro component compares the difference between the set point temperature that is desired at *Point 2* with the process variable, i.e. actual temperature at *Point 2,* and calculates the error. The desired temperature is achieved by changing the mass flow rate $\dot{m}$.

The approximation steps taken by a PID controller are shown in Figure 3.15. Once the PI controller detects an error, it alters the process variable $\dot{m}$ to adjust it to the set point value. However, it inevitably overshoots the needed value to *Point A*. Then, it measures again, and decreases the process variable to return to the set point. However, a lower value, i.e. *Point B,* is achieved. The process can be repeated several times until the closest possible value to set point is reached (*Point C*). In each case an insignificant steady-state error is present.
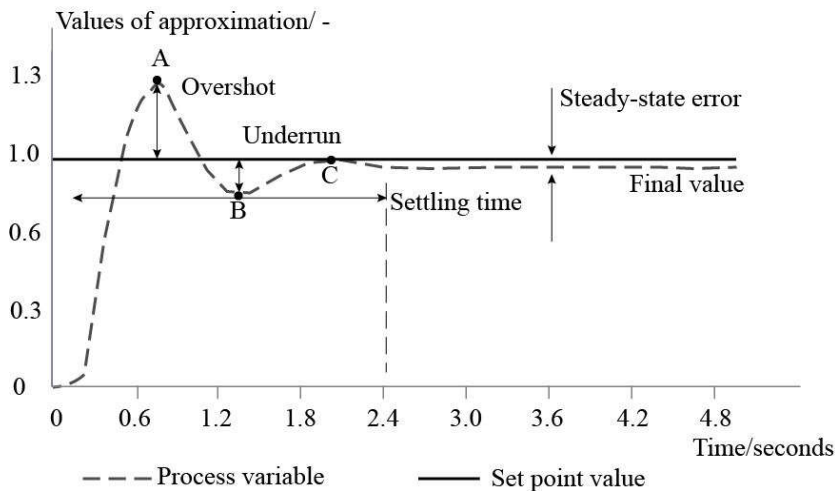

Figure 3.15: Process of approximation steps taken by a PI controller in a feedback loop.[7]

In regards to Figure 3.12, if the temperature at *Point 2* is higher than the required value of 60 ˚C, the pump speed is altered to reduce the mass flow rate $\dot{m}$ through the HE in order to minimize the error. A similar pump control mechanism would be applied when the system is designed in reality. If there is not enough heat available from the furnace to have 60 ˚C at *Point 2*, the PI controller still works to provide the maximum nearest value that is available by operating the pump at its full capacity. This is where the second PI controller in the Macro component comes in play to control the flow as shown in Figure 3.13.

The boiler shown in Figure 3.12 represents the district heating connection and adds the deficient heat (if any). The *COPs* of all boilers and chillers components are set to 1, to directly

---

[7] Figure is adapted from National instruments (2016).

incorporate the measured profiles of available heat and heating demands. The control signals for all boilers and chillers components are also set to 1, to maintain a constant operation. The complete IDA ICE model is shown in Figure 3.16.
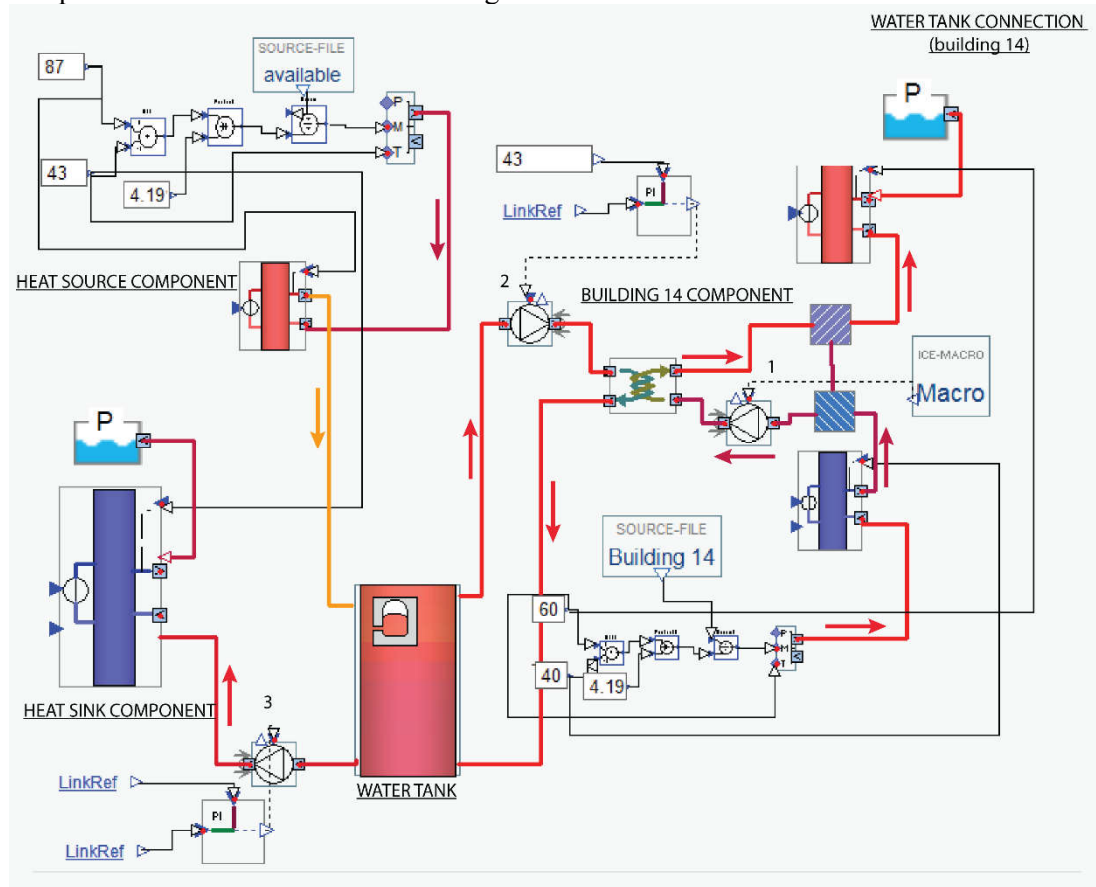

Figure 3.16: Plant model in IDA ICE showing the connection between furnace and Building 14 using the storage tank.

Hot water at 87 ˚C is taken from the furnace to the tank. *Pump 2* sends hot water from the tank to the HE, facilitating the heat exchange between the tank and the building component. *Pump 3* sends the chilled water from the tank to the heat sink component represented by the chiller. The chiller has a set point of 43 ˚C. If the water from the tank is higher than that temperature, the chiller cools it down to the set point. Thus, the amount of thermal energy provided by the chiller indicates the amount of thermal energy that is not utilized and dumped to the DH network.

Heat transfer for the heat exchanger at rating is set to 1 MW, which is the peak demand of Building 14. *Pump 2* is controlled by another PI controller and stops operating when the temperature in the bottom layer of the tank reaches 43 ˚C. *Pump 3* maintains the same mass flow rate that comes to the tank from the furnace.

There are several models of water tanks available in IDA ICE. In this study, the model for *Water tank with stratification* (*TANKSTRAT*) has been used. It allows the user to specify the

number of layers in the tank to account for the stratification phenomenon, thus providing more accurate results.

The volume of the tank in the IDA ICE model is specified by its radius and height of each layer. According to the information obtained by Helenius Ingenjörsbyrå from one Swedish manufacturer of large-sized storage tanks, a 150 m³ tank has a radius of 1.9 m and a height of 13 m. Changes in the tank volume are provided by varying the tank height. Therefore, for all simulations, radius of the tank is kept fixed at 1.9 m, while the height is altered to get the desired volume. Number of tank layers is also kept fixed in all the considered cases.

First, the U-value of the tank is set to zero to eliminate thermal losses and make a comparison with the spreadsheet calculations. In the following calculations, the U-value equals to 0.075 W/(m²·K), which corresponds to 400 mm of insulation (according to the manufacturer).

It should be mentioned that the model does not entirely represent the actual process. The part of the system concerning the instantaneous heating of the building by waste heat during the furnace operation time is not included. It is, however, not relevant since the demand profile already accounts for that. Additionally, *Pump 3* is only required for running the model and is not considered as a part of the real system.

3.3.1.4   Tank connections and results processing

Another important setting for the tank is the location of its inlets and outlets. A parametric study has been carried out to determine the optimum connection heights. It is mainly focused on the heights of the two inlets – hot water supply to the tank and cold water return to the tank, shown in Figure 3.17 and denoted as *Zin1* and *Zin2,* respectively. Various combinations have been studied and the amount of energy delivered to the building (tank output) has been used as a criterion for the comparison. Various tank volumes (heights) are analysed to identify the common behaviour in relation to the tank height (H_{tank}). Overall, a range of tank volumes from 80 m³ to 180 m³ have been studied (with only height being adjusted). The starting point is the connection *Zin1* at the very top of the tank (*Zin1* = H_{tank} - 0.1 m) and *Zin2* at the very bottom (*Zin2* = 0.1 m).

Figure 3.17: Tank inlets and outlets.
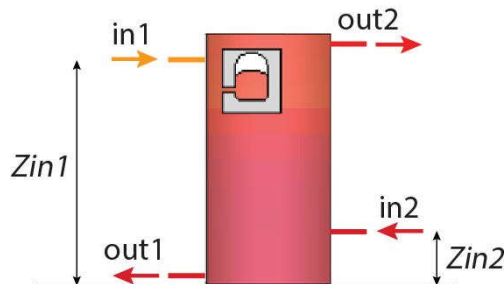
Besides the tank output, the efficiency of the tank is also calculated for each option to analyse the losses. It is defined as ratio of the energy extracted from the tank to the energy delivered to the tank. After defining the optimal positions of the inlets for each particular tank size, the results are used in the LCC analysis to find out the most economically feasible size.

3.3.1.5 Costs

Based on the information obtained by Helenius Ingenjörsbyrå during the preliminary studies, the price of the tank has been derived per cubic meter of the volume. The price has been estimated to be 1,400 SEK/m^3. Even though it is a rather simple way to estimate the tank price, it allows to make quick price estimations for various options. Additional system components and auxiliary equipment, including piping, pump, heat exchanger, valves, etc are also accounted for. Table 3.3 below provides the costs of these components as considered in this work. More details are provided in the following text.

Table 3.3: Material, installation and operating costs of the additional equipment for the storage tank option.

Pump / SEK	Pump operation / (SEK/year)	Piping / SEK	Heat exchanger / SEK	Other / SEK
92,950	3,290	520,000	155,160	60,000

The pump sizing is performed using an online tool from Grundfos (2017). The nominal flow rate is calculated in the same manner as described in Section 3.3.1.3 using Eq. 3. Pressure drop for piping is considered to be 100 Pa/m and the distance from the technical room to the tank is estimated to be 100 m. Piping costs are estimated according to Uponor pricelists (Uponor, 2017). In addition, Sektionsfakta database for cost estimation from Wikells (2017) has been used for estimating heat exchanger prices and all craftsmanship costs.

3.3.2 Direct use of waste heat

The direct use of waste heat is the second design option considered in this study. It is a simple and practical way to utilize the available waste heat and requires relatively low investment costs. Another benefit is that there are no issues related to storage. This design case is referred to as *Option 2* further in the text.

Figure 3.18 shows the operation principle of the direct connection. The amount of heat delivered is controlled by the mass flow rate. Once the heat reaches valve *1*, the control system determines the amount of heat required by Building 14, and divides the flow accordingly. The remaining heat is sent further down to valve *2*, where the heat needed for Building 15 is taken. The remaining heat is sent further to remaining buildings. The same process is repeated again, in valves *3* and *4*. In case there is surplus heat remaining after covering heating demands of all four buildings, it is dumped to the DH network. When the opposite happens, i.e. there is a heat shortage, the pump is reversed, and the heat is added from the DH network instead.
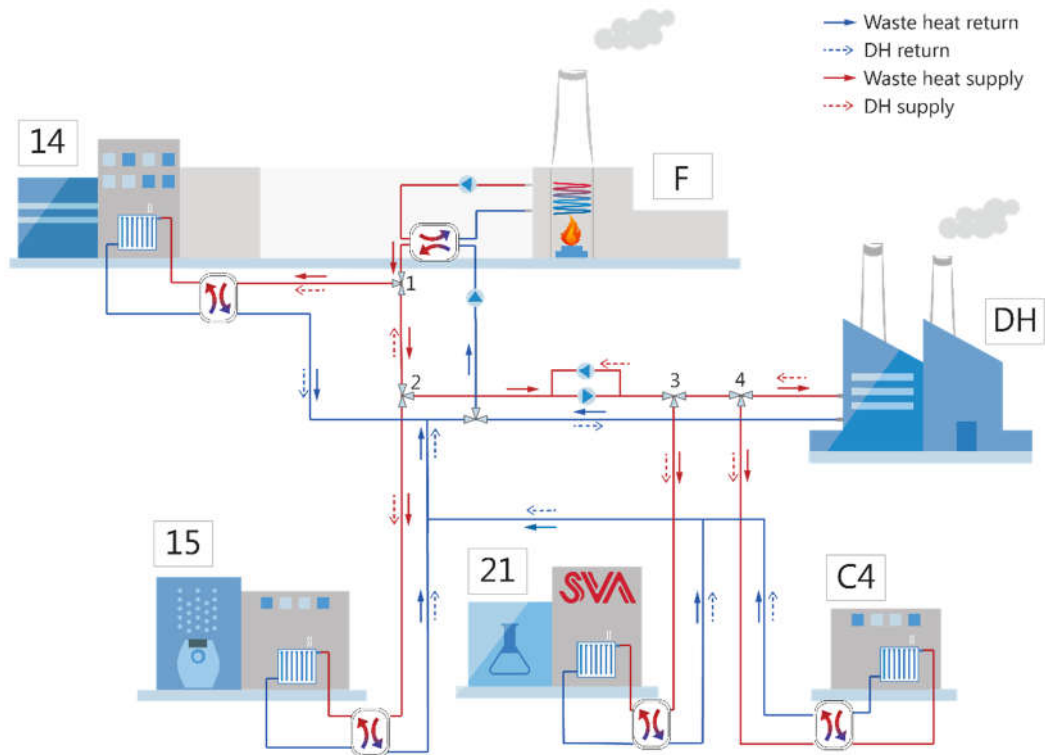
Figure 3.18: Schematic diagram of the heating system connection of Buildings 14, 15, 21 and C4 with the furnace (F) and DH network for instantaneous supply of heat.

3.3.2.1   Order of connecting buildings

It is not possible with the instantaneous connection to address the mismatch between the available waste heat and the heating demands of the buildings. Hence, the design should incorporate sending all the available waste heat to the buildings and to consume the maximum possible amount of heat.

The criterion used for selecting the appropriate order to connect buildings to the available waste heat depends on the potential of the building to cover the maximum demand (Figure 3.2 and Table 3.2) and the distance of the building from the heat source (Figure 3.19)[8]. The first criterion characterizes possible savings, whereas the second criterion affects the investment costs.

---

[8] The order of connection means that all the available heat is sent to the building connected first. If there is any heat left after meeting the heating demand of the first building, it is sent to the building connected second and so on.
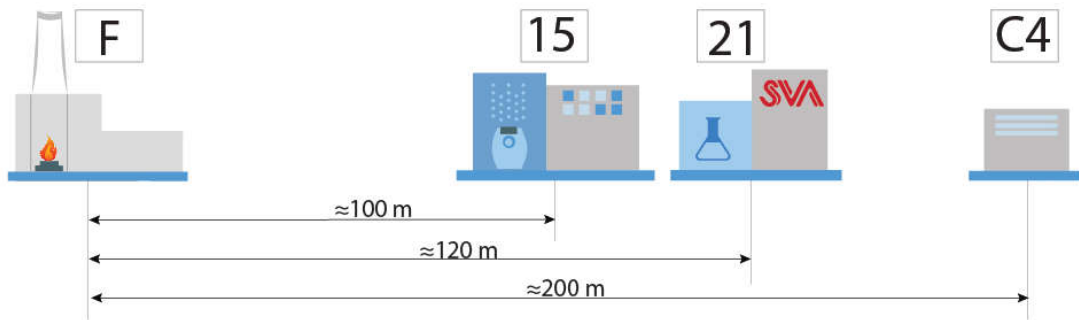
Figure 3.19: Piping distance from the furnace (F) to the technical room in Buildings 15, 21 and C4.

The criterion for maximum covered demand is relatively easy to evaluate since it solely depends on the heating demand and the available heat at the same time step. The evaluation of the criterion for the distance from the furnace is more complicated and is influenced by required piping length, size of the pump and electricity for its operation. A heat loss of 10 W/m from the pipe is taken into consideration for manual calculations. The size of the pump is determined based on the mass flow rate needed to cover the maximum peak demand and the pressure drop. The heat exchanger size is also chosen to cover the peak value.

It was decided that the best option for the connection should provide the highest savings-to-investment ratio (*SIR*). This ratio represents the present value savings to the present value costs (Short et al., 1995). This implies that the building with the highest covered demand and the shortest distance to the furnace should be connected first and so on. Since the total available waste heat is limited and its availability changes depending on building's connection order, the following set of procedure has been used for determining the optimal connection order.

The strategy is depicted in Figure 3.20. Prior to connecting the buildings in a series connection, the *SIR* for each building has been studied independently. This calculation makes it clear which building can bring the maximum savings if connected first. Thus, Building "*i*" with the maximum *SIR* is connected first; it is denoted as *max SIR$_i$* building in the figure. In the second step, the *SIR* is recalculated again for each of the buildings. The resulting Building "*j*" with the highest recalculated *SIR* is connected second (*max SIR$_j$* building). The procedure is repeated *n* times until the last building is connected (*n* is a number of buildings considered for connection).
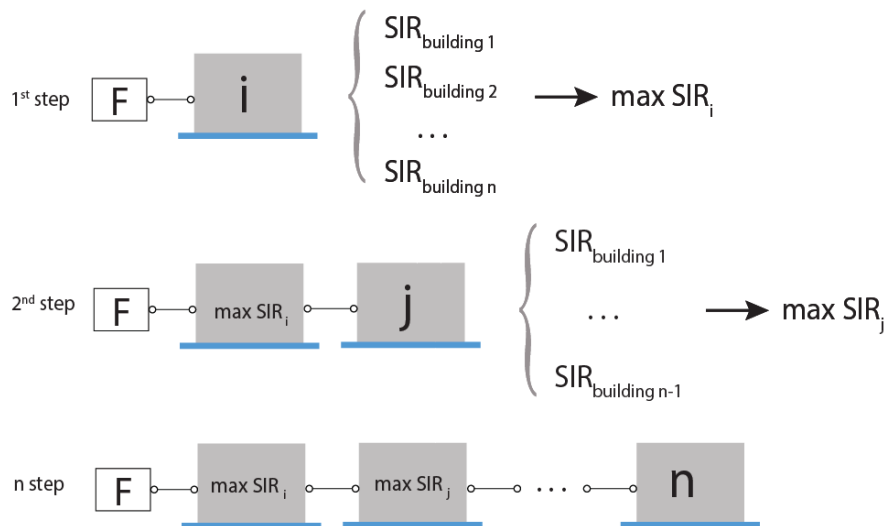
Figure 3.20: Procedure used for choosing the connection order.

3.3.2.2 Calculations

The manual calculations for the direct connection has been performed in Excel using the existing hourly profiles of available and needed heat. The savings associated with the coverage of building heating demands by the waste heat have been calculated. The building heating demands not covered by the furnace are covered through the purchased energy from DH network. On the contrary, the surplus heat that could not be utilized is dumped to the DH network free of charge.

The procedure discussed in Figure 3.20 has also been supplemented by IDA ICE simulations. A detailed explanation of the main components used in the plant has already been provided in Section 3.3.1.3. An example of two buildings connected in series is provided in Figure 3.21. Firstly, the available heat from the furnace is supplied through the heat exchanger to the Building 15. Next, the surplus heat is sent to the second heat exchanger, where the required heat for Building 21 is extracted. The remaining is sent to the heat sink.
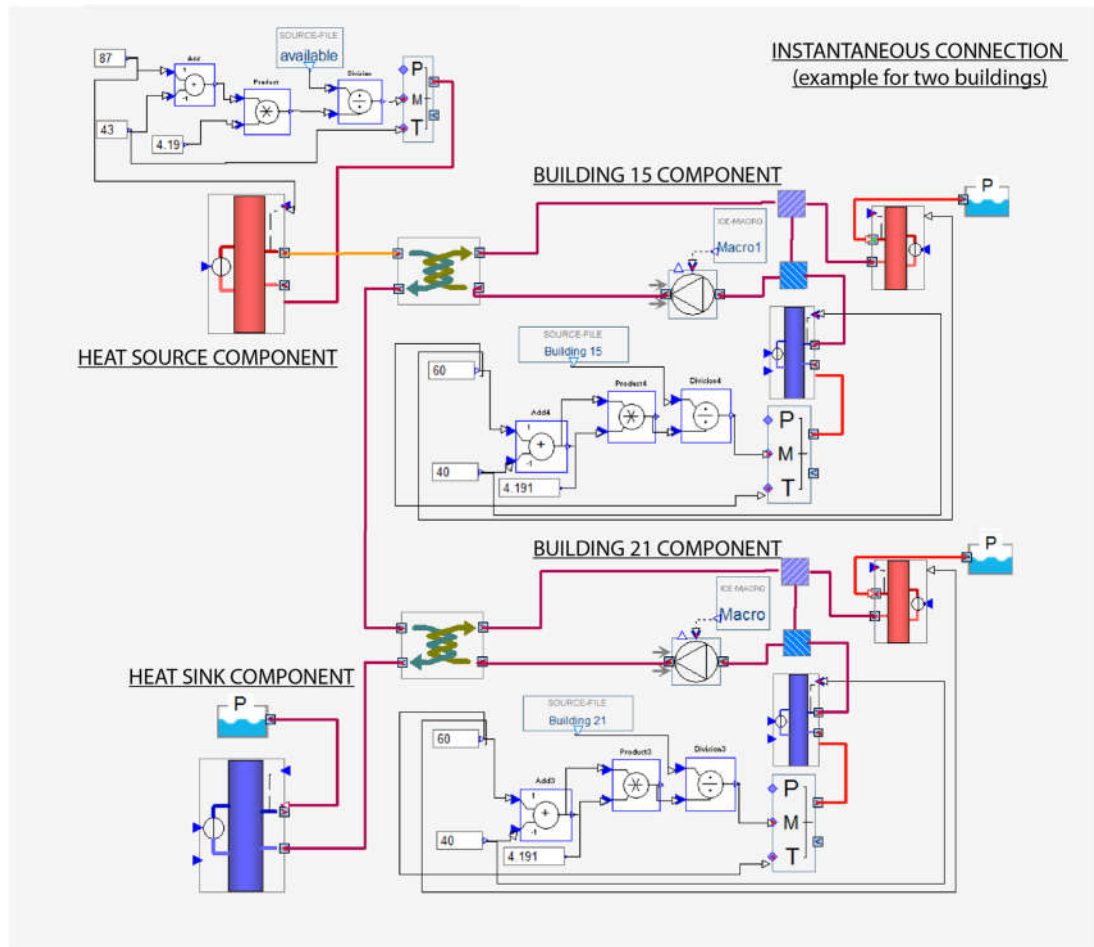
Figure 3.21: Modelling of direct connection in IDA ICE.

3.3.2.3   Sensitivity analysis of the piping distance
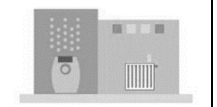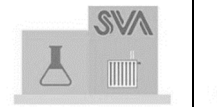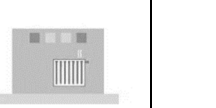
In addition to analysing the *SIR* for buildings at initially estimated distances from the heat source (Figure 3.19), a sensitivity analysis has also been performed to determine the maximum allowable piping lengths at which the *SIR* is still positive. The opposite illustrates the situation when installation and operation costs for pumping exceed savings that are achieved if the purchased district heating energy is replaced with the waste heat. The distances are increased gradually for all three buildings starting from 100 m from the source and finishing with 2 km.

3.3.3   Combination of direct use and storage tank

The strategy behind combining the direct connection and the storage tank implies that the buildings are supplied with the waste heat directly during the furnace operating hours and if any surplus heat is left, it is used to charge the tank to cover the heating demands of buildings during non-operating hours of the furnace. For this third design alternative, denoted as

Option 3, four different combinations have been considered. The details of these options are provided in Table 3.4 below.

Table 3.4: Different options considered for using the direct connection and the storage tank.

		Building 14	Building 15	Building 21	Building C4
Option 3a	Direct	n/a[9]	✔	-	-
	Tank	✔	-	-	-
Option 3b	Direct	n/a	✔	-	-
	Tank	✔	✔	-	-
Option 3c	Direct	n/a	✔	✔	✔
	Tank	✔	-	-	-
Option 3d	Direct	n/a	✔	✔	✔
	Tank	✔	✔	-	-

Option 3a is to connect Building 15 directly and to store the surplus heat in the storage tank to supply Building 14 afterwards (Figure B1, Appendix B). *Option 3b* is to use a larger tank to supply the stored surplus heat to both Building 14 and 15 as is illustrated in Figure 3.22. *Option 3c* is to supply waste heat directly to Buildings 15, 21 and C4, and to have a storage tank for Building 14 only (Figure B2, Appendix B). *Option 3d* is similar to *Option 3c* with tank sized for both Building 14 and 15. It can be noticed that for all options considered in Table 3.4, the tank is always designed for buildings with largest demands and shortest distances from the furnace.

---

[9] Building 14 is currently heated by the waste heat during the day.
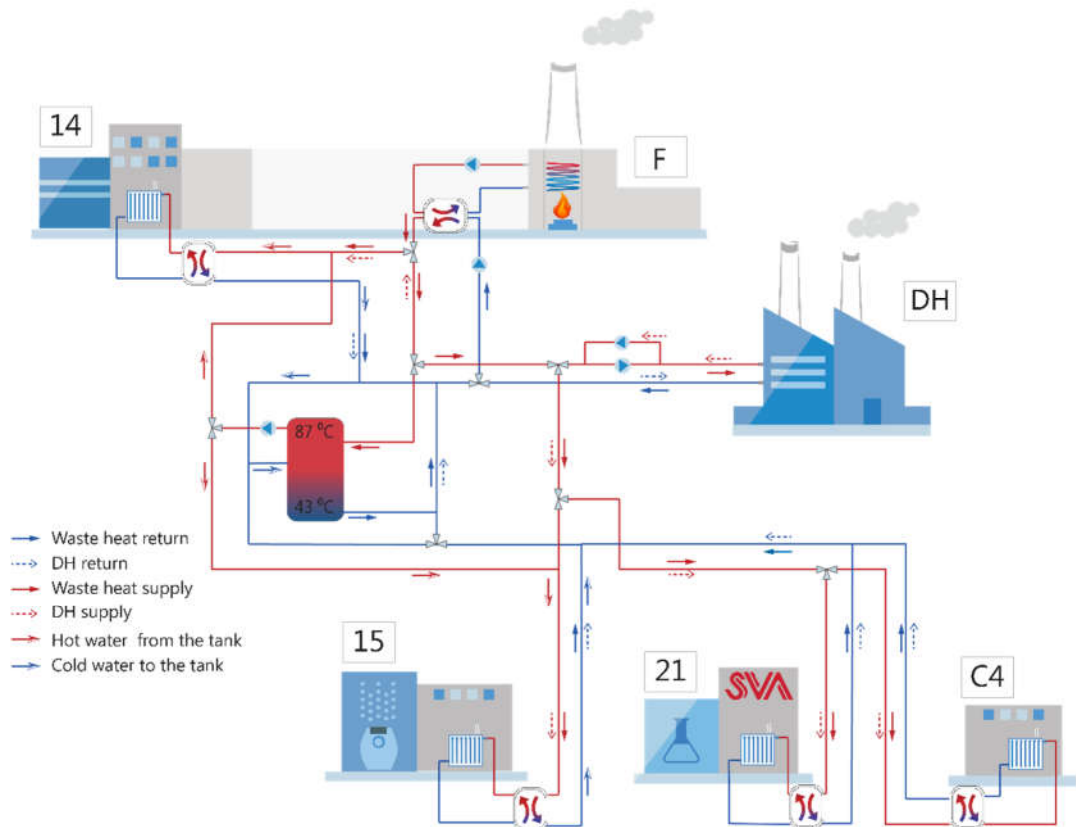
Figure 3.22: Schematic diagram showing direct connection for Building 15 and storage tank for Buildings 14 and 15 for Option 3b.

When sizing the tank for the options provided in Table 3.4, new heating demands and available waste heat profiles are analysed for each case. The maximum possible size of the tank is chosen following the same procedure explained earlier in Section 3.3.1.1.

An IDA ICE model has been created for each option with corresponding heating demand and available waste heat profiles. Figure 3.23 shows an example of the IDA ICE model developed for *Option 3b*. First, the waste heat is directly supplied to Building 15 from the *heat source component*. In case any surplus heat is left, it is sent for storage to the tank. If the tank is fully charged and the heat is still available, it is dumped to the *heat sink component*. The heat stored in the tank is supplied to Buildings 14 and 15. When the furnace and the tank cannot meet the heating load, the DH network provides the excess demand.
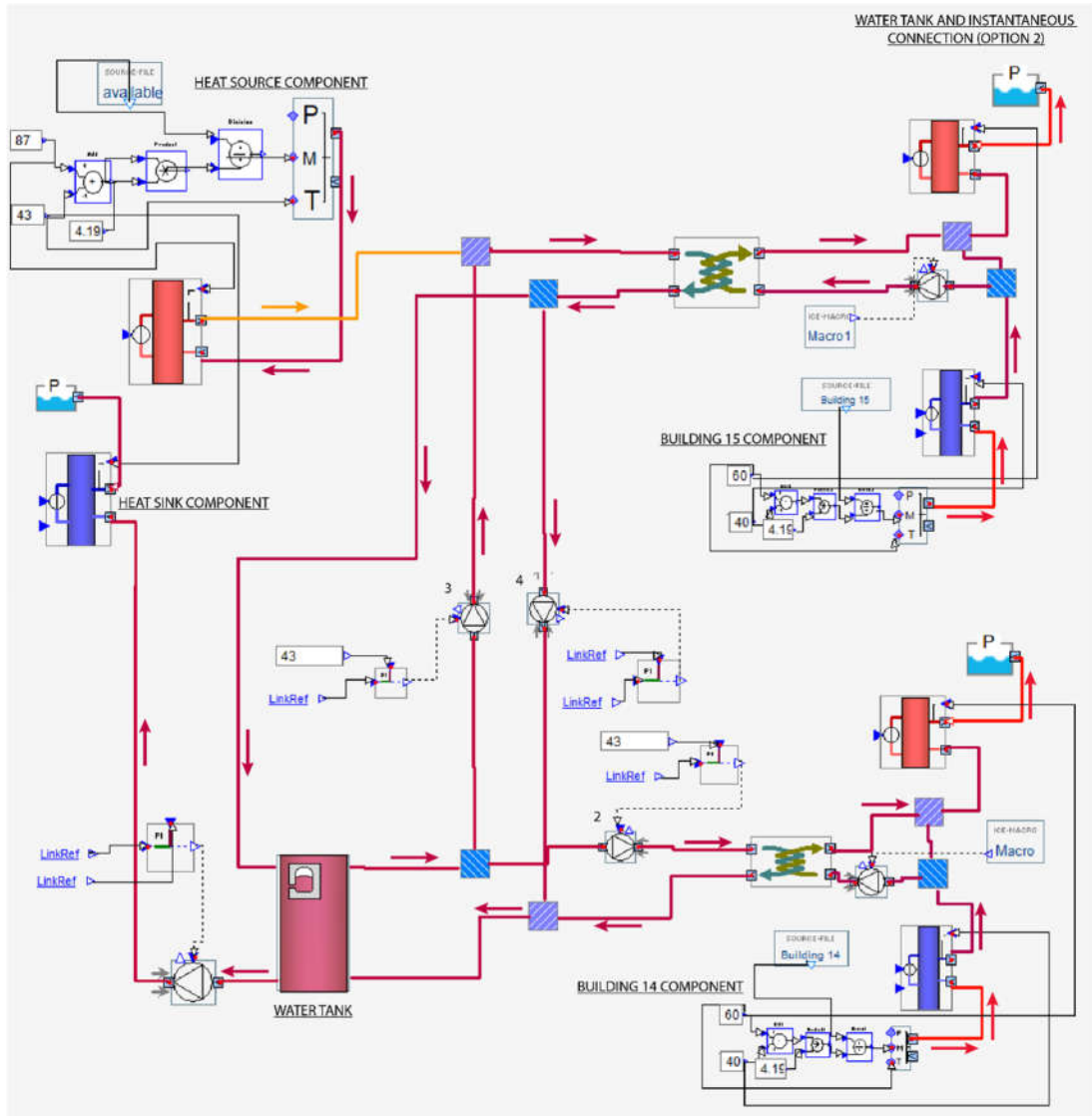
Figure 3.23: IDA ICE modelling of Option 3b with direct supply to Building 15 and storage tank for Buildings 14 and 15.

The control strategy for *Pump 3* is similar to that of *Pump 2* (see Section 3.3.1.3). It supplies water from the tank to Building 15 as long as the temperature in the lower layer of the tank is above 43 ºC. *Pump 3* has a nominal flow rate of 2.4 kg/s which is required to meet the peak load of Building 15. *Pump 4* is controlled to have the same mass flow rate as *Pump 3* to ensure that the same volume is returning to the tank.

Costs are estimated in the same way as described in Sections 3.3.1 and 3.3.2 for *Option 1* and *Option 2*, respectively.

3.3.4 Thermal energy storage using boreholes

Another possibility of storing waste heat is by using a borehole thermal energy storage (BTES) system with vertical loops. In a BTES system, ground is used as a thermal battery to store heat to be extracted afterwards (Javed et al., 2009). As a first step, the BTES system is used together with a ground-source heat pump to cover entire heating demands of the four buildings considered in this work. The storage is designed to be charged only after heating of all four buildings instantaneously. This design option is referred to as *Option 4a* from here onwards. Figure 3.24 provides the schematic diagram of this design option in charging mode.
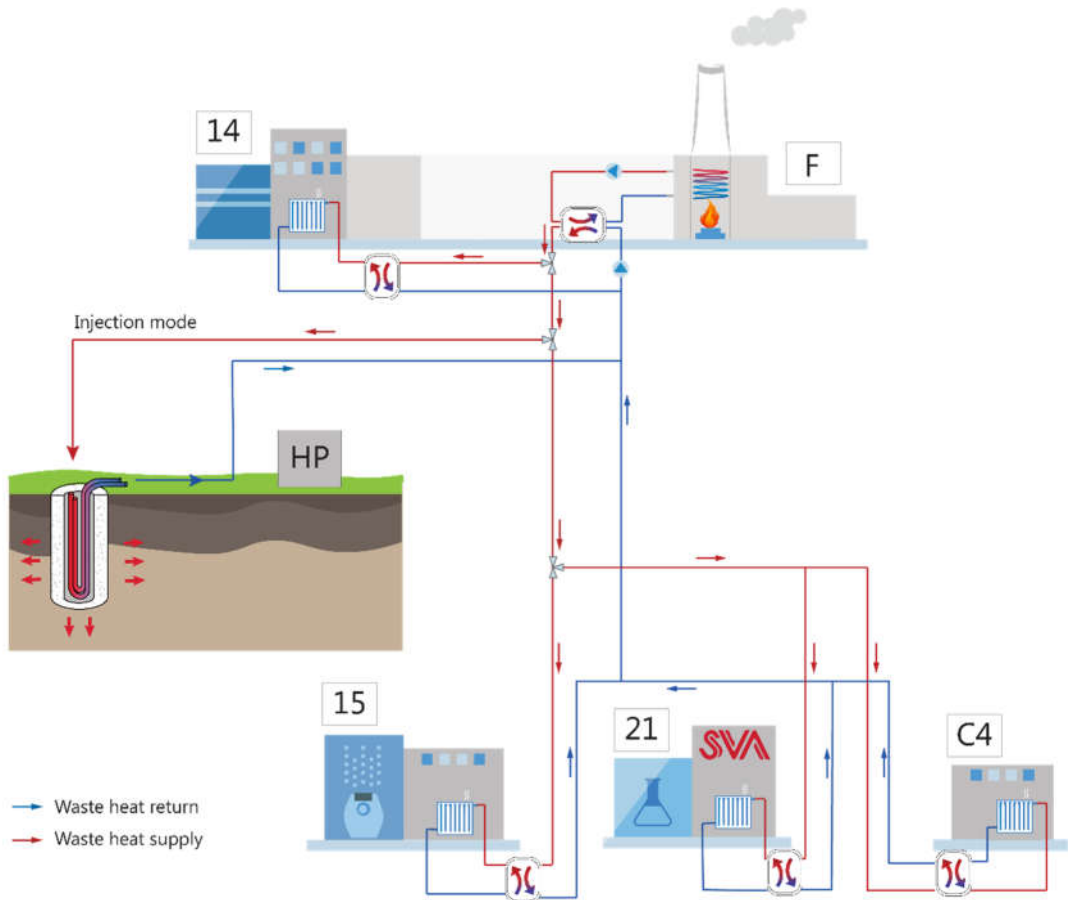
Figure 3.24: Schematic diagram of the BTES system in charging mode after heating of all buildings instantaneously.

Most of the BTES charging occurs during summer months. The discharging primarily occurs during night times in winter season, when there is no waste heat supply from the furnace (Figure 3.25). When discharging, the stored heat is extracted from the BTES system and is directed to the heat pump. The heat pump uses electricity to produce hot water at 60 ºC and supplies it to all four buildings. The BTES system is also discharged during the furnace operating time if the instantaneous heating is not enough for all buildings.
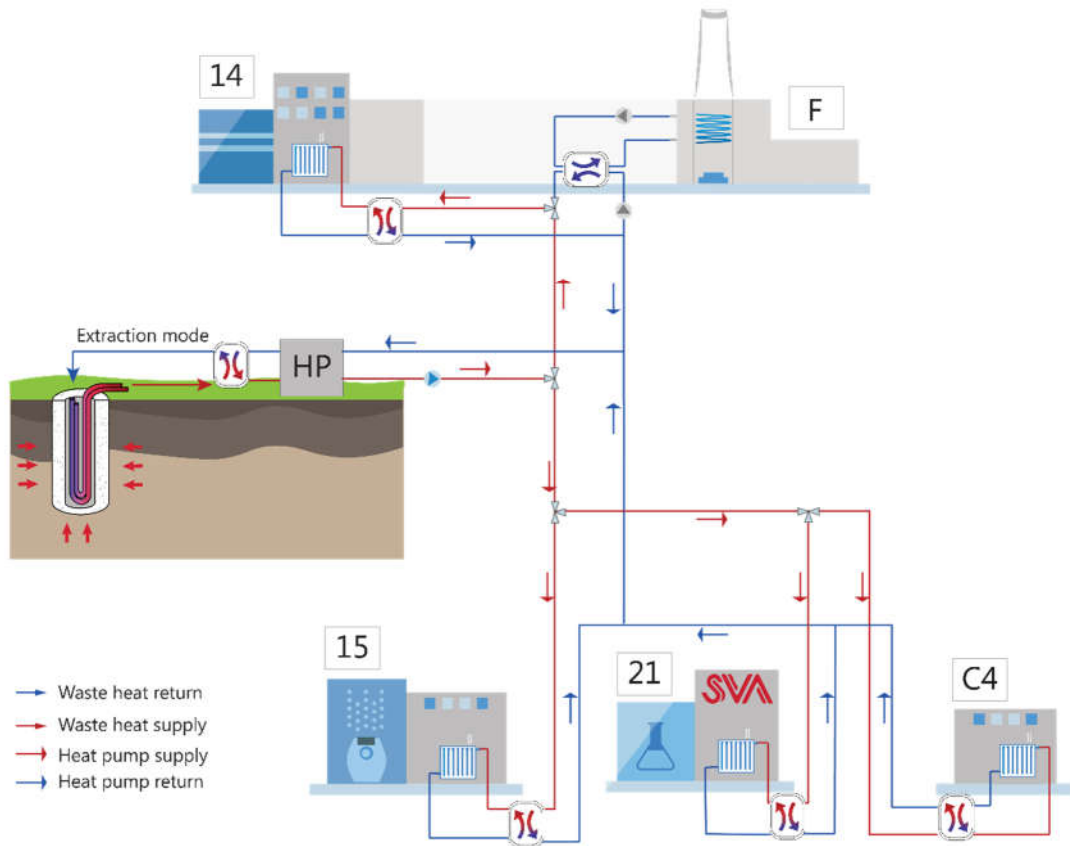
Figure 3.25: Schematic diagram of BTES system in discharging mode during furnace non-operating time.

To achieve a lower initial cost, several options for borehole system design are assessed in terms of the number of buildings connected to the heat pump. The considered options include cases providing heating to Building 15 only, and to Buildings 15 and 21 together. Various charging strategies, e.g. charging BTES for one and three years without any discharging, are also analysed. In this context, the optimal case, referred to as *Option 4b*, is found and compared to the large system of *Option 4a*.

3.3.4.1   Simulations

The BTES-GSHP system is modelled following the procedure below:

1. Modelling of borehole storage in EED with a constant assumed *COP* of 3,
2. Optimizing the BTES system to minimize costs using EED,
3. Importing the fluid temperatures from EED to IDA ICE,
4. Modelling of heat pump and buildings in IDA ICE,
5. Obtaining the dynamic *COP* values,
6. Assessing the borehole storage in EED with the new average *COP* value,
7. Repeating the process iteratively.

During the first step, BTES is simulated using EED software for dimensioning ground heat systems. The software is based on the dimensions temperature response function describing the thermal response of the borehole field (Claesson & Javed, 2011).

Hourly load profiles are uploaded to the program with negative values for heating demand and positive values for waste heat injection. The injection of waste heat to the ground is modelled as a cooling process in EED with heat being injected directly to the ground. In the program, this is set by assigning a very large value to the seasonal performance factor (*SPF*). The *SPF* is a measure which corresponds to average *COP* and indicates the energy-efficiency of a heat pump, describing the ratio of thermal output to the electrical input.

The extraction of heat from the ground in EED is modelled as a heating process with a constant *SPF* of 3. This means the heat pump uses one-third of electricity and two-thirds of thermal energy from the ground. Thus, the larger the *SPF*, the smaller is the electrical input and higher is the thermal output from the ground (Javed & Spitler, 2017). Using a *SPF* of three suggests that the ground storage should be designed to provide approximately two-thirds of the total heating demand. The total heating load of all four buildings after direct supply is 3,168 MWh, and the amount of heating to be provided by the ground storage is 2,112 MWh. The annual energy injected to the ground system from the furnace is 1,210 MWh (Figure 3.26). Hence, the ground system should provide the remaining 900 MWh and should also make up for the thermal losses from the storage.
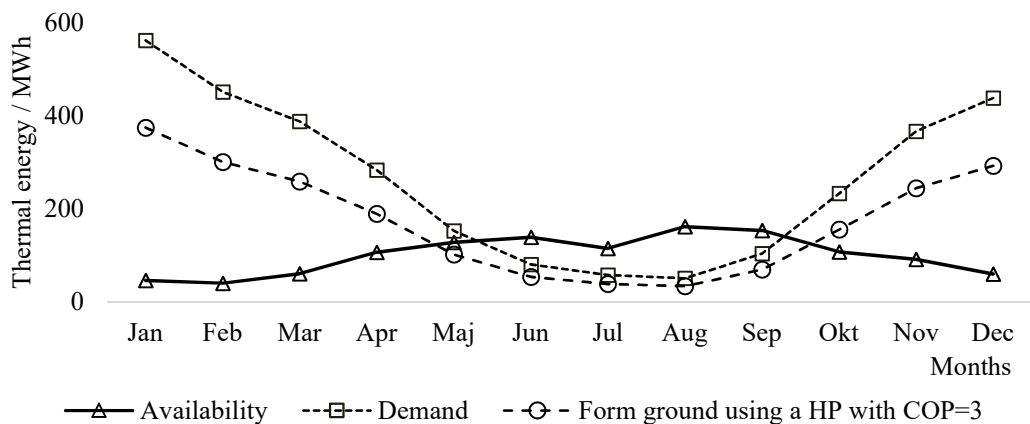
Figure 3.26: Monthly profile of available waste heat and total heating demand of Buildings 14, 15, 21 and C4 after direct heating from the furnace.

Ground specific properties and parameters used for the simulation and design of BTES-GSHP system are provided in Table 3.5. The bedrock in Sweden mostly consists of crystalline rocks with a value of thermal conductivity amounting to 3.47 W/(m·K) on average (Sundberg, 1988). After analysing the depth to bedrock (SGU, 2017), which is presented in Figure C1 in Appendix C, it is found that in the SVA proximity the depth to bedrock is 10–20 m. Considering the lower thermal conductivity of the soil above the bed rock and based on estimated ground conductivity values for the area, a value of 3 W/(m·K) is used for simulations. Double U-tube configuration with parallel connection is used. Borehole thermal resistance has been calculated using the multiple method (Javed & Claesson, 2017).

Table 3.5: Parameters used for BTES-GSHP system design and simulations.

Parameters	Value	Comments / illustrations
Ground specific properties (granite based rock)		
Thermal conductivity / (W/(m·K))	3.00	Estimated value
Volumetric heat capacity / (MJ/(m³·K))	2.16	From experience
Ground surface temperature / ºC	6.60	Value for the Stockholm region (Earh
Geothermal heat flux / (W/m²)	0.05	Energy Designer 4.18, 2000)
Borehole and heat exchanger properties		
Depth of boreholes[10] / m	100-300	Double-U tube
Spacing between boreholes[10] / m	5-15	
Diameter of boreholes / mm	110	
Filling thermal conductivity / (W/(m·K))	1.50	
Volume flow rate per borehole / (m³/h)	1.80	
Outer diameter of U-pipe / mm	32	
Wall thickness / mm	3	
Thermal conductivity of U-pipe / (W/(m·K))	0.42	
Shank spacing / mm	70	

Simulations are performed using water as the heat carrier fluid. Fluid temperature constrains for minimum and maximum mean fluid temperature are set to 2 and 20 ºC respectively. The lower limit is set so that the minimum water temperature does not drop below the freezing point.

The EED calculations return a number of configurations suitable for prescribed conditions. The selection of the BTES system is based on the lowest costs (estimated costs are explained in Section 3.3.4.3 below). Simulation outputs from EED include entering and leaving temperatures from the ground storage for a 15-year period. The goal is to get as high temperatures from the storage as possible to positively influence the heat pump performance. The borehole out temperatures obtained from EED are then fed to the heat pump model in IDA ICE along with the total flow rate for the BTES system.

Since the hot water temperature from the heat pump is not as high as from the furnace, it is required to connect the buildings to the heat pump in parallel by splitting the total flow from the heat pump proportionally to the heating demands of each building. This ensures that each building gets hot water at reasonably high temperature. IDA ICE model of BTES-GSHP system with four buildings connected in parallel is presented in Figure E1 in Appendix E. The model checks if building demands are met and calculates the actual *COP* values based on the exit fluid temperatures from the boreholes. Then, in course of optimization, the *SPF* parameter is changed in EED and new fluid temperatures are obtained.

---

[10] Preliminary range of values used for BTES-GSHP system optimization.

3.3.4.2   Heat pump

Two heat pump models are considered for the design of BTES-GSHP system. Their main characteristics are provided in Table 3.6 below (Carrier, 2017; GEA, 2017). The performance of both heat pumps is studied in the simulations to choose the optimal option.

Table 3.6: Rated parameters and conditions of the considered heat pump models.

Model	Heating capacity / kW	*COP* / -	Evaporator entering/leaving water temp. / °C	Condenser entering/leaving water temp. / °C	Max. condenser temp. / °C
Carrier 30XWHP1012	1,570	4.11	+10/+7	+40/+45	+63
GEA RedAstrum 1900	985	2.70	+10/+5	+40/+70	+80

As can be seen *GEA* heat pump has a much lower *COP*, however, it is able to supply higher temperature. Also, since the peak load of all four buildings is 1,560 kWh, installation of two *GEA* heat pumps is needed. There are several approaches to connect multiple units: in parallel, in series, and various combination of both. Figure 3.27 explains the first two alternatives.
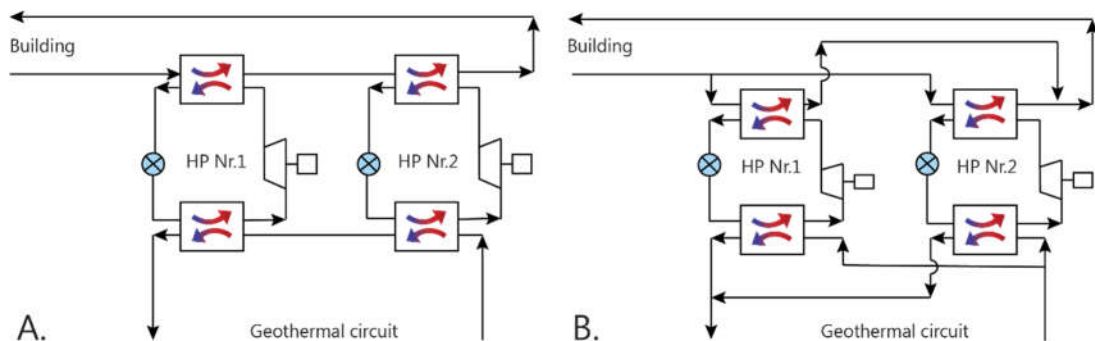
Figure 3.27: Possible arrangements of heat pump systems (HP): A) in series with counter flow in condenser and evaporator, B) in parallel.[11]

Piatti et al. (1992) pointed out that connecting the heat pumps in series with counter flow in evaporator and condenser as shown in Figure 3.27 (A) often appears to be the most profitable solution. In addition to that, when fluid temperatures from the ground are low, it is worth trying connecting evaporators in parallel and condensers in series. Therefore, in the course of the simulations, various arrangements have been tested to achieve the highest output from heat pump units.

---

[11] Figure is adapted from Piatti et al. (1992).

3.3.4.3 Costs

Some of the costs that are required for the BTES installation and are taken into consideration in this work are presented in Table 3.7 below (Manonelles, 2014).

Table 3.7: Costs of various BTES system components.

Expenses/units	Value	Comments
Fixed drilling cost / (SEK/borehole)	2,500	If the distance between boreholes is smaller than 15 m, then there is no fixed charge per borehole. However, a container should be used for each borehole when drilling through soil.
Soil drilling / (SEK/m)	440	Including double-U tube
Rock drilling / (SEK/m)	230	Including double-U tube. The price is shown for the drilling depth of 200–300 m. For shallower depths price is slightly lower.
Piping costs. Connection between boreholes / (SEK/m)	235	
Piping costs. Connection between storage and distribution centre / (SEK/m)	377	
Heat exchangers / SEK	310,300	2×550 kW
Pumps / SEK	200,000	
Other equipment / SEK	200,000	Valves, measurement devices, etc.

The price for the heat pump(s) and its installation is roughly 1.2 MSEK. Cost for pumping the water from the heat pump to the buildings is calculated in the same way as for *Option 2* of this work, determined in Section 3.3.2. Energy for pumping through the borehole field is estimated to be roughly 250 MWh/year.

3.3.5 LCC calculations

The economic feasibility of the four proposed solutions including water storage tank, direct use of waste heat, combination of direct connection with storage tank and BTES-GSHP system, is determined using a LCC analysis. The net present value (*NPV*) method is used for carrying out the economic analysis.

The *NPV* is calculated as the sum of the initial investment cost and the present value of the annual energy expenses during the considered project life-cycle. Thus, the *NPV* describes the total costs associated with implementing the project and consequent running expenses throughout the considered period. Hence, the lowest *NPV* indicates the most profitable solution. The present value (*PV*) of the annual payments is determined using the formula for geometric gradient series (Eq. 4).

$$PV = A_1 \cdot \left[\frac{1-(1+g)^N \cdot (1+i)^{-N}}{i-g} \right] \qquad [PV] = \text{SEK} \qquad (4)$$

Where:
i = discount rate;
g = energy price growth rate;
N = analysis period;

A_1 = energy costs after one year:

$$A_1 = A_0 \cdot (1 + i) \qquad [A_1] = \text{SEK} \tag{5}$$

Eq. 5 is a formula for a single compounded payment, where A_0 is today's annual energy cost, i.e. amount of energy used in kWh multiplied by its price in SEK/kWh. The parameters used for LCC calculations are same as used by Akademiska Hus for their in-house economic estimations and are provided in Table 3.8. Values of the discount rate and energy price growth are nominal.

Table 3.8: Parameters used for LCC calculations.

Parameter	Value
Discount rate, i / %	5.00
DH price / (SEK/kWh)	0.70
Electricity price / (SEK/kWh)	0.85
DH/Electricity price growth, g / %	3.00
Lifetime, N / years	15

Each of the considered cases is calculated for a lifetime of 15 years. Analysis of the results is based on net savings, i.e. difference in LCC values. Other costs necessary for the proposed solutions are explained in the corresponding sections of the thesis. Maintenance as well as design and administration costs are not accounted for in this project.

4 Results

This chapter presents results of different design options discussed in Chapter 3. The chapter is divided into five sections. The first four sections provide results of the four main design options of waste heat utilization identified in Sections 3.3.1 – 3.3.4, and highlight the major trends apparent from the parametric studies. The last section compares possible savings for all design options.

4.1.1 Water tank

Before analysing the results of the simulations and comparing different volumes of the tank, the optimal height of the tank inlets was determined. Figure 4.1 shows how the tank output changes with different heights of the inlets for a 180 m³ tank (15.4 m high). The tank output represents the amount of thermal energy provided by the tank to cover the annual demand. As seen from the figure, if the cold-water inlet ($Zin2$) is located at the bottom of the tank, a lower position of the hot-water inlet ($Zin1$) results in higher tank performance. The peak tank output is reached at $Zin1$ height of two-meters. On the contrary, if the hot-water inlet ($Zin1$) is located at the top of the tank, a higher position of the cold-water inlet ($Zin2$) results in higher tank performance. The peak tank output is reached at $Zin2$ height of ten-meters.
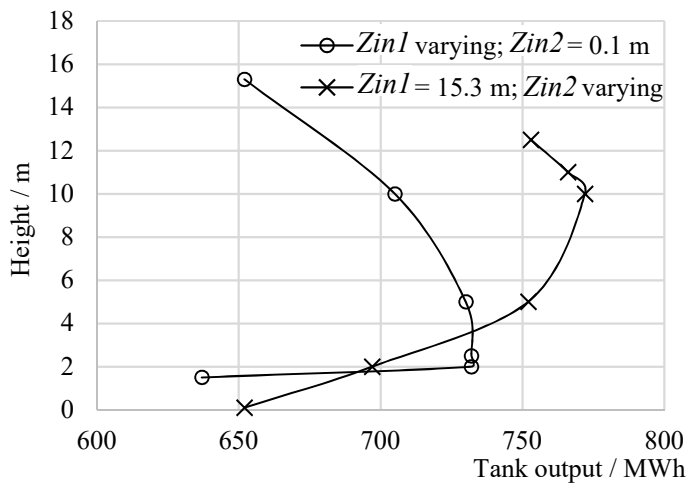

Figure 4.1: Influence of cold- and hot-water inlets on tank output.

The analysis mentioned in Figure 4.1 signifies the importance of considering the water-inlet locations in relation to each other. Also, the advantage of having two inlets in the upper part of the tank is apparent from the figure. Figure 4.2 illustrates temperature distribution in the same tank for various combinations of inlet heights (several cases have been chosen for demonstration purposes). The analysis has been performed for 24-hour period between December 19–20 (7:00 a.m. to 6 a.m.). The highest tank output is achieved at $Zin1 = 12$ m and $Zin2 = 10$ m. This option provides the highest temperature difference between the bottom and the top of the tank, as well as the highest temperature in the upper most layer.
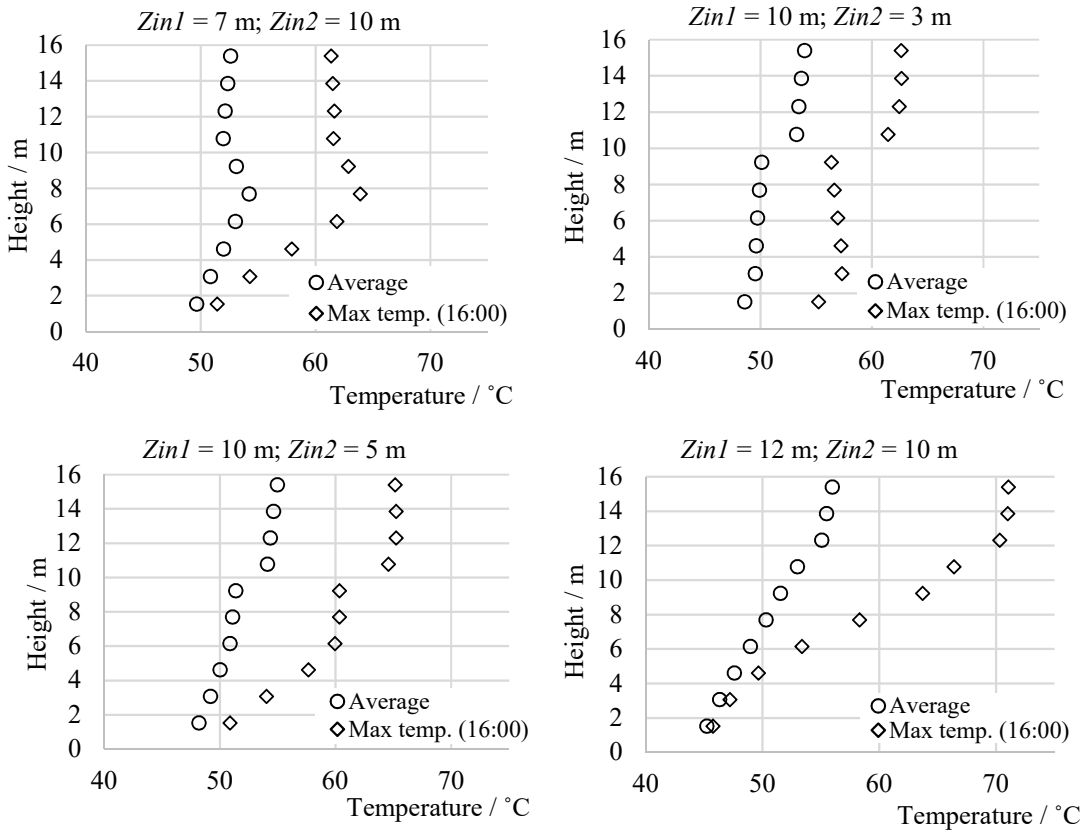
Figure 4.2: Water temperature at different levels in the tank (180 m³) based on different heights of cold- and hot-water inlets.

The same analysis has been performed for different tank sizes. The diameter of the tank was kept constant. Thus, variations in tank sizes were only due to different tank heights. After analysing various tank sizes, it is concluded that the highest tank output is achieved when *Zin1* and *Zin2* are around 0.8 and 0.6 of the total tank height, respectively. This result will be used in all further simulations.

For Building 14, the maximum required storage capacity of 6.5 MWh results in a water tank of 130 m³ at a ΔT of 44 K between the tank operating temperatures (see Section 3.3.1.1). Table 4.1 presents information on the tank output and its efficiency.

Table 4.1: Tank output and efficiency for 130 m³ storage tank of 11.5 m height for different levels of inlet connections.

Connection options	*Zin1* = 5 m; *Zin2* = 6 m	*Zin1* = 10 m; *Zin2* = 3 m	*Zin1* = 11 m; *Zin2* = 6 m	*Zin1* = 8 m; *Zin2* = 6 m
Tank output / MWh	684	687	718	726
Tank efficiency / -	0.994	0.985	0.982	0.988

For Building 14, the largest tank output is achieved at $Zin1 = 8$ m and $Zin2 = 6$ m, considering a proposed tank height of 11.5 m. As can be seen from Figure 4.3, such a tank will decrease the total purchased energy from the DH network by approximately 40 %.
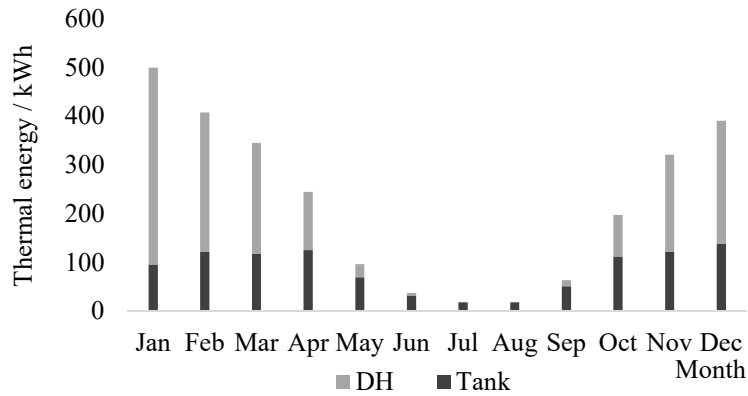

Figure 4.3: Thermal energy coverage of Building 14 using a tank of 130 m³ storage volume.

Figure 4.4 shows the temperature profiles within the tank and the thermal energy coverage of Building 14 for one February week. Temperatures are shown for the bottom and top layers of the tank. Charging (C) and discharging (D) of the tank and the portion of the thermal demand covered by the tank is also presented. Similar results for one week in April are presented in Figure D1 in Appendix D.
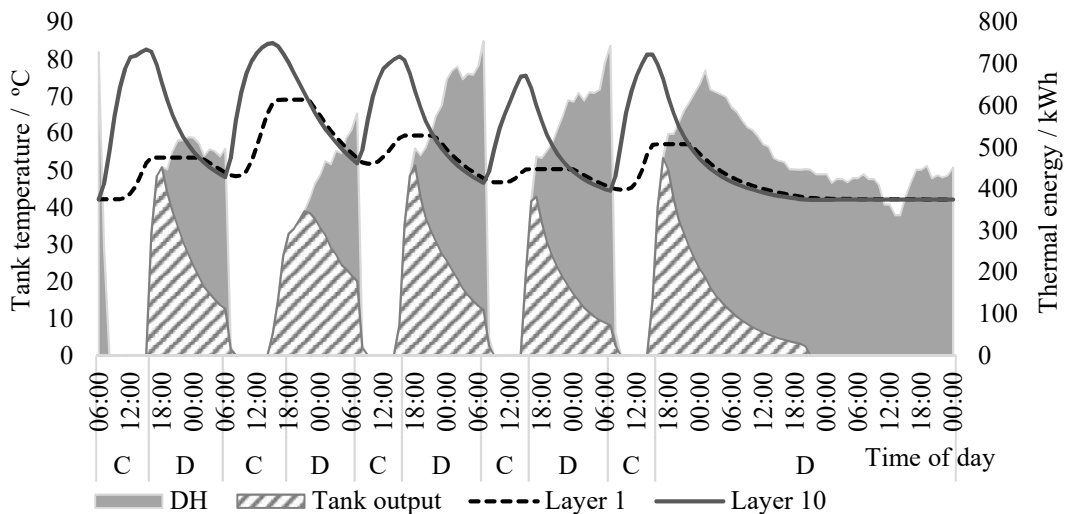
Figure 4.4: Water temperatures and thermal energy supplied by the 130 m³ tank for Building 14.

Figure 4.5 shows results of varying the tank volume in economic terms. Tank sizes between 110 and 150 m³ have small differences in *NPV* for 15 years. They all have a payback time of approximately six years. The size calculated for the maximum storage capacity (130 m³) appears to be the optimal one. A larger tank size provides a higher thermal output but has a higher *NPV* due to higher initial costs. On the other hand, a smaller tank size provides a lower

thermal output and is not as profitable as the 130 m³ tank in the 15-year period considered in this work. The shortest payback time of approximately five years is achieved with tanks of 80–90 m³ storage volumes. As can also be seen from Figure 4.5, the installation of 130 m³ tank can result in savings of 3.88 MSEK in 15 years as compared to the current situation. The investment required for this option is 2.64 MSEK and thus the resulting savings-to-investment ratio (*SIR*) is 1.47.
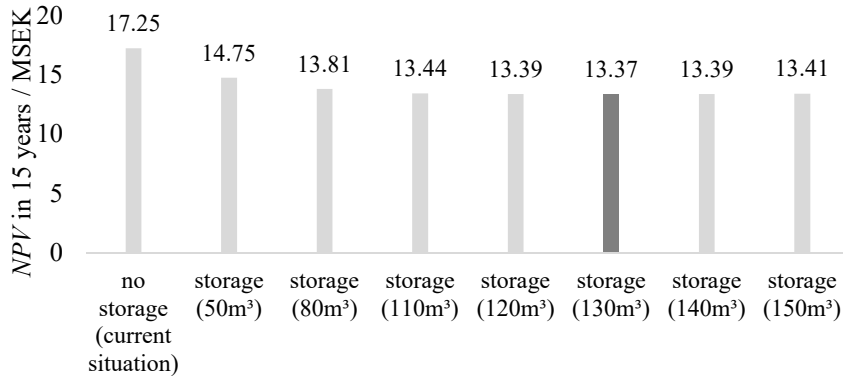

Figure 4.5: Comparison of NPV for different tank sizes.

4.1.2   Direct use of waste heat

Based on the procedure described in Section 3.3.2, the results reported in this section present the optimal order of connecting Buildings 15, 21 and C4 to the available waste heat to optimise its use. As can be seen from Table 4.2, Building 15 has the highest *SIR*. Hence, it is selected for instantaneous connection in Step 1. Thereafter, Building 21 has the next higher *SIR* when connected second after Building 15. Hence, it is selected for the instantaneous connection in Step 2. Finally, Building C4 is selected for the instantaneous connection in Step 3. Table 4.2 presents *SIR* values for all possibilities considered in Steps 1-3. A higher *SIR* value suggests a more feasible connection.

Table 4.2: SIR for different possibilities of instantaneous connections.

	Order of connection	*SIR* / -			
		1st place	2nd place	3rd place	Total
Step 1	Building 15	7.16	-	-	7.16
	Building 21	3.28	-	-	3.28
	Building C4	1.01	-	-	1.01
Step 2	Building 15 - Building 21	7.16	2.27	-	9.43
	Building 15 - Building C4	7.16	0.53	-	7.69
Step 3	Building 15 - Building 21 - Building C4	7.16	2.27	0.40	9.83
	Building 15 - Building C4 - Building 21	7.16	0.53	2.02	9.71

Table 4.3 summarizes *NPVs*, savings and payback times anticipated for the optimal connection of the three buildings as well as for each building. This connection covers 33, 25 and 33 % of heating demands of Buildings 15, 21 and C4, respectively.

Table 4.3: Key economic figures for investing in instantaneous use of waste heat.

	Total for the connection	Building 15	Building 21	Building C4
NPV in 15 years / MSEK	12.53	7.26	3.85	1.43
Savings / MSEK	3.43	2.59	0.66	0.18
Payback time / years	4	2	5	10

Table 4.4 presents the results of the sensitivity analysis performed to investigate the influence of the distance from the source on the *SIR*. The total thermal energy provided by the furnace depends on specific thermal requirements of each building as well as on the availability of the waste heat. At the same time, installation and operation costs increase with increasing distance from the source. A negative *SIR* value indicates that the connection is not profitable.

Table 4.4: Results of sensitivity analysis for different piping distances from the source.

	Distance/m				
	100	**200**	**500**	**1 000**	**2 000**
Building 15					
Thermal energy provided by the furnace / MWh	327	327	327	327	327
Flow rate / (l/s)	2.4	2.4	2.4	2.4	2.4
Head / kPa	20	40	100	200	400
Pump cost / SEK	8,770	11,610	23,510	19,560	24,890
Pump installation cost / SEK	1,646	1,646	1,646	1,646	1,646
Electricity for pumping / SEK	294	515	1,570	2,865	5,336
Pipes cost and installation / SEK	192,040	384,080	960,200	1,920,400	3,840,800
SIR / -	7.2	4.3	1.6	0.4	**-0.3**
Building 21					
Thermal energy provided by the furnace / MWh	156	156	156	156	156
Flow rate / (l/s)	2.0	2.0	2.0	2.0	2.0
Head / kPa	20	40	100	200	400
Pump cost / SEK	7,810	9,640	10,550	11,350	16,030
Pump installation cost / SEK	1,646	1,646	1,646	1,646	1,646
Electricity for pumping / SEK	238	413	1,434	2,422	4,576
Pipes cost and installation / SEK	192,040	384,080	960,200	1,920,400	3,840,800
SIR / -	3.9	1.9	0.3	**-0.3**	-0.7
Building C4					
Thermal energy provided by the furnace / MWh	76	76	76	76	76
Flow rate / (l/s)	1.2	1.2	1.2	1.2	1.2
Head / kPa	20	40	100	200	400
Pump cost / SEK	6,810	7,570	8,330	9,410	12,430
Pump installation cost / SEK	1,646	1,646	1,646	1,646	1,646
Electricity for pumping / SEK	152	275	1,021	1,711	3,080
Pipes cost and installation / SEK	116,900	233,800	584,500	1,169,000	2,338,000
SIR / -	2.1	1.0	**0.0**	-0.5	-0.7

The *SIR* value depends on two factors: distance from the source and the thermal energy covered by the waste heat. The first factor determines the required investment, whereas the second factor influences the potential savings. The effect of these factors is shown in Figure 4.6. It is apparent from this figure that the *SIR* is negatively influenced by the distance. However, what is even more interesting here is the magnitude of these changes for different buildings with different amounts of thermal energy provided by the furnace (referred to as *saved energy* in the figure). For distances up to 500 m, there is a significant difference in the *SIR* values between the buildings. But this difference diminishes gradually with increasing distance and becomes nearly unnoticeable at a distance of 2 km.
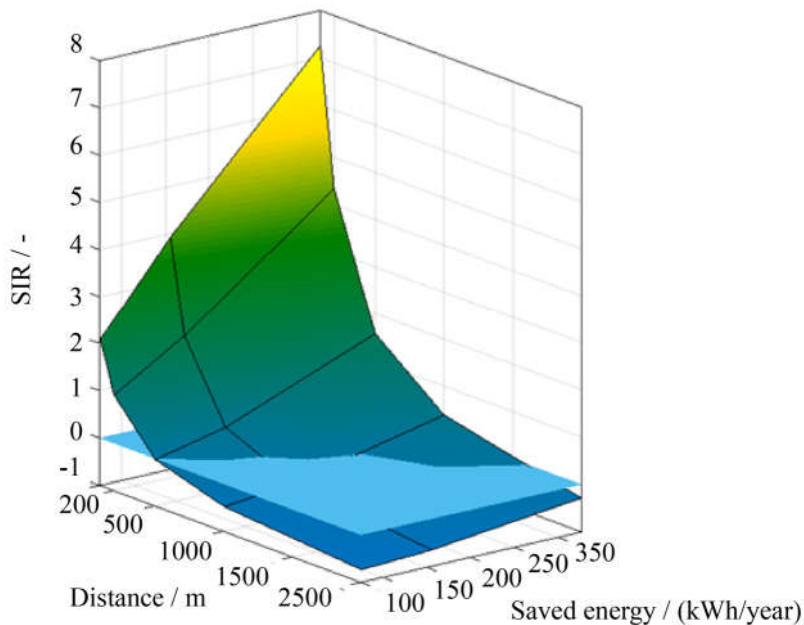

Figure 4.6: SIR as a function of the distance to the heat source and thermal energy requirements covered by the waste heat. The connection is not profitable below zero SIR i.e. light-blue plane.

4.1.3   Combination of direct use and storage tank

Option 3a

As explained in Section 3.3.3, this option considers direct connection of Building 15 to the heat source and storage of surplus heat in a tank to heat Building 14 during non-operating time of the furnace. By analysing the zero-difference between available waste heat and building thermal demands in Figure D2 (Appendix D), the required capacity of the tank is determined to be 5.6 MWh. This in turn suggests a tank of 110 m³ storage volume at $\Delta T = 44$ K, as discussed in Section 3.3.1.1. However, the results of economic analysis, presented in Figure 4.7, suggest that a tank of 120 m³ storage volume will be marginally more feasible for the considered lifespan of 15 years.
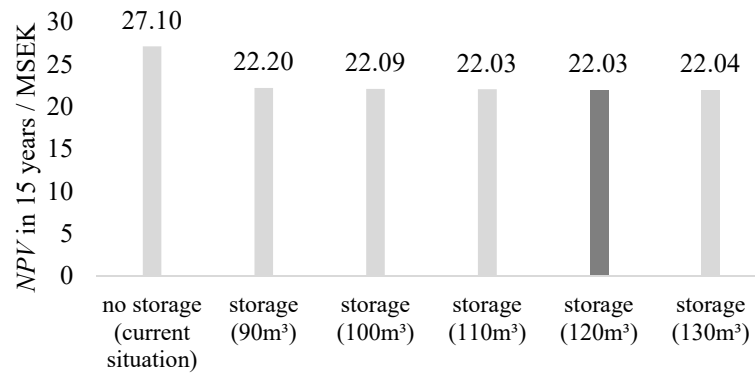
Figure 4.7: NPVs for Buildings 14 and 15 for different tank sizes considered in Option 3a.

Table 4.5 presents further details of optimal tank size for *Option 3a*. The connection covers 30 % of the heating demand of each building.

Table 4.5: Results for optimal tank size for Option 3a.

Savings / MSEK	Payback time / years	Covered portion of total heating demands / %
5.07	5	30

Option 3b

In addition to directly connecting Building 15 to the heat source and having Building 14 connected to the storage tank as considered in *Option 3a*, this option also considers connecting Building 15 to the storage tank system. As can be seen from Figure D3 (Appendix D), the required capacity of the tank for *Option 3b* is around 7 MWh. This leads to a tank of 140 m³ storage volume. The economic analysis presented in Figure 4.8 also confirms that 140 m³ is the optimal tank size in this case.
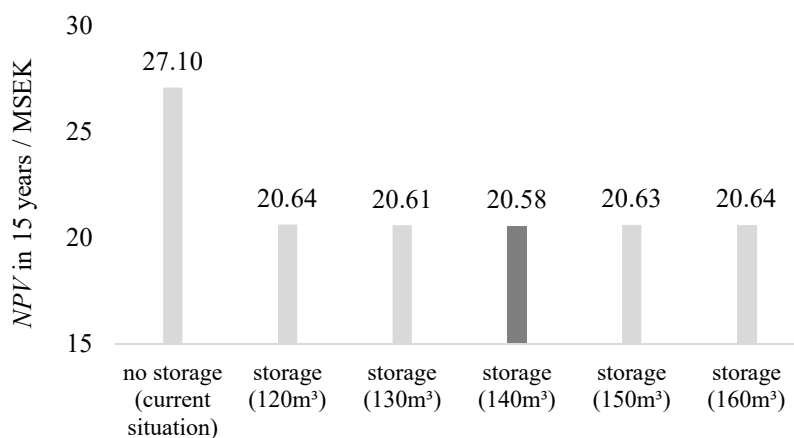

Figure 4.8: NPVs for Buildings 14 and 15 for different tank sizes considered in Option 3b.

Table 4.6 provides more results for this option. The waste heat covers nearly 23 and 60 % of the heating demands of Buildings 14 and 15, respectively.

Table 4.6: Results for optimal tank size for Option 3b.

Savings / MSEK	Payback time / years	Covered portion of total heating demands / %
6.5	5	37

Option 3c

This option is to supply Buildings 15, 21 and C4 instantaneously from the heat source and to have a tank only for Building 14. As seen from Figure D4 (Appendix D), the zero-difference between the available waste heat after instantaneous use in three buildings and Building 14's thermal demand indicates the required tank capacity of 4.8 MWh. This gives a tank of 90 m³ storage volume. In terms of *NPV,* Figure 4.9 shows that a tank of 110 m³ storage volume appears to be the most optimal.
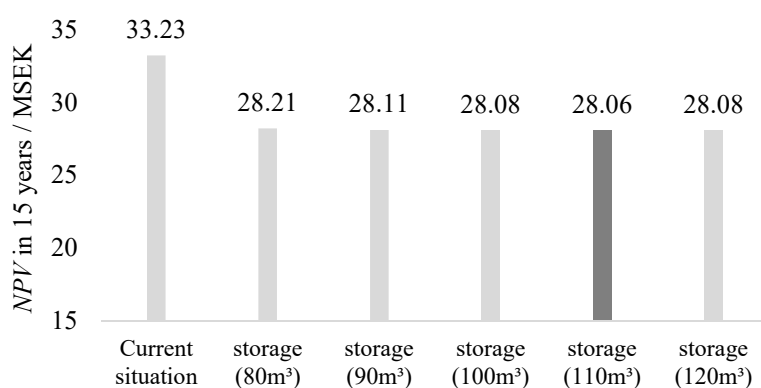
Figure 4.9: NPVs of various tank sizes considered in Option 3c.[12]

In addition to what is covered by instantaneous supply of waste heat, i.e. 33, 25 and 33 % of heating demands of Buildings 15, 21 and C4, respectively (see Section 4.1.2), the storage tank covers 21 % of Building 14's heating demand. Additional details are provided in Table 4.7 below.

Table 4.7: Results for optimal tank size for Option 3c.

Savings / MSEK	Payback time / years	Covered portion of total heating demands / %
5.17	6	27

Option 3d

In this case a tank, charged after supplying heat instantaneously to Buildings 15, 21 and C4 from the heat source, is used for heating of Buildings 14 and 15. The tank size is calculated

---

[12] Total figures are given, i.e. for the operation of four buildings in 15 years.

to be 6 MWh, as shown in Figure D5 in Appendix D. This gives a tank of 120 m³ storage volume. LCC analysis of various tank sizes for this option is shown in Figure 4.10.
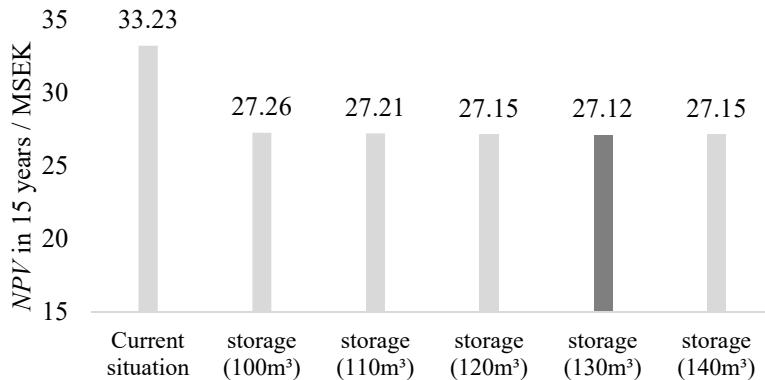

Figure 4.10: NPV for various tank sizes for Option 3d.[13]

For this option, a tank of 130 m³ storage volume yields savings of 6.1 MSEK with a payback period of six years. The thermal demands of Buildings 15 and 14 covered by waste heat are 56 and 17 %, respectively.

Table 4.8: Results for optimal tank size for Option 3d.

Savings / MSEK	Payback time / years	Covered portion of total heating demands / %
6.1	6	31

4.1.4 Thermal energy storage using boreholes

4.1.4.1 BTES

The borehole storage for the considered design conditions requires a land area between 6,000–17,000 m², depending on it's configuration. Accordingly, the area to the south-east of SVA can be used for the borehole field. Figure 4.11 shows the most suitable solution found using EED. The total drilling length is 50 km.

---

[13] Total figures are given, i.e. for the operation of four buildings in 15 years.
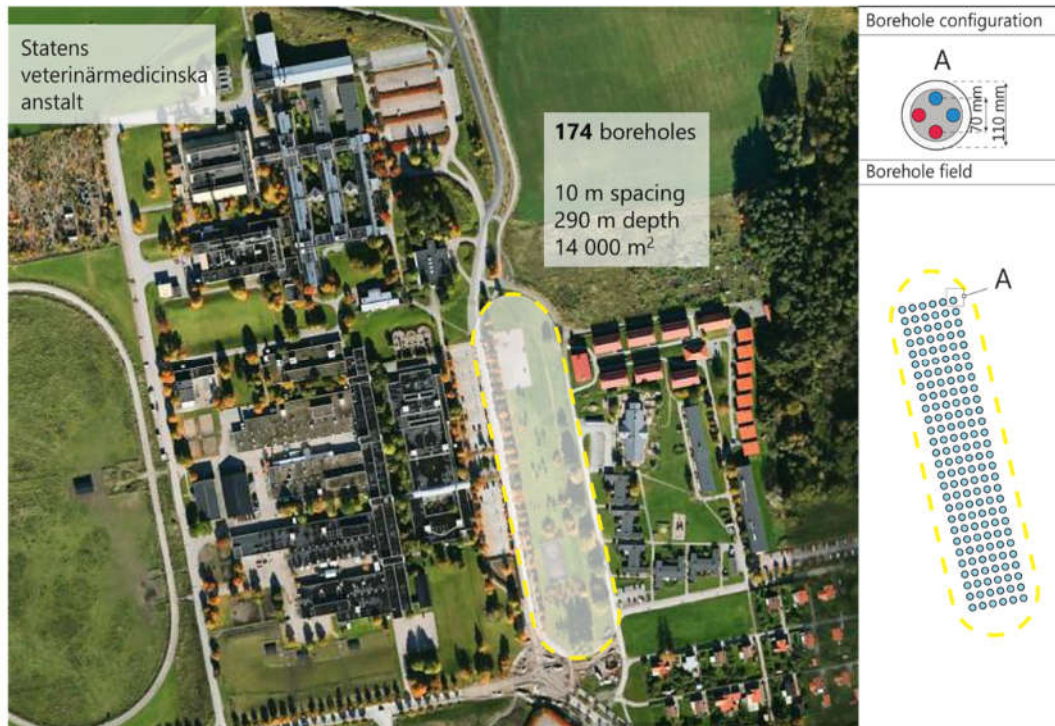
Figure 4.11: Proposed location for the borehole field (marked area).

The design ensures that the minimum fluid temperature in the boreholes does not fall below 0 °C. Figure 4.12 shows the fluid temperatures exiting the borehole field and entering the heat pump for the entire fifteen-year lifecycle period considered in this work.
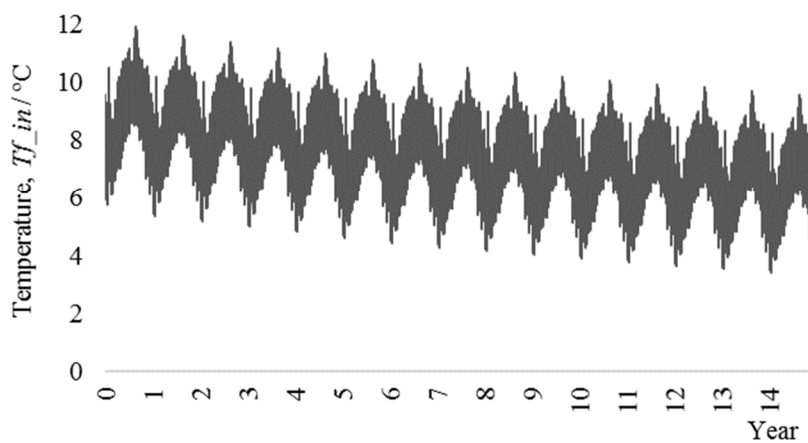

Figure 4.12: Fluid temperature entering the heat pump from the boreholes (Tf_in).

Since the annual heat extraction of 2,112 kWh/year from the ground system is larger than the annual heat injection of 1,210 kWh/year, the fluid temperatures exiting the ground system

have a decreasing trend over the years. When performing IDA ICE simulations, the temperatures of the last year of the EED simulations are fed to the heat pump model. As the ground is simulated to work in two modes – i.e. cooling and heating (when the heat is injected and extracted from the ground, respectively) – it returns temperatures for both modes. The temperatures that are actually used by the heat pump for heating lie between 3.5 and 7 ºC.

4.1.4.2 Heat pump

Table 4.9 compares different arrangements of two *GEA* heat pumps in terms of their *SPF*.

Table 4.9: Performance of the heat pumps in various settings.

Arrangement type	*SPF* / -		
	Unit 1	Unit 2	Average
Parallel	2.71	2.71	2.71
Series, parallel flow in evaporator/condenser	2.31	2.79	2.55
Series, counter flow in evaporator/condenser	2.33	2.77	2.55
Evaporator in parallel, condensers in series	2.32	2.76	2.54

As can be seen from the above table, the parallel connection of the heat pumps proves to be the most efficient one. However, even the best arrangement of two *GEA* heat pumps results in a lower *SPF* compared to one *Carrier* heat pump. The *SPF* of the latter was calculated to be 3.0 (the rated COP was 4.11). Thus, results presented here onwards have been determined with *Carrier* heat pump.

Figure 4.13 shows the extent to which various sources cover the heating demands of the four buildings. These results are further analysed in the LCC section.
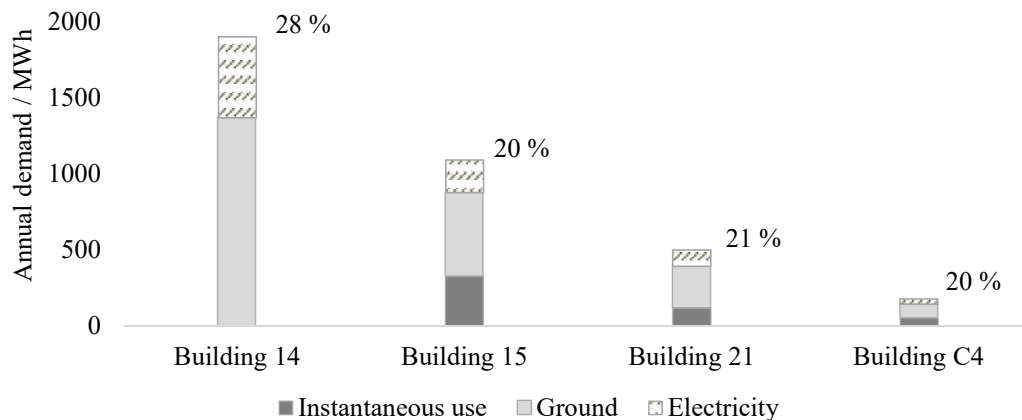

Figure 4.13: Portion of the purchased energy (electricity) to cover the heating demand.

4.1.4.3 LCC analysis and optimization

Table 4.10 summarizes the main costs related to the installation and operation of the system, which first meets the heating demands of Buildings 15, 21 and C4 directly through the available waste heat, and then provides the remaining heating requirements of all four

buildings (14, 15, 21 and C4) using a ground-source heat pump system. Costs of operating the current system are also provided for comparison purposes.

Table 4.10: Costs of existing and proposed design with GSHP system.

	GSHP system	Direct use	Existing system
Investment / MSEK	17.02	1.03	-
Electricity for heating / (KSEK/year)	752.30	-	-
Electricity for pumping[14] / (KSEK/year)	212.50	0.80	-
Heat from DH / (KSEK/year)	-	-	2,200.00
NPV for 15 years / MSEK	30.50		33.10

The results from Table 4.10 show that the proposed GSHP system can provide 2.6 MSEK savings in 15 years. Payback time of the investment is 13 years.

Parametric study, which has been performed to optimize the BTES-GSHP system in terms of investment and temperatures from the ground, suggests that entering water temperatures to the heat pump can be maximized and kept over 20 ºC if only Building 15 is connected to the system. However, in this case temperatures in the borehole system continue to increase rapidly, and rather excessively, over the years. Thus, it is assumed beneficial to have higher heating demand to balance the temperatures in the ground system.

The connection of Buildings 15 and 21 only is considered using two alternate scenarios of one and three years of charging the UTES before extracting any heat. In the first case of one year of charging, the fluid temperature (*Tf_in*) from the ground system to the heat pump stays between 10–20 ºC and remains rather stable over the years. In the second case of three years of charging, the fluid temperatures remain slightly higher and lie between 15–25 ºC.

For the first case of charging the ground for one year, the GSHP system should consist of 70 boreholes (temperatures to the heat pump are shown in Figure E2 in Appendix E), resulting in an *SPF* of 4.64 and electricity use of 228 MWh/year for the two buildings. Resulting savings amount to 4.1 MSEK in 15 years with an investment of 3.8 MSEK. This option is further referred to as *Option 4b*.

For the second case of charging the ground for three years, a GSHP system with 60 boreholes has been used for further analysis. Temperatures to the heat pump are provided in Appendix E, Figure E3. The value of *SPF* is calculated to be 5.2 with 208 MWh of electricity used for the two buildings. Resulting savings amount to 3.4 MSEK in 15 years, making it unreasonable to have the ground charged for three years in this case.

---

[14] Under the category *Electricity for pumping* only additional costs for pumping, associated with new system design, are considered. Pumping costs of the existing system are neglected and will be same for new and existing designs.

4.1.5 Summary of results

Table 4.11 summarizes the economic parameters of all design options considered in the project along with amount of waste heat left after.

Table 4.11: Summary of results. Comparison of design options.

	Investment / MSEK	Savings / MSEK	*SIR* / -	Payback time / years	Heat left / MWh
Tank (*Option 1*)	2.64	3.88	1.47	6	1,110
Direct use (*Option 2*)	1.03	3.43	3.33	4	1,211
Direct + Tank. (*Option 3a*)	2.86	5.07	1.77	5	900
Direct + Tank. (*Option 3b*)	3.33	6.53	1.96	5	729
Direct + Tank. (*Option 3c*)	3.39	5.17	1.52	6	724
Direct + Tank. (*Option 3d*)	3.86	6.11	1.58	6	636
Direct + GSHP (*Option 4a – all buildings*)	18.05	2.60	0.15	13	0
Direct + GSHP (*Option 4b – B.15+B.21*)	3.80	4.10	1.08	8	0

As shown in the above table, *Option 3b* where instantaneous supply is combined with the storage tank results in the largest savings over a 15 years lifespan. Direct connection of the three buildings is shown to be the most promising investment with the highest *SIR*. Due to the fact that GSHP system requires significantly higher investment costs, its benefit is only starting to grow after 15 years. However, as such a system is usually designed and assessed for 25-30 years lifespan, it is reasonable to take a look at its performance in a longer time perspective.

Figure 4.14 compares long-term savings resulting from *Option 3b*, as well as from two options with underground storage and the heat pump.
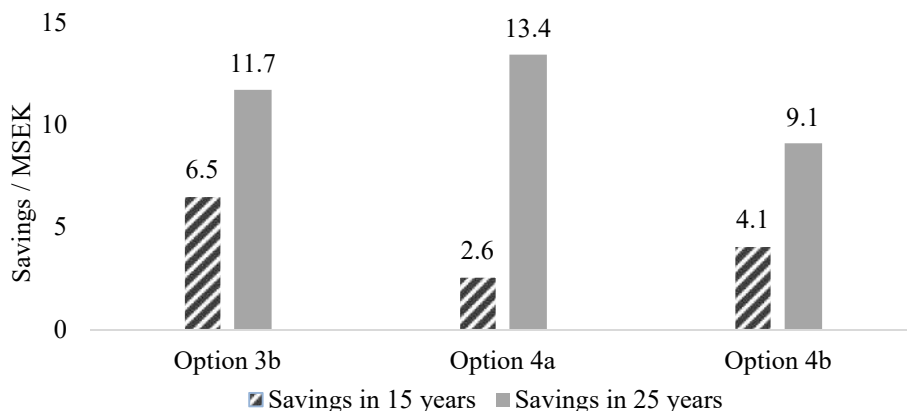

Figure 4.14: Comparison of savings in 15 and 25 years.

The above figure shows that the potential savings for *Option 4a* (i.e. the large borehole system that covers heating demands of all building) rise dramatically for larger life-cycles, making this option the most profitable for the 25-year lifecycle period.

5 Discussion and conclusions

This thesis has studied different solutions to utilize a large amount of waste heat (approximately 2,000 MWh/year) available from an incineration process at National Veterinary Institute (SVA) in Uppsala, Sweden. Four options, primarily focusing on thermal energy storage and direct use of heat, have been assessed to use the available heat for heating of SVA premises. Buildings considered for this study include one main building (Building 14) where the furnace is located and three neighbouring buildings - Buildings 15, 21 and C4. At present, more than 3,600 MWh of heat is purchased annually from a DH network to provide heating to these buildings. Considerable savings can be achieved by using the available waste heat instead of district heating.

5.1 Water tank

The first option considered is to install a hot water storage tank and accumulate the available heat for night-time heating of Building 14. Special attention has been paid to the tank sizing technique to determine the optimal capacity of the tank. The analysis has been performed based on the difference between the available energy and the heating demand on a twenty-four-hour basis. It was anticipated that optimum storage capacity would lie at the point when this difference would be equal to zero. To verify this, LCC analysis of various tank sizes has been performed to determine the most feasible economic solution. The performance of the tank has been studied in a spreadsheet using hourly energy profiles and has also been simulated in IDA ICE Advanced level.

The IDA ICE simulations for analysing the performance of the tank suggest that the location of hot- and cold-water inlets have a direct influence on the heat output from the tank. The analysis of water temperatures of the tank layers indicates that better stratification is achieved when supply hot-water inlet *Zin1* and return cold-water inlet *Zin2* are located approximately at $0.8 \cdot H_{tank}$ and $0.6 \cdot H_{tank}$, respectively. However, in the studied case of direct water inflow to the tank (without a heat exchanger), stratification depends on the mass flow rate entering the tank. In the simulations carried out in IDA ICE, the temperature difference between the water supplied from and returned to the furnace has been kept constant, thus, resulting in high mass flow rates at peak loads. This in turn disturbs stratification in the tank. In reality, the temperature difference between supply and return flows from the furnace varies over time, whereas the flow rate does not fluctuate so much. Hence, stratification in a real tank will be better compared to the modelling results presented here. Moreover, changes in tank diameter may also influence stratification.

It is worth mentioning that study of inlet heights improves the tank performance in simulations. A real tank generally has fixed inlet locations and uses other measures e.g. baffle plate, porous mesh, etc. to smoothen the inflow of water (Han et al., 2007). Some optimization of inlets is generally done by the manufacturer for each tank.

Using water tank (*Option 1*) allows to cover around 40 % of the heating demand of Building 14 and has a potential to provide relatively high savings in 15 years. However, more than half of the available waste heat cannot still be utilized when using this option.

5.2   Direct use of waste heat

The second option considered in this work is to directly supply the buildings with the available waste heat during the operating time of the furnace. In this context, a strategy has been developed to determine the optimal connection order and the number of buildings that can be connected directly to the available waste heat. The strategy is based on the relation between energy savings and the costs required for installation and operation. Energy savings are achieved when purchased energy is replaced by the available waste heat, while the installation and operation costs are the expenses required for the direct connection of a particular building at a certain piping distance from the source. In the present conditions, the connection order of the buildings is rather straightforward as buildings with the highest demand are located closer to the furnace. Nevertheless, the developed strategy allows to generalise the results and to make them applicable for different conditions (piping distances from the source and the demands). Regarding the application of the strategy, it should be noted that in case different buildings have similar demand profiles, then based on the calculated *SIR* values the connection order can already be decided during *Step 1* of the strategy (Section 3.3.2).

Apart from looking at buildings at the prescribed distances, the effect of the piping distance from the source on savings-to-investment ratio has been studied. Parametric studies reveal that *SIR* diminishes significantly with increasing distance from the source. For example, at a piping distance of 500 m, *SIR* drops by approximately 80 % even for the building with large energy savings potential. Also, at this distance it becomes unreasonable to connect a small building. The results suggest that buildings with the highest portion of the heating demand covered by the waste heat have larger potential to remain profitable, even if connected at further distances. These results also allow to determine the distance beyond which it is not feasible anymore to connect a building.

As with *Option 1*, IDA ICE has been used to simulate the performance of the systems with instantaneous connection of several buildings to the furnace. In engineering practice when several buildings are connected to a heat source or a DH plant, the connection is typically made in parallel and is regulated by a control system. Nevertheless, for the given task, it is important to facilitate the building connected first to take as much of heat as required and then send the remaining heat to the next building. This would require more sophisticated control algorithm in IDA ICE, which is beyond the scope of this work; thus, sequential connection has been applied. Despite the simplifications in the model, simulation results show good correlation with the manual spreadsheet calculations based on hourly energy profiles.

In economic terms, such a direct or instantaneous connection proves to have the highest *SIR* providing large savings against low initial investments among all other options considered in this thesis. This option ensures the fastest payback time. There is a possibility to cover 30 % of the total demand of the three neighbouring SVA buildings. Nonetheless, as in *Option 1*, more than half of the available waste heat cannot be utilized by direct heating of buildings.

5.3   Combination of direct use and storage tank

In the third option, instantaneous connection and hot water storage tank have been studied together in four different combinations to maximize the use of the available waste heat. The tank size has been determined by comparing the amount of heat left after the instantaneous supply to the building demands. The LCC calculation of various tank sizes has been carried out for each case to determine the most economically reasonable tank size. Result of these calculations show that in some cases it is more beneficial to install volumes larger than those determined from analysing of the difference between available heat and heating demands. The biggest deviation has been observed for *Option 3c* (see Section 3.3.3). The zero difference between the amount of waste heat left after supplying Buildings 15, 21 and C4 instantaneously and the heating demand of Building 14 suggested a tank capacity of 4.8 MWh, which in turn results in a tank size of 90 m³. Figure 5.1 shows the distribution of the difference for this case (the whole profile is provided in Figure D3 in Appendix D). As can be seen from the figure, there are instances when higher demand can be covered (areas marked black) by means of a larger tank size. The LCC analysis suggests a tank size of 110 m³, which corresponds to nearly 5.4 MWh capacity.
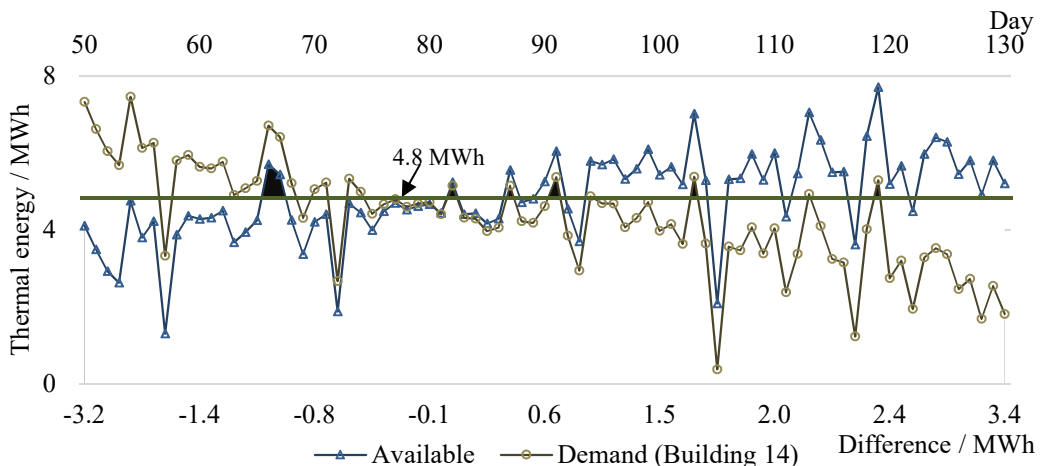

Figure 5.1: Distribution of the difference between available waste heat and heating demand for Option 3c.

Furthermore, for periods when the available waste heat exceeds heating demands of one single night, heat from the tank can be used for heating at weekends. The approach taken for sizing the tank, as well as manual estimations of tank performance both fail to take this consideration into account. Nevertheless, the sizing strategy has been rather accurate for determining the optimal tank volume over the fifteen-year period. On the contrary, as briefly discussed above, larger tank sizes will be more feasible if longer operation times are considered.

Among the combinations considered within *Option 3*, the case where Building 15 is supplied instantaneously and the tank is sized for Buildings 14 and 15 to cover the demand during the non-operating time of the furnace (*Option 3b*) proves to be the most profitable. Moreover, this option provides the highest savings in 15 years among the other options considered in this work. The design proposal allows to cover 23 and 60 % of the heating load for Buildings 14 and 15, respectively, utilizing approximately 64 % of the available waste heat.

5.4 Thermal energy storage using boreholes

The fourth option considered in this work is a borehole thermal energy storage (BTES) system assisted by a ground-source heat pump (GSHP). Firstly in *Option 4a*, the system has been designed to cover the heating demands of all four buildings. At the same time, the borehole storage is only charged with the waste heat that is left after the instantaneous heating of all buildings during the furnace operating time. This results in a large borehole system requiring significant investment costs, which in turn results in a rather long payback time of 13 years. Due to these reasons, savings in 15 years are the lowest among all other options considered in this work.

As the results in Section 4.1.4 suggest, the temperature in the ground storage drops over time when the system is designed for all the buildings. This occurs due to the fact that amount of heat extracted from the ground storage is larger than the heat injected into it. A heat pump with an *SPF* of 3.0 should extract nearly 2,100 MWh/year from the ground. However, only 1,200 MWh/year of heat is available for ground storage after direct heating of all buildings during furnace operating hours. This implies that there is roughly an imbalance of 900 MWh/year between the heat extracted and the heat injected into the ground. Consequently, by the fifteenth winter, the water temperature from the ground to the heat pump drops down to 3.5–6 ºC. However, without injection of waste heat into the ground, these temperatures would have dropped down to even lower 1–3 ºC.

To optimize the performance of the BTES and the GSHP system and to provide as high temperatures to the heat pump as possible, different loads on the ground have been simulated. By considering a lower heat extraction load on the ground system, e.g. having the BTES designed for two buildings instead of four, it is possible to achieve higher supply temperatures to the heat pump. In this case, it is beneficial to have fewer boreholes with smaller depth (100 m). However, attention should be paid to the maximum temperatures occurring in the borehole system because too high temperature in ground system may complicate the usage of water as a heat carrier. In general, the results have shown that considering a lifespan of 15 years, a smaller borehole system for two buildings is more profitable than a larger one for all the buildings. This is mainly due to the significantly lower initial investment. In addition, higher temperatures from the ground increase the heat pump's *SPF* by 55 %. As a result, *Option 4b* of having the borehole system designed for two buildings provides almost 60 % higher savings compared to *Option 4a* when a fifteen-year lifespan is considered.

It has been shown that the BTES system is negatively influenced by the high initial cost, and consequently results in lower savings-to-investment ratio compared to other options. However, in practice, a system is usually designed and assessed for a longer lifespan. When the LCC is performed considering a lifespan of 25 years, *Option 4a* of having a large borehole system for all buildings provides the highest savings among the options considered in this thesis. This occurs because the annual energy expenses are reduced more noticeably than with other options. Figures 5.2 and 5.3 illustrate a steeper growth of the curves of LCC savings for the large borehole system compared to *Option 3b*. This explains the dramatic increase in savings for the BTES system, from 2.6 MSEK to 13.4 MSEK when the analysis period is increased from 15 to 25 years. *Option 3b* of using instantaneous connection together with a storage tank yields largest savings in 15 years, however, *Option 4a* becomes the most profitable design option if a lifespan of 25 years is considered instead. Figures 5.2 and 5.3 also cover different scenarios of changes in energy price and discount rates. The 0 % scenario

presents the settings used in this study for all LCC calculations, i.e. nominal discount rate of 5 % and energy price growth of 3 %. The scenario of 50 % increase means the nominal discount rate of 7.5 % and energy price growth of 4.5 %.
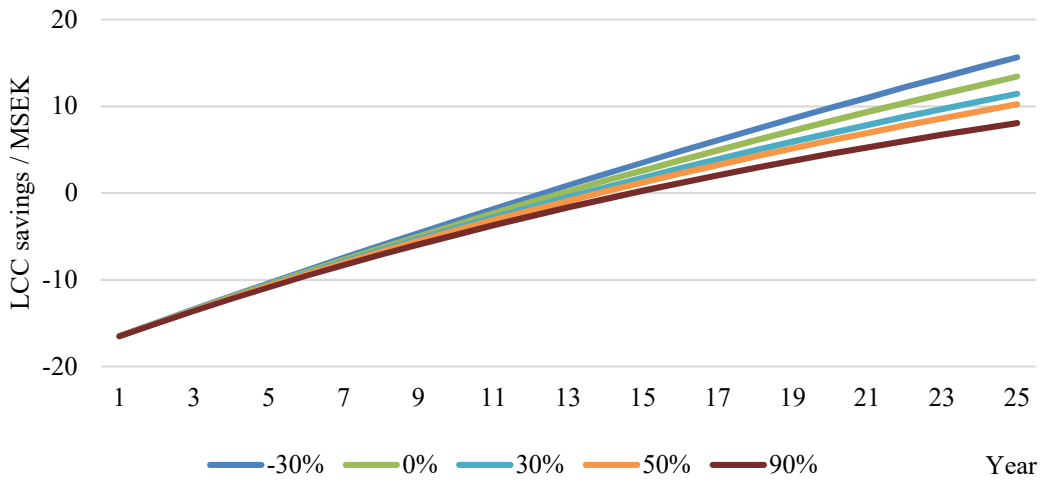

Figure 5.2: LCC savings for various economic scenarios for Option 4a considering instantaneous connection and BTES combination for all buildings.
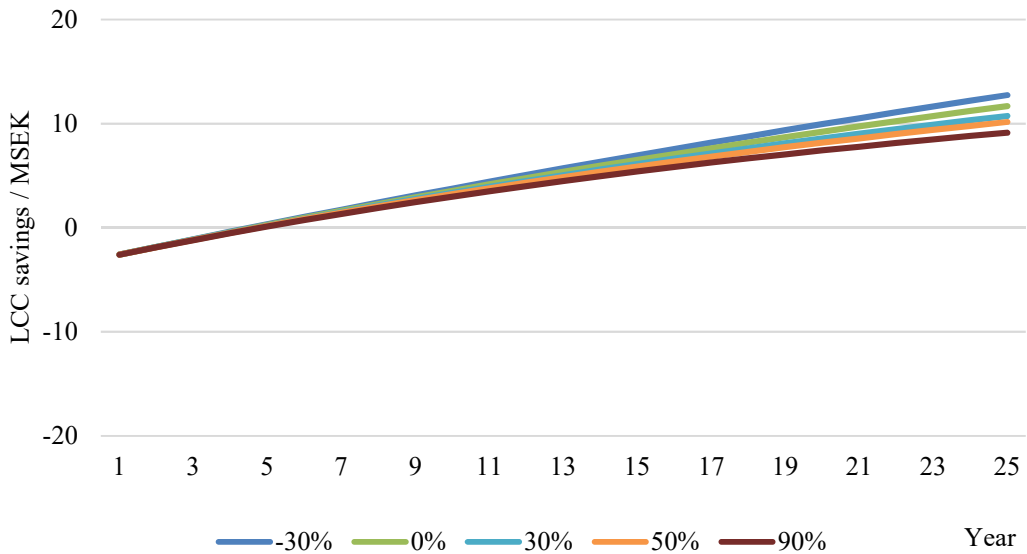

Figure 5.3: LCC savings for various economic scenarios for Option 3b considering instantaneous connection and water tank.

As can be seen from the figures, system with BTES is more sensitive to changes in economic parameters. This occurs due to the fact that it entirely relies on electricity, which is more expensive than district heating energy. Moreover, for the scenario of 90 % increase on Figures 5.2 and 5.3, i.e. nominal discount rate of 9.5 % and energy price growth rate of 5.7 %,

Option 4a will not be the most profitable in 25 years anymore (8.0 MSEK savings in 25 years compared to 9.1 MSEK for *Option 3b*).

It should be noted that design cases involving BTES systems (*Options 4a and 4b*) are the only two options that utilize all the available heat. There are several additional factors favouring BTES systems. In future, building owner may have to pay a special fee for the peak loads to the DH company. In addition, there is a yearly connection fee for DH services. These considerations have not been taken into account in this project, but they will not be applicable if the heat pump and borehole system are installed. On the contrary, there is a concern that installation of the heat pump will put the buildings into the category of electrically heated. This may pose specific requirements if the buildings are to be environmentally certified.

As to the simulations and assessment of the performance of the BTES and the GSHP system, the study has shown that when modelling a heat pump, it is important to set the parameters as close to reality as possible. This especially concerns the temperatures on the building side, which should vary over the year, and a parallel connection of the buildings.

Performance of the heat pump depends on both the evaporator fluid temperatures from the ground and the condenser fluid temperatures provided by the heat pump. The *COP* of a heat pump decreases with increasing supply temperatures. The two heat pump models tested in this work have shown different performances. This is mainly due to the fact that they have different operating limits. The maximum condenser temperature of the *Carrier* unit is only +63 ºC, whereas for *GEA* unit it is 80 ºC. This plays significant role in the considered system design. When modelling the heating system with constant supply and return temperatures of 60 ºC and 40 ºC on the building side, the authors encountered a problem with the *Carrier* heat pump, since it failed to provide 60 ºC over the entire demand duration. In a real system, heat pump supply and return temperatures will vary and the maximum supply temperature of 60 ºC will only be required occasionally during the peak loads. In this study, the temperatures on the building side have been decreased slightly to calculate the performance of the *Carrier* heat pump, yet it is evident that the system should have been modelled in a more realistic way, with temperatures in the heating system varying with the outside air temperature. It should also be mentioned that parameters of the heat pump models have not been optimized according to the product performance tables, thus the actual output from the heat pumps considered in this work may be slightly different.

It is also crucial for the heat pump model to have a parallel connection of the buildings to ensure that all buildings are supplied with the maximum temperature from the heat pump. On the other hand, it is not that important when direct connection to the furnace is modelled, since the supplied temperature is very high (87 ºC) and even after giving off heat to several buildings remains above 60 ºC.

As stated earlier, temperature from the ground also influences the performance of the heat pump. In this context, it should be highlighted that increase in temperatures from the ground to the heat pump has more significant effect on the improvement of the *SPF* when lower temperatures are provided by the heat pump.

All in all, despite all the advantages of the TES systems, direct use of the available waste heat results in much higher *SIR* compared to other options considered in this work. This option

also ensures the fastest payback time. The water storage tank option can also be profitable. Even though it does not use all of the available waste heat, it brings significant savings, especially in combination with the direct connection. When the considered systems are evaluated for a lifespan of 15 years, the BTES system is negatively influenced by the high initial cost, and consequently results in low savings-to-investment ratio. However, when the LCC analysis is performed for a lifespan of 25 years, the large BTES and GSHP option gives highest savings due to lower annual expenses. BTES system is the only option that allows to utilize all the available heat. It is possible to optimize the borehole system in terms of investments and savings, by extracting lower amount of energy from the ground.

It is also worth mentioning that if the available waste heat could have been sold to the district heating company for only 0.25 SEK/kWh, any design option considered in this work would not be needed.

References

Andersson, O., Rydell, L. & Algotsson, T., 2009. *Efficient usage of waste heat by applying a seasonal energy storage (BTES) at ITT Water & Wastewater AB, Emmaboda, Sweden*

Ataer, O. E., 2006. Storage of Thermal Energy. In: *Energy Storage Systems, in Encyclopedia of Life Support Systems (EOLSS).* Oxford, UK: Eolss Publishers.

Boer, R., Smeding, S. F. & Bach, P. W., 2006. *Heat storage systems for use in an industrial batch precesses.* New Jersey, The tenth international conference on thermal energy storage.

Bourne-Webb, P. et al., 2016. Analysis and design methods for energy geostructures. *Renewable and Sustainable Energy Reviews,* Volume 65, pp. 402-419.

Boverket, 2015. *Regelsamling för byggande, BBR,* Karlskrona: Elanders Sverige AB.

buildingphysics.com, 2017. *EED - Earth Energy Designer.* [Online]
Available at: http://www.buildingphysics.com
[Accessed 1 May 2017].

Cabeza, L. F., 2015. *Advances in Thermal Energy Storage Systems. Methods and Applications.* Sawston, Cambridge: Elsevier Ltd.

Carrier, 2017. *30XWH Vätska/vatten värmepump (252 - 1752 kW).* [Online]
Available at: http://www.carrierab.se/produkter/vaermepumpar/vaetskavatten-vaermepumpar/30xwh-vaetskavatten-vaermepump-(252-1752-kw).aspx
[Accessed 26 April 2017].

Claesson, J. & Javed, S., 2011. An analytical method to calculate borehole fluid temperatures for time-scales from minutes to decades. *ASHRAE Transactions,* 117(2), pp. 279-288.

Dincer, I. & Rocen, M., 2011. *Thermal energy storage. Systems and applications.* 2nd ed. Ontario: Wiley.

EnergyNest, 2017. *energy-nest.* [Online]
Available at: www.energy-nest.com
[Accessed 16 May 2017].

EQUA, 2017. *IDA Indoor Climate and Energy.* [Online]
Available at: http://www.equa.se/en/ida-ice
[Accessed 14 February 2017].

Freiberg, I., 2015. *Seasonal Storage of Distant Industrial Excess Heat for District Heating,* Gothenburg: Chalmers University of Technology.

GEA, 2017. *Heat Pumps.* [Online]
Available at: http://www.gea.com/en/productgroups/chillers_heat-pumps/heat-pumps/index.jsp
[Accessed 25 April 2017].

Göran Hellström, B. S., 2000. *Earth Energy Designer User Manual.* Lund: s.n.

Grundfos, 2017. *Find products and solutions.* [Online]
Available at: product-selection.grundfos.com
[Accessed 10 March 2017].

Gurtner, R., 2015. *Industrial waste heat recovery and efficient use of energy in the industry. Illustrative Examples from Germany.* Kolding, Conference on Renewables in the industry.

Hammock, C., 2015. *Underground thermal energy storage via borehole and aquifer thermal energy storage systems,* Houston, TX: s.n.

Han, Y. M., Wang, R. Z. & Dai, Y. J., 2007. Thermal stratification within the water tank. *Renewable and Sustainable Energy Reviews,* 13(2009), pp. 1014-1026.

Javed, S., 2010. *Design of ground source heat pump systems - Thermal modelling and evaluation of boreholes,* Gothenburg, Sweden: Building Services Engineering, Licentiate thesis, Chalmers University of Technology.

Javed, S., 2012. *Thermal modelling and evaluation of borehole heat transfer,* Gothenburg, Sweden: Building Services Engineering, PhD thesis, Chalmers University of Technology.

Javed, S. & Claesson, J., 2017. *Second-Order Multipole Formulas for Thermal Resistance of Single U-tube Borehole Heat Exchangers.* s.l., Research Conference Proceedings-IGSHPA Conference & Expo 2017.

Javed, S. & Spitler, J., 2016. Calculation of borehole thermal resistance. *Rees S, editor. Advances in ground-source heat pump systems*, pp. pp. 63-95.

Javed, S. & Spitler, J., 2017. Accuracy of borehole thermal resistance calculation methods for grouted single U-tube ground heat exchangers. *Applied Energy,* Volume 187, pp. 790-806.

Kiran, S. C. & Reddy, M. R., 2015. Experimental Analysis of a Thermal Energy Storage System-Waste Heat Recovery. *International Journal of Innovative Research in Science,Engineering and Technology, Vol. 4, Issue 8*, August.

Lavan, Z. & Thompson, J., 1976. Experimental study of thermally stratified hot water storage tanks. *Solar Energy,* Volume 19, pp. 519-524.

Manonelles, J. J., 2014. *Large-scale underground thermal energy storage. Using industrial waste heat to supply district heating,* Lleida: Universitat de Lleida.

Mickelsson, A., 2016. *Fortsättning på förstudie. Värmeåtervinning från förbränning. SVA Hus 14 samt hus 14 och 15,* Uppsala: Helenius.

Pavlov, G. K. & Olesen, B. W., 2011. Building Thermal Energy Storage - Concepts and Applications. *Proceedings,* p. Paper No 283.

Peacock, F., 2016. *Control solutions Minnesota.* [Online]
Available at: https://www.csimn.com/CSI_pages/PIDforDummies.html

Piatti, A., Piemonte, C. & Szegö, E., 1992. *Planning of geothermal district heating systems.* Dorderecht, The Netherlands: Kluwer Academic Publishers.

Prinsloo, G. & Dobson, R., 2015. Combined solar heat and power with microgrid storage and layered smartgrid control toward supplying off-grid rural villages. *Energy Science & Engineering,* 3(2), pp. 135-144.

Romagnoli, A., 2015. *Waste heat recovery in industrial precesses via thermal energy storage. Strategic Energy Management For Resilience,* Nanyang: Energy Research Institute NTU.

SADEV, 2017. *SADEV Architectural glass systems.* [Online]
Available at: http://www.sadev.com
[Accessed 18 May 2017].

SGU, 2017. *Map generator.* [Online]
Available at: http://www.sgu.se/en/products/maps/map-generator/
[Accessed 15 April 2017].

Short, W., Packey, D. J. & Holt, T., 1995. *A manual for the economic evaluation of energy efficiency and renewable energy technologies.* Golden, Colorado: National Renewable Energy Laboratory (NREL).

SMHI, 2016. *Enegi-Index, Graddagar och Kyl-Index - utökad information.* [Online]
Available at: www.smhi.se

Spitler, J., Javed, S. & Ramstad, R., 2016. Natural convection in groundwater-filled boreholes used as ground heat exchangers. *Applied Energy,* Volume 164, pp. 352-365.

Sundberg, J., 1988. *Thermal Properties of Soils and Rocks,* Göteborg: Geologiska Institutionen.

SVA, 2017. *SVA.* [Online]
Available at: http://www.sva.se/
[Accessed 12 February 2017].

SVEBY, 2013. *SVEBY Brukaring data kontor.* Stockholm: s.n.

The Swedish Environmental Protection Agency, 2009. *Climate Investment Programmes. An important step towards achieving Sweden´s climate targets,* Stockholm: Naturvårdsverket.

Uponor, 2017. *Uponor VVS Prislista 2017.* [Online]
Available at: http://www.uponor.se
[Accessed 9 March 2017].

Wang, W., 2010. *Mobilazed thermal energy storage for heat recovery for distributed heating.* Västerås, Mälardalen University.

Way, J., 2008. *Storing the Sun: Molten Salt Provides Highly Efficient Thermal Storage.* [Online]
Available at: http://www.renewableenergyworld.com/articles/2008/06/storing-the-sun-molten-salt-provides-highly-efficient-thermal-storage-52873.html
[Accessed 2 May 2017].

Wikells, 2017. *Sektionsfakta VVS 17/18.* [Online]
Available at: www.wikells.se
[Accessed 5 March 2017].

Worthington, M., 2017. *Underground Energy, LLC (Applied Hydrogeology and Geothermal Innovation).* [Online]
Available at: http://www.underground-energy.com/About-Us.html
[Accessed 6 May 2017].

Appendix A. Existing system

Figure A1: Flow diagram of the heating system connection with furnace for Building 14.

Appendix B. Direct use and storage tank
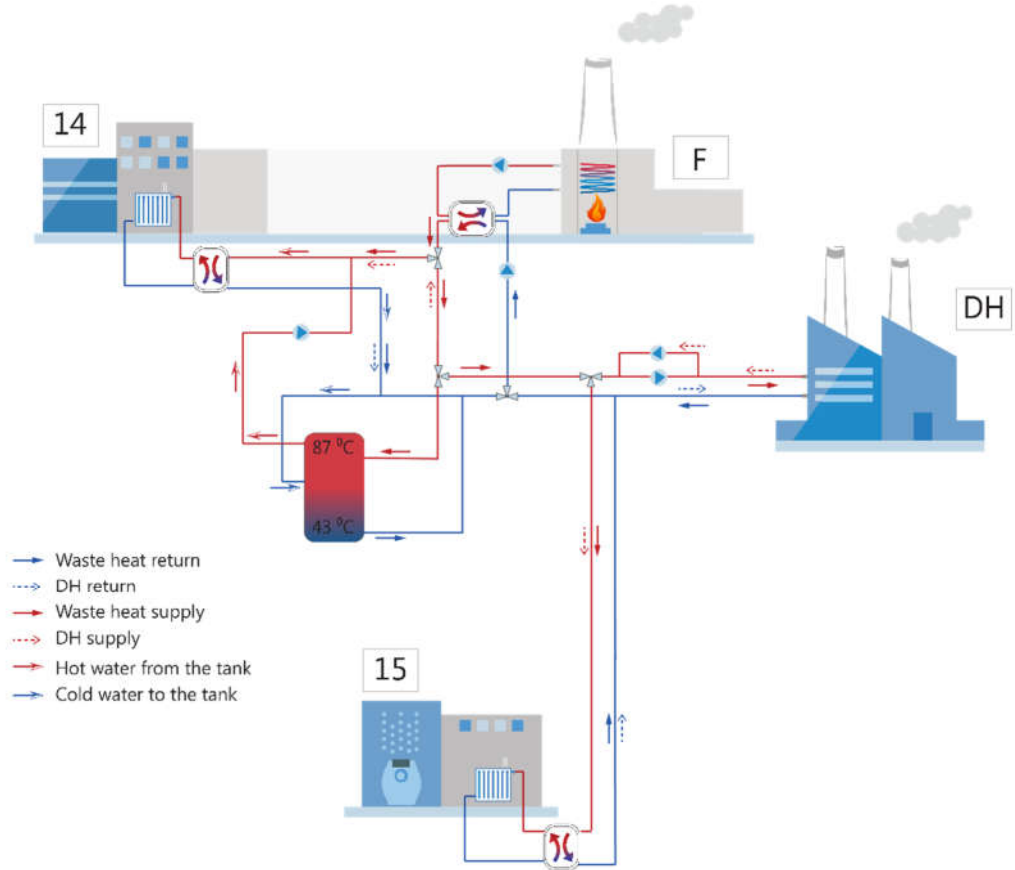
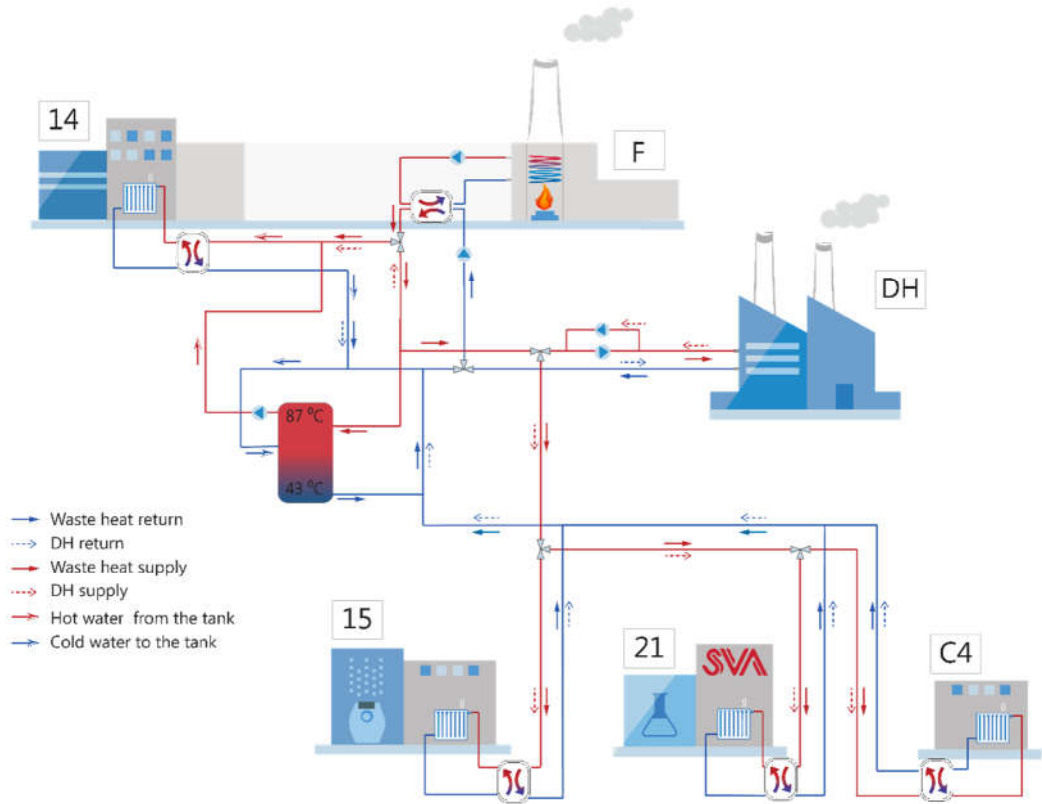*Figure B1: Direct supply of Building 15, and storage tank for Buildings 14 and 15 (Option 3a).*

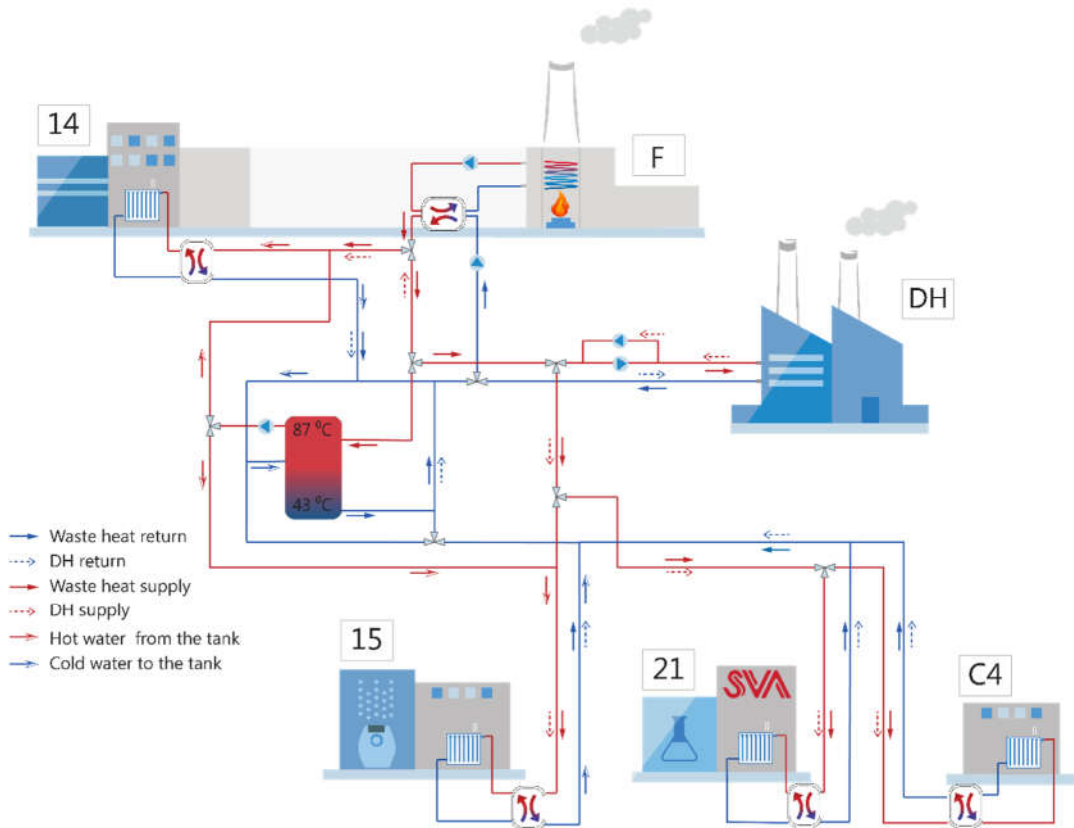*Figure B2: Direct supply of Buildings 14, 15, 21, C4 and storage tank for Building 14 (Option 3c).*

Figure B3: Direct supply of Buildings 14, 15, 21, C4 and storage tank for Buildings 14 and 15 (Option 3d).

Appendix C. Depth to bedrock in Uppsala
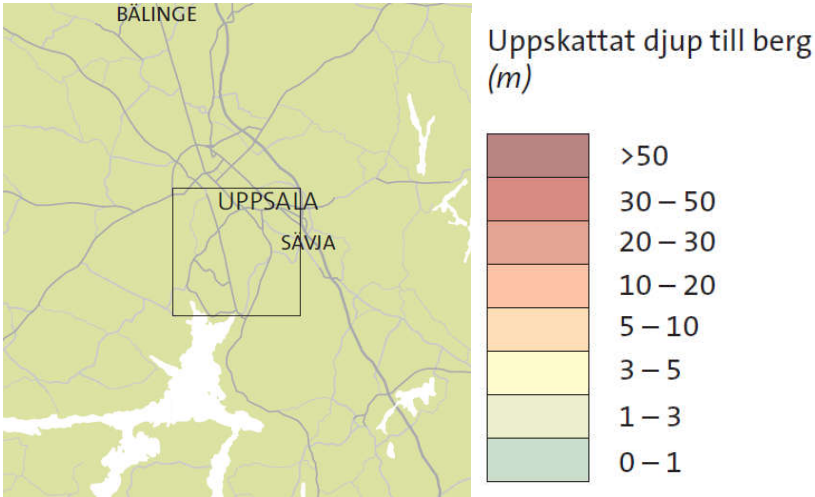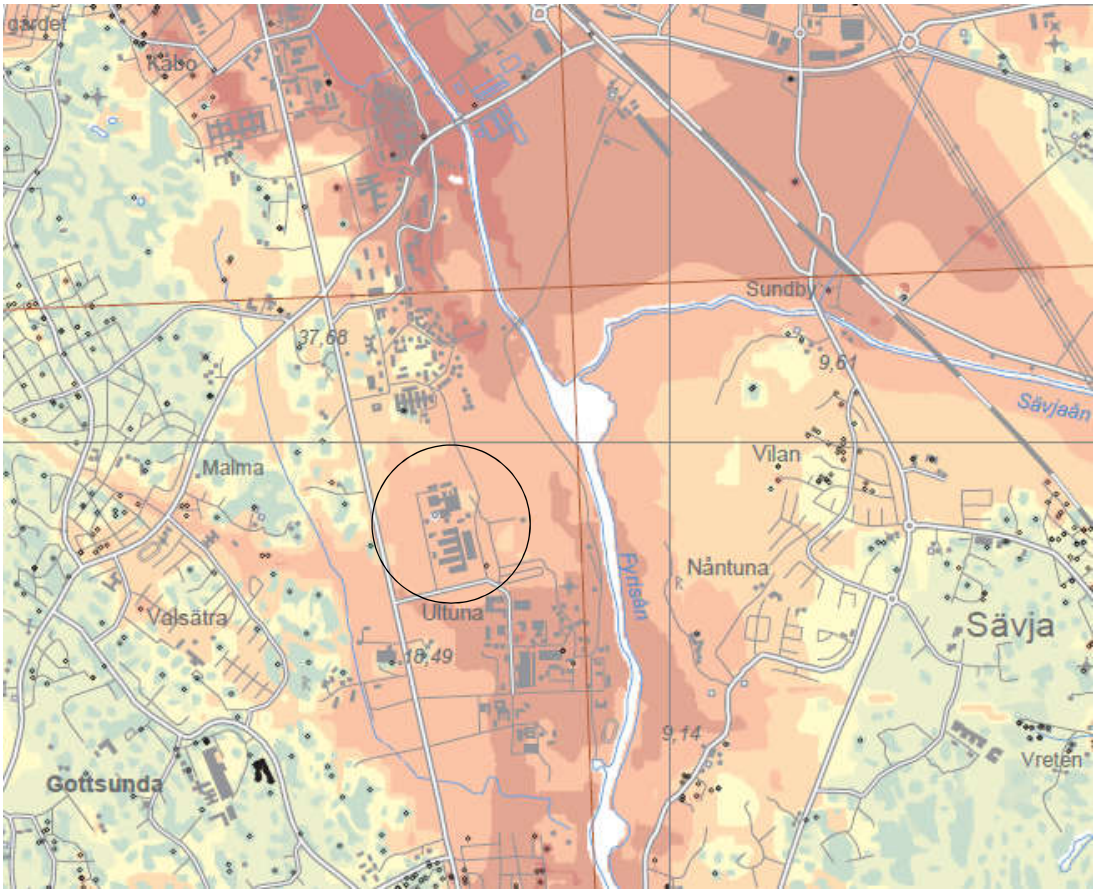
Figure C1: Map of the depth to bedrock of the considered site (SVA, Uppsala, circled on the map).

Appendix D. Water tank temperatures and sizing
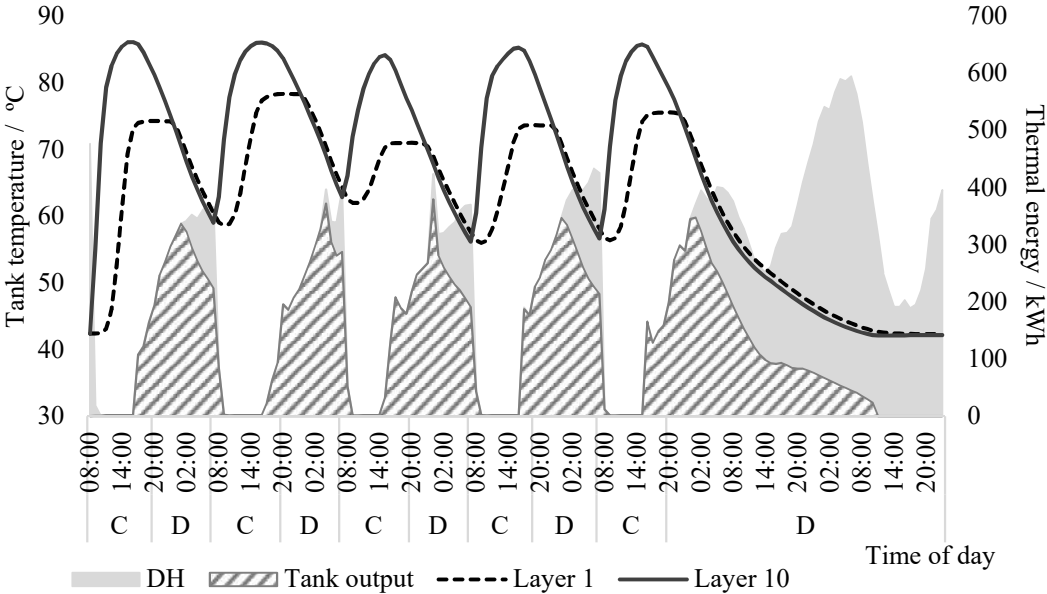
Figure D1: Temperatures at the bottom (Layer 1) and top (Layer 10) layers of the tank in the beginning of April. Portion of Building 14's demand covered by the tank is also shown. Letters 'C' and 'D' indicate charging and discharging periods respectively.
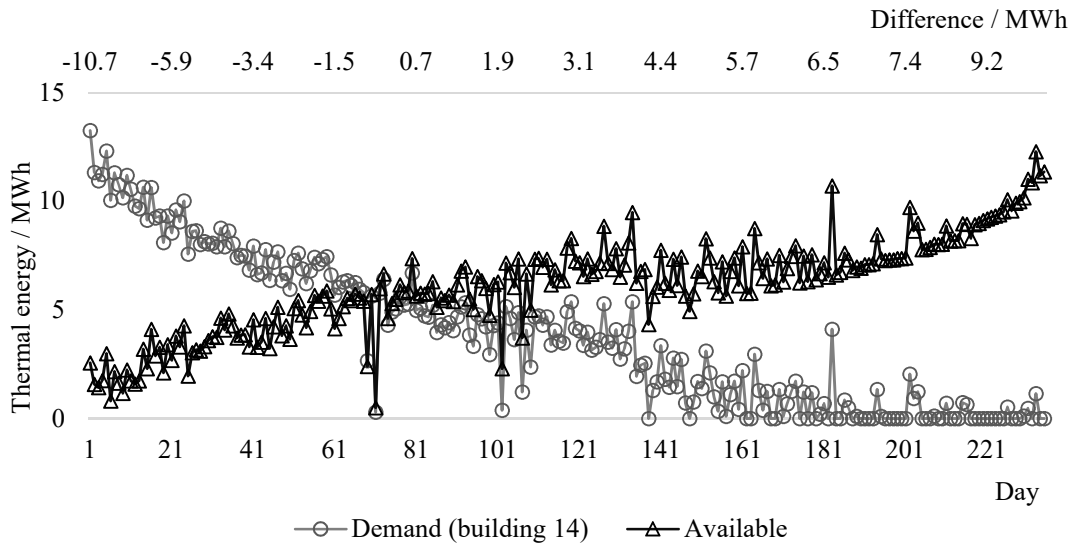
Figure D2: Difference between available heat and demand for Option 3a of direct connection and water storage tank.
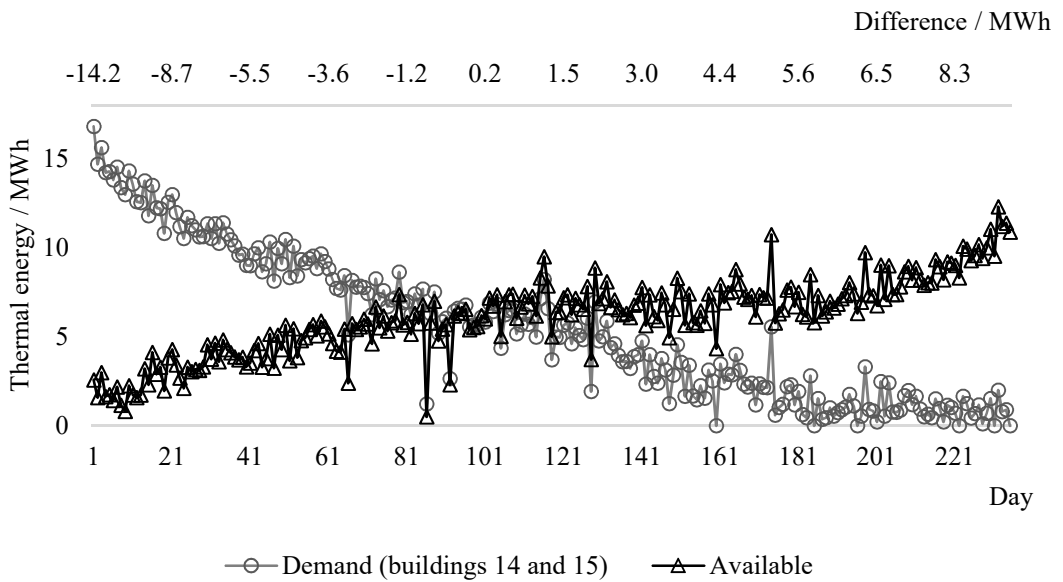
Figure D3: Difference between available heat and demand for Option 3b of direct connection and water storage tank.
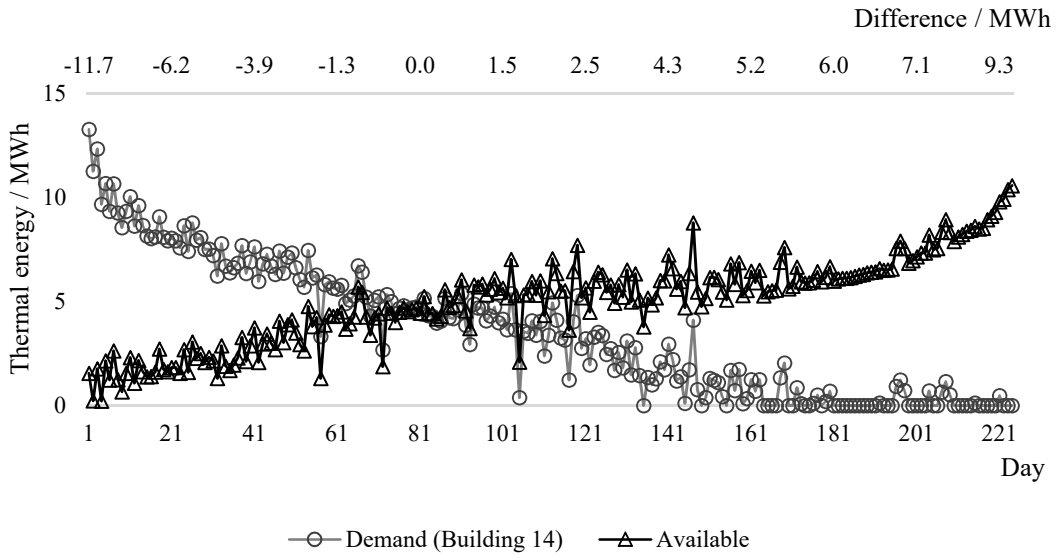
Figure D4: Difference between available heat and demand for Option 3c of direct connection and water storage tank.
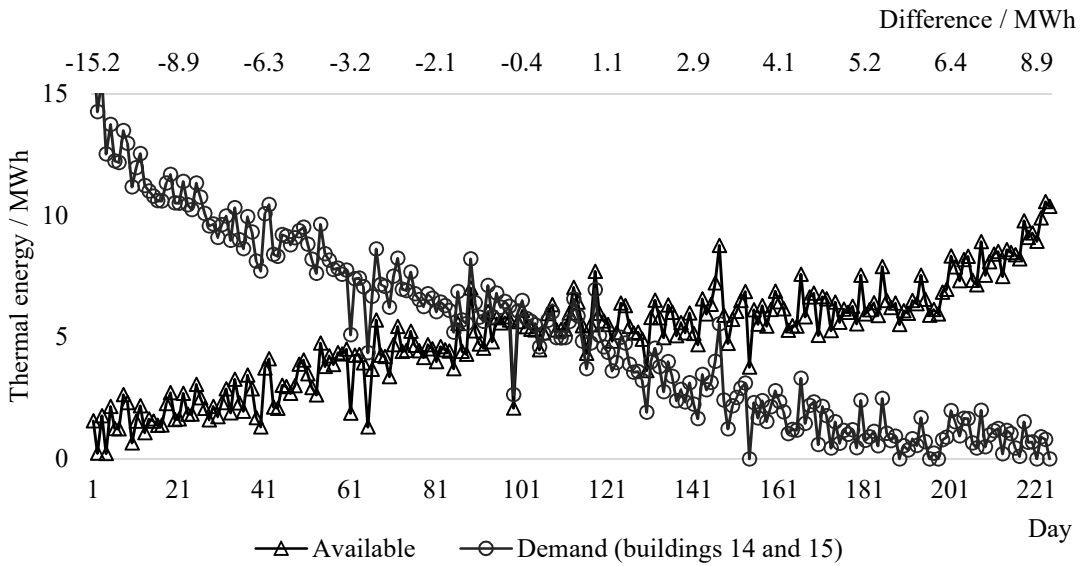

Figure D5: Difference between available heat and demand for Option 3d of direct connection and water storage tank.
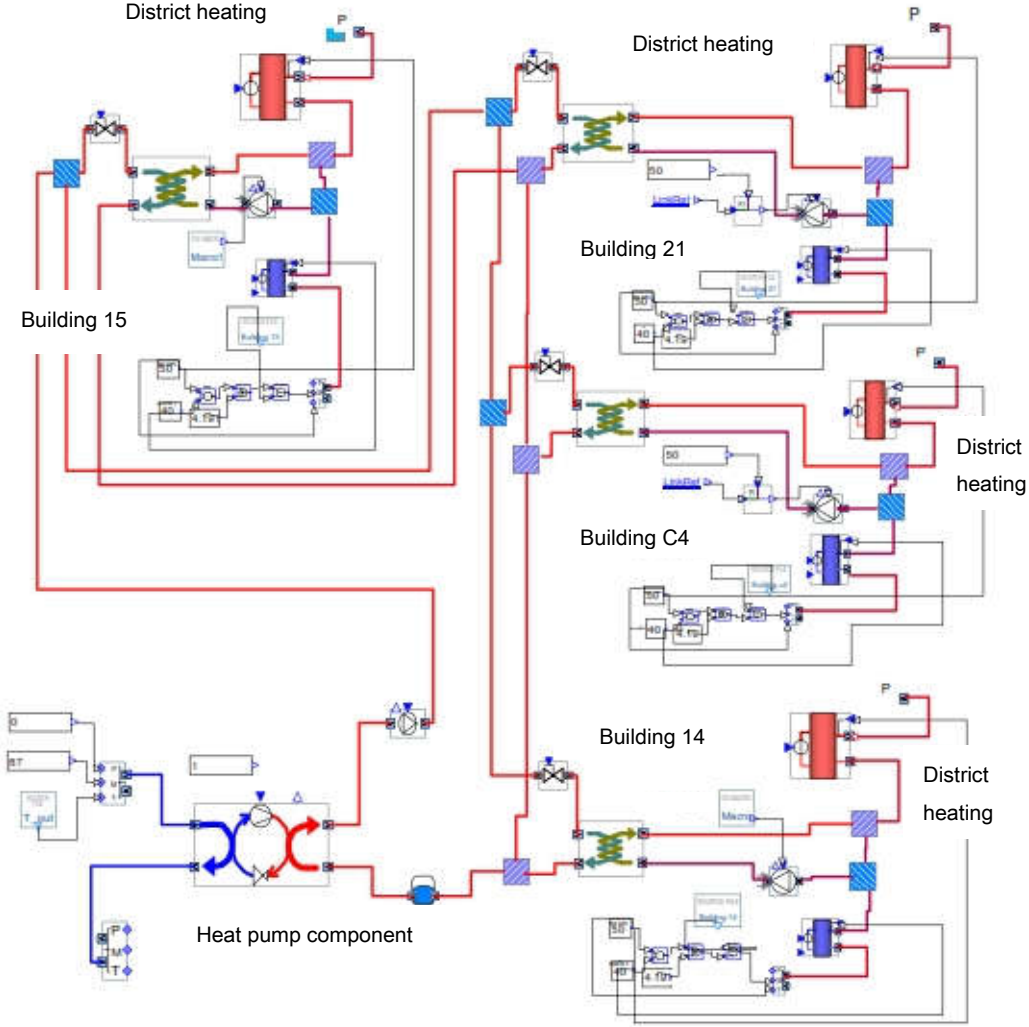
Appendix E. GSHP model

Figure E1: The resulting plant model in IDA ICE with heat pump and four buildings connected in parallel.
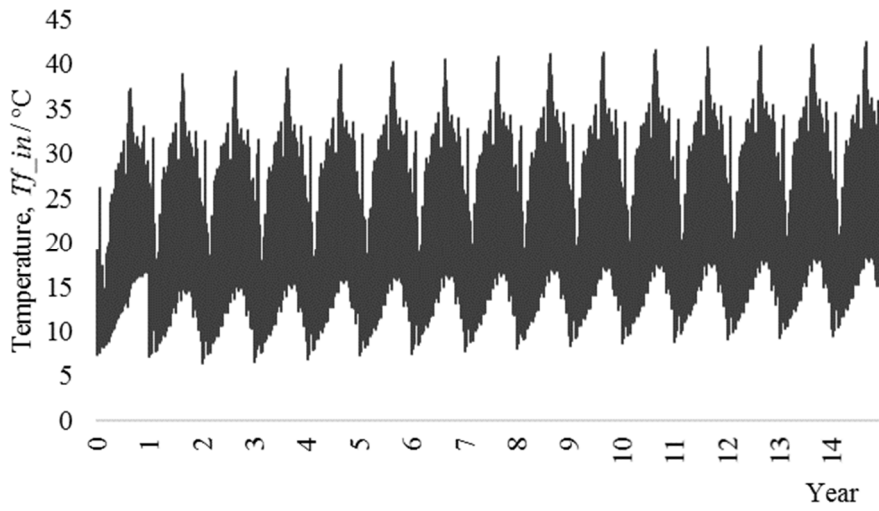
Figure E2: Temperatures to the heat pump in case of BTES sized for Buildings 15 and 21 and one year of ground charging.
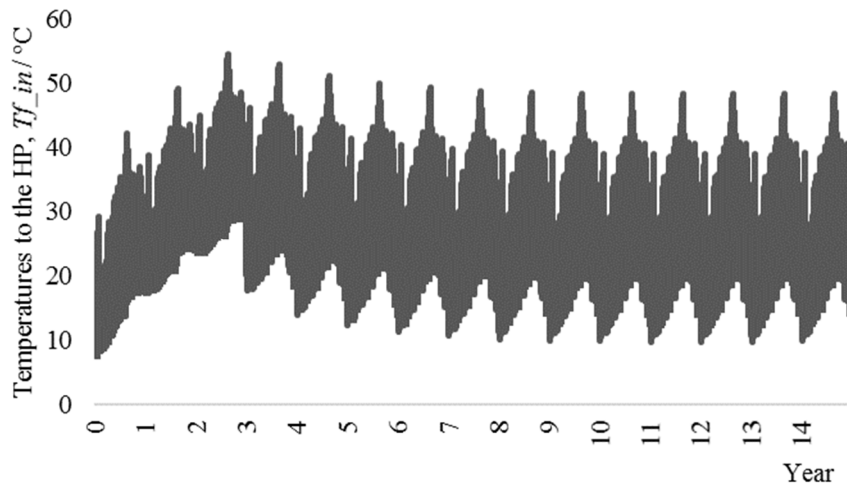

Figure E3: Temperatures to the heat pump in case of BTES sized for Buildings 15 and 21 and three year of ground charging.

LUND UNIVERSITY

Dept of Architecture and Built Environment: Division of Energy and Building Design
Dept of Building and Environmental Technology: Divisions of Building Physics and Building Services